2001

Conceptual analysis of a four -stroke linear engine

Sorin Petreanu
West Virginia University

CONCEPTUAL ANALYSIS OF A FOUR-STROKE LINEAR ENGINE

By

Sorin Petreanu

Dissertation

Submitted to
The College of Engineering and Mineral Resources
at
West Virginia University
in partial fulfillment of the requirements
for the degree of

Doctor of Philosophy
in
Mechanical Engineering

Christopher M. Atkinson, Sc.D., Chair
Nigel N. Clark, Ph.D.
Parviz Famouri, Ph.D.
Donald W. Lyons, Ph.D.
Gary J. Morris, Ph.D.

Department of Mechanical and Aerospace Engineering

Morgantown, West Virginia
2001

Keywords: Linear Engine, Engine Modeling, Diesel Engines, Homogeneous Charge Compression Ignition

ABSTRACT

CONCEPTUAL ANALYSIS OF A FOUR-STROKE LINEAR ENGINE

By Sorin Petreanu

During the past five years at West Virginia University, research into new auxiliary power generation devices has led to the development of a novel crankless reciprocating internal combustion engine. This dissertation presents a conceptual design of a Four-Stroke Linear Engine based on the numerical simulation of the operation of this type of linear engine. The engine consists of four opposed pistons linked by a connecting rod to a linear alternator. A series of numerical simulations was developed and employed to investigate the operation and performance of this crankless, four stroke linear engine. Since this linear engine is crankless, the numerical analysis of this particular engine is a time-based analysis. Two numerical models permit the simulation of the Four-Stroke Linear Engine employing Direct Injection Compression Ignition mode and a Homogeneous Charge Compression Ignition (HCCI) mode. The engine computational model combines dynamic and thermodynamic analyses. A detailed analysis of the engine operation range allows results to be obtained from a parametric study. The parametric study was performed to predict the engine behavior over a wide operating range, given intake parameters, variations in fuel combustion properties, reciprocating mass of the piston shaft assembly, frictional load and the externally applied load, and injection and valve timing. Based on the parametric study a conceptual design for a 15 kW linear engine was developed, showing the effects of reciprocating mass and air to fuel ratio on frequency of operation, power output, and efficiency. The engine analysis shown that this engine has a limited range of operation. The engine operating in as a direct injection compression ignition permitted high efficiency with values between 46 and 49 % corresponding to a compression ratio range between 17 and 35.

The analysis performed for the engine operating as a HCCI mode revealed that this particular operating mode depends critically on the start of combustion, which depends in turn on piston motion which is not prescribed. Although the HCCI operation permitted to achieve high values of the efficiency (over 60%) and power output it was observed that the operation domain for the engine was much narrower than for the direct injection case. The results obtained from the numerical simulation show that the FSLE operating under HCCI is difficult to control and this observation extends to any mechanical arrangement of the linear engine with unconstrained piston motion.

ACKNOWLEDGEMENTS

My past five years as graduate student at West Virginia University represent one of the greatest experiences of my life. During this period I had the chance to meet new people and to make a lot of friends. It is very difficult to write this section since there are so many people to mention.

I must first thank Dr. Christopher M. Atkinson for giving me the opportunity to attend graduate school and for being my advisor and especially for his for his unvaluable help and understanding during this long period. I want to assure Dr. Atkinson that I learn so many things from him. I hope he is not upset for the fact that I probably was the most stubborn student he has ever had.

I also wish to thank to Dr. Nigel N. Clark for his excellent guidance and help towards my work. I wish to thank my other committee members, Dr. Famouri, Dr. Lyons, and Dr. Morris for their help along theses years as graduate student at WVU and also to Dr. Greg Thompson.

Next, I want to thank my colleagues (staff from ERC) who have been helping me during this long period at WVU, Richard Atkinson, Michael Hildebrand, Tom McDaniel Andreas Pertl and Tom Spencer.

Evidently that I have to mention some the friends I made at ERC (unfortunately not all of then since it would take a phone directory) and I hope I would not offend them if I mention their names in alphabetical order: Emily Cirillo, Jennifer Hoppie, Nene Azu, Eric Corrigan, James Daley, David McKain, Eric Meyer, Scott Richmond, Christopher Tennant, Michael Traver. Also I have to thank to the other people who helped me and I have not mentioned their names. I wish all the recognized people the very best and I will do my very best to stay in contact with each and everyone of you.

TABLE OF CONTENTS

LIST OF FIGURES

LIST OF TABLES

NOMENCLATURE AND SYMBOLS

a	Wiebe Function Coefficient
	Coefficient for Frictional Force
A	Area
b	Coefficient for Friction Force
CI	Compression Ignition
C_{d_d}	Diffusive Combustion Duration
C_{d_p}	Premixed Combustion Duration
c_f	Friction Coefficient
DI	Direct Injection
D	Diameter
E_A	Activation Energy
F_f	Frictional Force
F_p	Total Pressure Force
EGR	Exhaust Gas Recirculation
$fmep$	Friction Mean Effective Pressure
FSLE	Four-Stroke Linear Engine
h	Oil Film Thickness
h_c	Convection Heat Transfer Coefficient
h_r	Radiation Heat transfer Coefficient
γ	Specific Heat Ratio

IC	Internal Combustion
ID	Ignition Delay
IVC	Intake Valve Closing
L_{st}	Maximum Stroke Length
LHV	Fuel Lower Heating Value
λ	Relative Air/Fuel Ratio
MAP	Manifold Air Pressure
MAT	Manifold Air Temperature
μ	Dynamic Viscosity
NO_x	Oxides of Nitrogen
Nu	Nusselt Number
η_v	Volumetric Efficiency
p	Cylinder Pressure
Pr	Prandtl Number
R	Gas Constant
$\widetilde{R}$	Universal Gas Constant
Re	Reynolds Number
S_p	Mean Piston Speed
SI	Spark Ignition
σ	Stefan-Boltzmann Constant
T	Cylinder Charge Temperature
	Temperature

T_w	Cylinder Wall Temperature
TSLE	Two-Stroke Linear Engine
τ_{id}	Ignition Delay
$\hat{U}$	Characteristic Velocity
$\frac{dQ}{dt}$	Heat Transfer Rate
$\frac{dQ_p}{dt}$	
χ	Mass Fraction Burnt
$[O_2]$	Oxygen Molar Concentration
$[Fuel]$	Fuel Molar Concentration

CHAPTER 1 INTRODUCTION

Since the start of the Industrial Revolution many types of power producing devices based on conversion of the chemical potential energy of a fuel into mechanical work (so called heat engines, or combustion driven engines) have been developed. Based on the fuel-engine interface the heat engines can be categorized into two main groups: internal combustion engine and, external combustion engine. Another classification of the heat engine is based on the way that combustion takes place intermittent or continuous, or based on the fuel ignition as: spark ignition compression versus compression ignition. The subject of this dissertation is an internal combustion engine and therefore this particular category will be further emphasized. It is generally accepted today that the internal combustion engine represents a main source of power production. Driven by environmental concerns and resource shortages the internal combustion engine has been the subject of continuous research and development for more than a century with significant improvements in this area.

The most common mechanical configuration of an internal combustion engine is represented by the traditional slider-crank mechanism, which permits the conversion of the reciprocal linear motion of the piston to the rotational motion of the crankshaft. Another mechanical configuration of an internal combustion engine is represented by the rotary engine known as the “Wankel” engine. This engine offers a more compact size than the reciprocating engines and multifuel capability. Having fewer moving parts than reciprocating engines, they have a lower weight and therefore high specific power density. However these engines have their own weaknesses and these is represented by the leakage encountered at the interface between the rotor apex seals and housing. Most piston engines are of the slider-crank mechanism type,

but there is a second class of piston engines, termed free-piston or linear engines, in which the engine's pistons reciprocate freely without the use of a rotating crankshaft or flywheel. This work describes the development of a new linear engine for power generation applications.

The internal combustion engine is a relatively inefficient machine, its efficiency varies from 20 to almost 50% the upper limit corresponding to the compression ignition engine, therefore only a small amount of the fuel available energy is transformed into useful work, the rest being lost through heat transfer and friction. The efforts to improve the overall efficiency of the conventional slider crank mechanism engines were focused mostly toward the improvement of the thermodynamic efficiency, although the mechanical losses associate with friction were also reduced due to the improvement of the materials used in the manufacturing. The elimination of the slider-crank mechanism which involves a substantial reduction of the losses associated with friction, represents a potential source of improving the efficiency of an internal combustion engine. From the design point of view, this mechanical arrangement will be much simplified due to fact that there are less moving parts than in a slider crank mechanism configuration.

A new crankless reciprocating internal combustion engine type with a real potential of improving the “weaknesses” of the common slider-crank mechanism internal combustion engine, will make the subject of this dissertation.

CHAPTER 2 OBJECTIVES

The objective of this dissertation was to develop a design for an alternative diesel fueled auxiliary power plant able to produce a nominal power of 15 kW. The evaluation of the performance of Four-Stroke Linear Engine was based on a numerical simulation of the engine cycle. A parametric study was performed to study the influence of different variables on the engine operation and, to determine the operation range of this particular engine. These objectives were accomplished through the following tasks:

- A literature survey was conducted to review the existent work in the area of free piston engines.
- A review of existent compression ignition engine modeling techniques was undertaken.
- A review of the operation and characteristics and combustion models of the Homogenous Charge Compression Ignition engines was undertaken.
- Two effective, yet simple, thermodynamic time-based numerical models were developed to study the operating characteristics of the Four-Stroke Linear Engine operating in a direct injected compression ignition mode.
- A thermodynamic time-based numerical model was developed to study the adaptability and operation of the Four-Stroke Linear engine as a Homogeneous Charge Compression Ignition engine.
- A parametric study was performed to determine the effect of various parameters on engine performance.
- Based on the engine modeling and simulations results, engine design recommendations were made.

CHAPTER 3 LITERATURE REVIEW

3.1 FREE PISTON ENGINES

Free-piston engines have been a subject of research and development for several decades. Free-piston engines utilizing internal combustion (as opposed to the external combustion Stirling engine, which suffers from poor power density) have their origin in the 1920's when R. Pescara [1] patented their use as air compressors. Junkers in Germany developed a free-piston engine for use in German submarines in World War II. The French SIGMA free-piston gasifier saw service for decades in stationary power generation. The use of free-piston engines in automotive application was most heavily promoted in the period 1952 to 1961, when both General Motors and Ford Motor Company produced running prototypes [2,3]. In both cases these engines were two-stroke, opposed piston spark ignited engines with combustion bounce/compression chambers. These engines where used as gasifiers to generate hot gases to drive exhaust turbines through which energy would be extracted. A schematic of a free piston engine used as a gasifier is presented in Figure 3.1 [4]. The free piston engine presented is a diesel combustion engine gasifier that incorporates a gas turbine expander for power output. The reciprocating devices, which are identical designed, consist of a large double-faced compression piston at one end and a small gas expansion piston at the other end. Both large double-faced pistons serve a twofold purpose; the inner face is utilized to compress air, and the outer piston face to work with a special closed air-bounce chamber. The smaller pistons are the ones that operate as a two-stroke engine piston. One mechanical cycle of a free piston engine begins with air compression. With the intake ports uncovered, air is compressed and moved into a clearance volume defined by the two small gas expansion

pistons. During this undergoing process, the inner face of the double-faced pistons, compresses the air through a valving system into a compressed air tank/volume, this particular mass of compressed air serving as intake air for the future scavenging process.

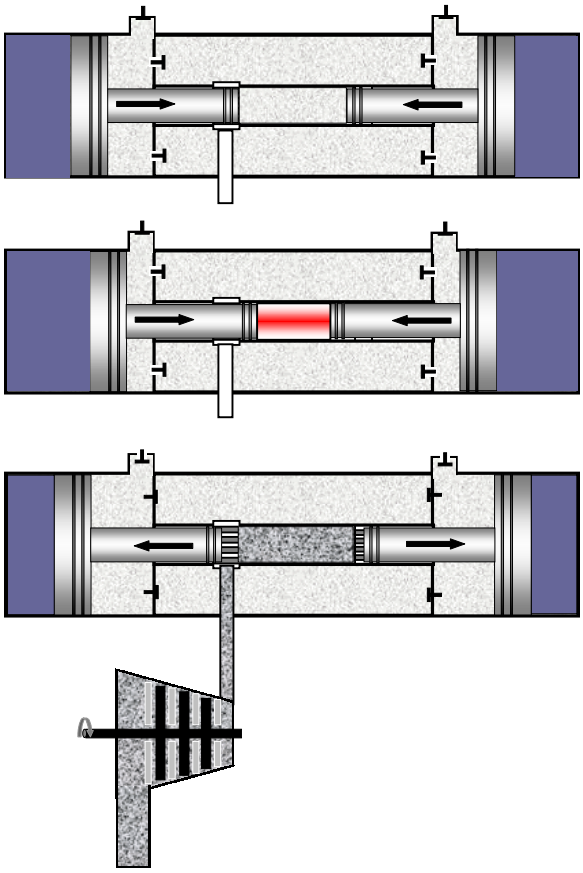

Figure 3.1: Free Piston Engine used as a Gasifier

Diesel fuel is injected into the volume of high-temperature and high-pressure compressed air mass, delimited by the two small pistons. The injected fuel mixed with the compressed air and ignites resulting a combustion process. Due to the high gas pressure developed within the combustion volume during the combustion process, the two small pistons start moving outwards and the combustion gas undergoes an expansion process. During this process the

large compression perform two tasks: the outer faces compress the air within the bouncing chambers and the inner faces serve as suction pump allowing the air enter a volume delimited by the inner face of the larger piston and the wall that separates the compressed air volume. As the smaller pistons undergo the expansion process, the exhaust ports are opened permitting the exhaust gases to expand through the turbine producing this way the power output. The development efforts for this gasifiers largely ceased by the 1960's as turbine powered vehicles were increasingly viewed as not commercially viable.

The elimination of the crankshaft mechanism in free-piston engines provides potential for reduction in mechanical losses. Due to the fact that the piston is not constrained in a free-piston engine, the piston motion is not prescribed, and it varies from one operating regime to another. Characteristic of the free-piston engines is the fact that they do not have a flywheel. As a result, they do not accumulate energy from the previous cycles for the subsequent cycles, except in terms of achieving a greater or lesser stroke associated with greater or lesser gas compression energy. A free-piston engine-pump system has been disclosed by Heintz [5]. The device consists of a pair of opposite pistons connected by a common rod operating a hydraulic pump. The free-piston engine pump has double acting power pistons and pumping pistons attached as a main reciprocating member and movable in a housing. The housing itself moves for mass balancing purposes. The engine is spark ignited, and stroke control is provided by a valving system. Air is supplied and the exhaust products are removed from the two combustion chambers by common intake and common valves. These valves are operated by a common actuator in response to the position of the main reciprocating member.

A linear engine operates somewhat similarly to a free-piston engine, the only difference

being that the reciprocating assembly consists of two pistons connected by a common connecting rod, with each piston operating in its own cylinder. In the last two decades there has been resurgence in interest in these engines for hybrid electric vehicle applications. Several linear engines have been designed but most of them have a complicated mechanical configuration. This complication is the result of the need for tight control of the length of the stroke of the piston assembly, to avoid having the piston contact the cylinder head at its furthermost outer position. Some notable recent work in the development of linear engines is reviewed below.

Bock [6] has developed a compression ignition linear engine. The engine incorporates a hydraulic pump cylinder arranged in the central part of the engine in order to provide useful work. The engine is gas cushioned and it uses a nitrogen filled elastic annular body serving as a shock absorbing body. Rittmaster et al. [7] have presented a spark ignition linear engine connected to hydraulic power system. Hydraulic fluid is stored and maintained under pressure in two pressurization chambers on the opposite side of the pistons forming an internal combustion engine. In order to time the operation of the engine, a set of proximity detectors located around the connecting rod are used. The hydraulic fluid flow in the two pressurization chambers is controlled by a set of cross-over valves. A hydraulic motor is interposed downstream of the cross-over valves to convert the flow of the fluid into the rotation of a shaft. The cylinders of the engine have intake and exhaust valves electronically operated. A flywheel is attached to the shaft of the hydraulic motor to dampen the pulsation induced by the shifting of the cross-over valves and to store the energy of the pistons between reciprocation. Iliev et al. [8], have presented a linear engine coupled to an electrical

alternator. The engine operates on a two-stroke cycle and is spark ignited. The engine is controlled by an electronic module, which also controls the linear alternator. The spark timing is regulated based on the quality of fuel and the electrical load. According to the inventors the engine is designed to operate at high frequencies thereby attaining a high thermal efficiency. Galitello [9] has proposed a linear engine controlled by a computer. The engine is a two-stroke compression ignition engine. According to the inventor the engine operates at ultra high speeds and is vibration free. During engine starting, ignition assist is provided by spark plugs. The engine can be connected to an electric generator or to a hydraulic power system. Deng et al. [10] disclosed a double acting tandem crankless internal combustion engine having combustion chambers at opposite ends and one in its center with double acting pistons displaceable between one end and the center chamber and between the other end and the center chamber. Each piston includes opposite piston heads with connecting rods between them coupled to a linear alternator. The presented device works based on the two-cycle engine, each combustion chamber having an inlet port and a valve and an exhaust valve. The engine uses a mechanism to provide a symmetrical piston displacement.

An interesting design has been presented by Kos [11]. The disclosed engine is a two-stroke cycle linear engine employing a reciprocating piston in conjunction with an electromagnetic transducer for control and power output. The engine can be spark or compression ignited (with multi-fuel operation possible). The engine is designed to be controlled by computer, with the engine stroke varied by tailoring the magnetic field. The inventor suggests an alternative arrangement of the engine by using a pair of opposite pistons linked by a

connecting rod.

Beachley and Fronczak [12], presented a two-stroke free-piston engine for hydraulic power generation. The engine consists of two double-ended, reciprocating opposed-pistons that serve a twofold purposes, the inner side of the pistons operate within the internal combustion engine while the outer ends operate a hydraulic pump.

Widener and Ingram [13] recently described a numerical model of a free-piston linear generator for a hybrid vehicle modeling study. The model addressed the use of a free-piston engine coupled with a linear generator as a potential auxiliary power unit in hybrid electric vehicles. The feasibility of such a model was analyzed with regards to power output and efficiency of the unit with reference to conversion of mechanical power output of the linear engine to electrical power output. The study was conducted on a two-stroke cycle engine and a reciprocating rig was developed to study and characterize the operation of the generator.

Van Blarigan et al. [14, 15] developed a two-stroke linear engine combined with a linear alternator for electrical power generation. The disclosed engine operates as homogeneous charge compression ignition engine, and the fuel used was hydrogen. The engine consists of two opposed pistons, rigidly connected by a connecting rod, which can oscillate back and forth within the combustion cylinders. The linear alternator was designed such that electricity was generated directly from the piston's oscillating motion, as permanent magnets fixed to the piston are driven back and forth through the alternator's coils. The linear alternator is also used as a stroke control device. A linear engine two-stroke spark ignition for electrical power generation has been developed at WVU over the past four years. The engine consists of a two horizontally opposed-pistons, mounted on a common shaft that is allowed to oscillate back

and forth between end mounted cylinders. Combustion occurs alternately in each cylinder, thus forcing the piston assembly back and forth in an alternating fashion. The piston motion is not constrained implying that each cylinder of the engine has an infinitely variable effective compression ratio. The intake and exhaust valves are ported for two-stroke operation, thus removing any necessity for external actuation of their operation or timing. The engine has been the subject of a number of investigations [16-20] with regards to the design modeling and simulation. This work will be generally presented in the following section.

3.2 PREVIOUS WORK AT WEST VIRGINIA UNIVERSITY

The cooperative effort between Mechanical and Aerospace Engineering department and Computer Science and Electrical Engineering department lead to the development over the past four years of a new device of power generation. First linear engine prototype developed at WVU for the past four years was a two-stroke spark ignition for electrical power generation A schematic of this engine is presented in Figure 3.2. The engine consists of a two horizontally opposed-pistons, mounted on a common shaft that is allowed to oscillate back and forth between end mounted cylinders. Combustion occurs alternately in each cylinder, thus forcing the piston assembly back and forth in an alternating fashion.

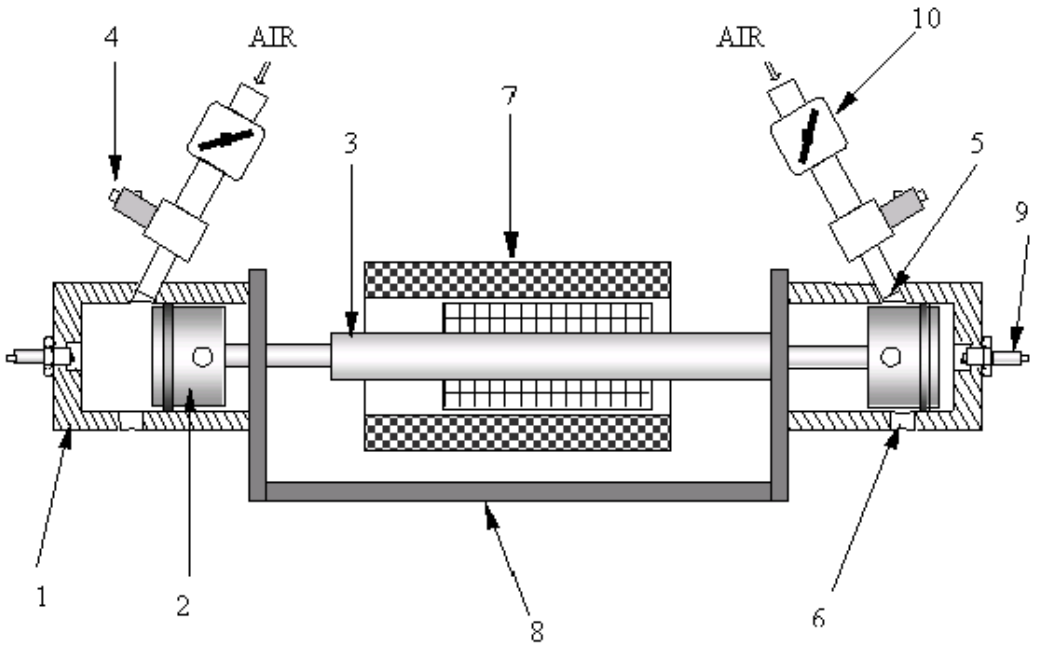

1. Cylinder, 2. Piston, 3. Connecting Rod, 4. Pulsed Solenoid Fuel Injector, 5. Intake Port, 6. Exhaust Port. 7. Linear Alternator. 8. Frame. 9. Spark Plug. 10. Throttle

Figure 3.2: Prototype Two-Stroke Spark Ignition Linear Engine

The piston motion is not constrained, implying that each cylinder of the engine has an infinitely variable effective compression ratio. The intake and exhaust valves are ported for two-stroke operation, thus removing any necessity for external actuation of their operation or timing. The geometric parameters of this engine are presented in Table 3-1.

Table 3-1: Geometric Parameters of a Spark Ignition Two-Stroke Linear Engine Prototype

Number Cylinders	2
Bore	36.4 [mm]
Maximum Possible Stroke	50 [mm]
Exhaust Port Opening	19 [mm] from the end of maximum theoretic stroke
Intake Port Opening	21 [mm] from the end of maximum theoretic stroke
Exhaust Port Height	10 [mm]
Intake Port Height	10 [mm]

Ref. [16-20]

The cylinders are ported such a manner to utilize a loop scavenging process, although this process was not optimized. The fuel is supplied to each cylinder by two pulse width-modulated gasoline fuel injectors. In order to keep the engine temperature within a reasonable operating range, water is forced through the cylinder heads. An electronic control device allows the adjustment of the ignition timing and fuel injection timing and quantity. The engine stroke is controlled on a stroke-by-stroke basis by the ignition timing and the amount of fuel injected. The engine is equipped with two motoring coils (also connected to the electronic control device) used as a starting device. These are automatically disengaged after the engine exceeds a certain reciprocation frequency. The motoring coils are also used in case of misfire in one of the cylinders, to reverse the motion of the piston assembly and to assist in restarting. A permanent magnet linear alternator connected to the engine shaft

transforms the kinetic energy of the reciprocating motion into electrical energy.

The prototype engine has been tested extensively under several different operating modes, with the load being provided by a friction brake, as well as with the load applied by a permanent magnet linear alternator. In-cylinder pressure profiles for different applied loads were experimentally determined through extensive engine testing. The results of the engine testing, using a friction brake to provide the load, are presented in Table 3-2.

Table 3-2: Experimental Data from the Linear Engine Operation using Load applied by a Friction Brake

Load	Average Indicated Work output per stroke [J]	Average Positive Power Output [W]	Average Stroke [mm]	Average Frequency [Cycles/min]
No	1.55	81.3	44.3	1574
Yes	6.25	262.5	35.3	1260
Yes	10.79	438.0	37.6	1197
Yes	16.40	804.0	47.0	1470

Ref. [16-20]

A further analysis of the experimental operation of the linear engine in combination with the linear alternator has been presented [17]. The linear alternator is of the permanent magnet-type, and has been shown to produce as much as 316W from the prototype engine-alternator combination. Based on the in-cylinder pressure data gathered during operation of the engine-alternator combination, an analysis of the cycle-to-cycle variation of integrated mean effective pressure (IMEPg) was performed. It was shown that there are significant cycle-to-cycle variations of the in-cylinder pressure versus time for different operating regimes. The results of the performance tests of the engine-alternator prototype combination are shown in Table 3-3.

Table 3-3: Experimental Data from the Linear Engine using Load applied by a Permanent Magnet Alternator

Test	Load [ohms]	Voltage [V]	Current [A]	Load Power Output [W]	Frequency [Hz]
1	Open Circuit	132.0	0.00	0	25.0
2	156.0	120.0	0.75	92	24.6
3	130.0	119.0	0.88	104	24.4
4	104.0	115.0	1.07	124	23.4
5	78.0	111.0	1.38	153	24.1
6	52.0	103.0	1.92	200	26.6
7	26.0	90.0	3.30	300	23.6
8	24.0	88.5	3.54	312	23.6
9	23.4	87.5	3.58	313	23.6
10	19.5	79.0	3.90	316	23.1
11	17.3	74.0	4.15	309	22.7

Ref. [16-20]

The modeling and simulation of the two-stroke gasoline linear engine [19] is summarized as follows. A numerical model was developed for the spark ignited linear engine prototype, with the possibility of being easily adapted for the case of the compression ignition engine simulation. The developed numerical model represents an idealized case due to the assumptions made and, it was validated using results from the tests performed on the linear engine prototype. The engine computational model combines dynamic and thermodynamic analyses. The dynamic analysis performed consists of an evaluation of the frictional forces and the load (in this case the alternator load) across the full operating cycle of the engine. The thermodynamic analysis consists of an evaluation of each process that characterizes the engine cycle, including scavenging, compression, combustion and expansion, based on the first law of thermodynamics. In order to simplify the modeling task, the numerical analysis

was divided into two distinct sub-models that are correlated, a dynamic model and a thermodynamic model. In the first sub-model, the dynamic model, it was performed an analysis and a evaluation of the forces that act on the reciprocating assembly, namely friction, load, inertia and pressure forces exerted on the two opposed-pistons faces.
The second sub-model performed the thermodynamic analysis of the engine cycle which consists of an evaluation of the thermodynamic parameters for each process that characterizes the engine cycle, for the two-cycle case, scavenging, compression, combustion and expansion. The thermodynamic model used in this numerical analysis was a single zone model. In single models the cylinder mixture composition, pressure and, temperature are considered to be uniform and, the energy released by the combustion of the fuel is specified or calculated after the fact from the measured in-cylinder pressure history data. Matching the experimentally derived and the numerically obtained in-cylinder pressure profiles was a complicated task due to the number of the unknown variables, namely the absolute value of the heat addition, the combustion duration, and the actual load on the engine. There is an infinite number of combinations of these unknowns that can match the given shape of the in-cylinder pressure profiles. Nevertheless, an important piece of information in the combustion process was that the spark timing was known. In these engine experiments, there is no explicit information regarding the combustion duration, so matching the experimental and numerical P-V diagrams is extremely complicated. Figure 3.3 and Figure 3.4 illustrate the in-cylinder pressure variation obtained from the tests performed on the two-stroke linear engine prototype and the in-cylinder pressure variation obtained from the numerical simulation of the engine cycle, respectively.

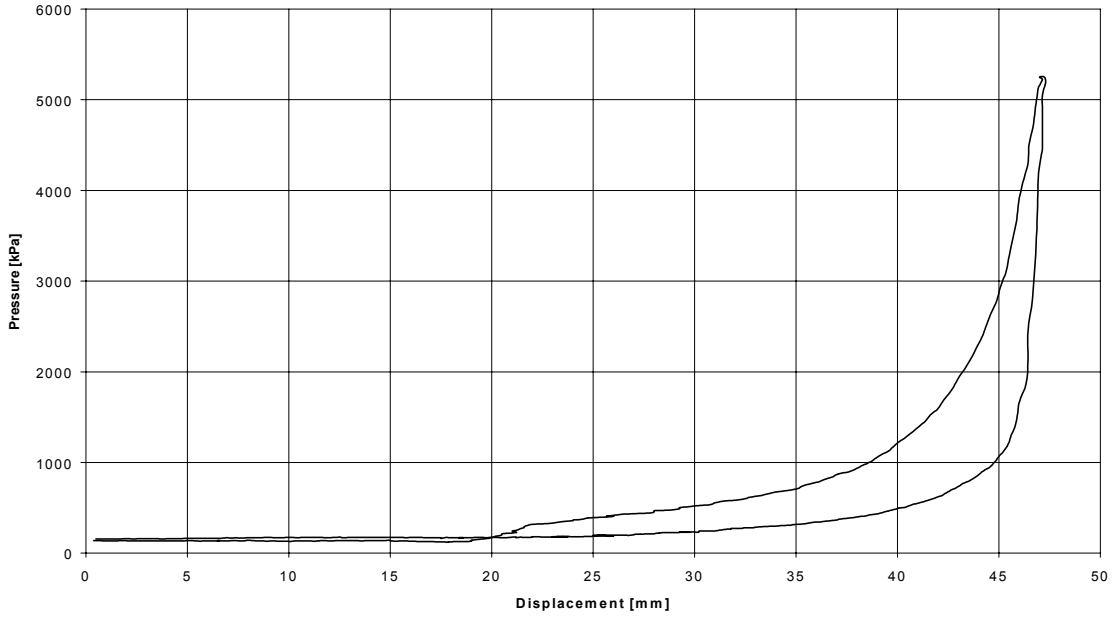

Figure 3.3: Experimental Data Derived from the Operation of the Prototype Linear Engine-Alternator Combination.

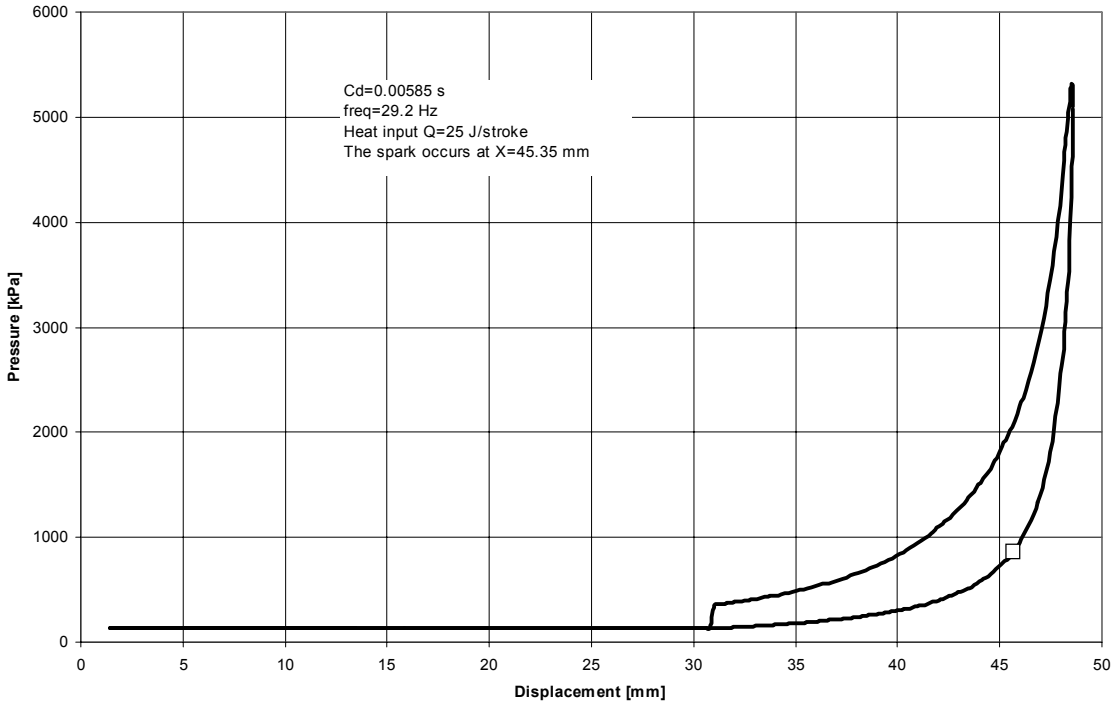

Figure 3.4: A "P-V" Diagram Obtained from the Numerical Simulation of a Two-Stroke Linear Engine.

The numerical simulation of the Two-Stroke Spark Ignition Linear Engine cycle, allowed a parametric study of the operation of this type of engine, absolutely new at that moment. The parametric study sought the prediction of the engine behavior over a wide operating range, given variations in fuel combustion properties, the reciprocating mass of the piston shaft assembly, frictional load and the externally applied electrical load. It was observed that the variation of the heat input influences the peak pressure, the frequency of the engine, and also the stroke length. The variation in the combustion duration also influences the peak pressure, the frequency of the engine, and the displacement in the same manner as for the heat input variation, is presented in Figure 3.5 and Figure 3.6. The experimental testing performed on the linear engine [17] showed that the linear alternator introduces a load that has a roughly sinusoidal shape throughout the stroke, therefore in the numerical simulation was taken as being a various power of a sinusoidal. A resultant resistant force was considered as being the summation of the friction force and the load introduced by the linear alternator. The shape of the resultant was varied considering three particular cases: first case considered the resultant force as being constant throughout the stroke, while the second case considered a triangular shaped force maintaining the same integrated area under the curve. Extending the analysis, the third case of more complex load functions was considered. Figure 3.7 illustrates the different shapes or profiles of the load that were used in the numerical model. These shapes were chosen to represent the cases of high load near the extremes of the piston stroke, or highest load in the center of the stroke. The case when the load is concentrated towards the end of the stroke corresponds to greater values of the shape factor k, (where k varies from 0 to 3.55).

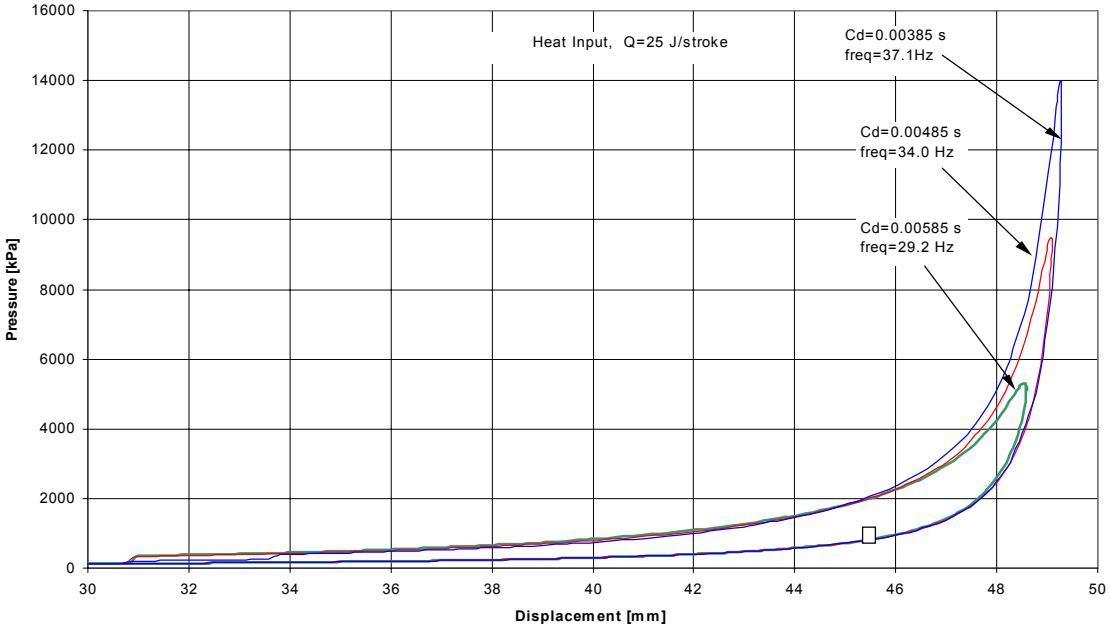

Figure 3.5: In-Cylinder Pressure vs. Piston Assembly Displacement for different values of the Combustion Duration for the same Heat Input

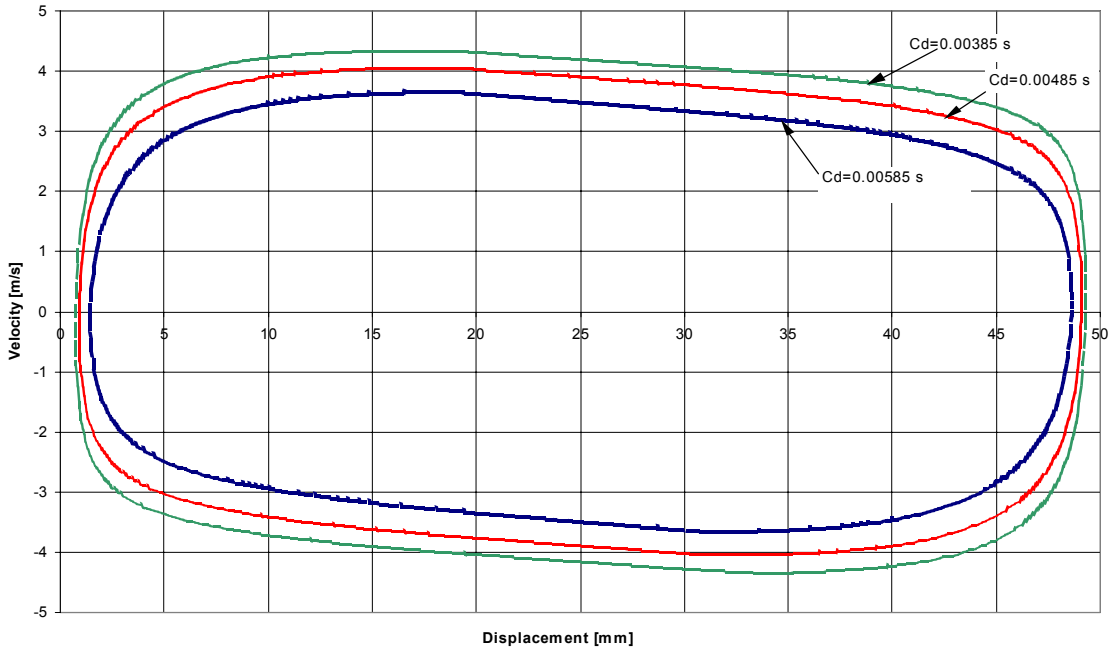

Figure 3.6: Piston Velocity vs. Displacement for different values of the Combustion Duration

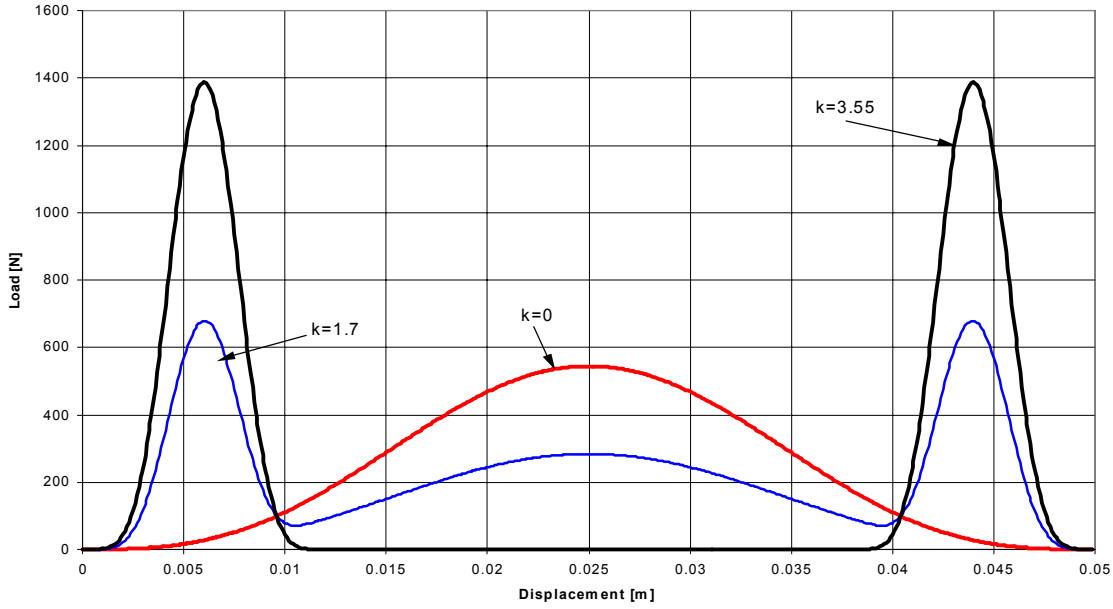

Figure 3.7: Different Shapes of the Load Considered in the Analysis

By varying the mass of the moving piston assembly, the peak pressure and maximum displacement, vary proportionally. For a greater mass, the peak pressure and the engine stroke both increase, shown in Figure 3.9. The frequency varies in an inverse proportional relationship with the mass of the reciprocating shaft, this aspect is presented in A further observation was that, for very low reciprocating masses, the operation of the linear engine becomes possible only if the heat input was increased significantly, due to the low inertial forces associated with low piston speeds.

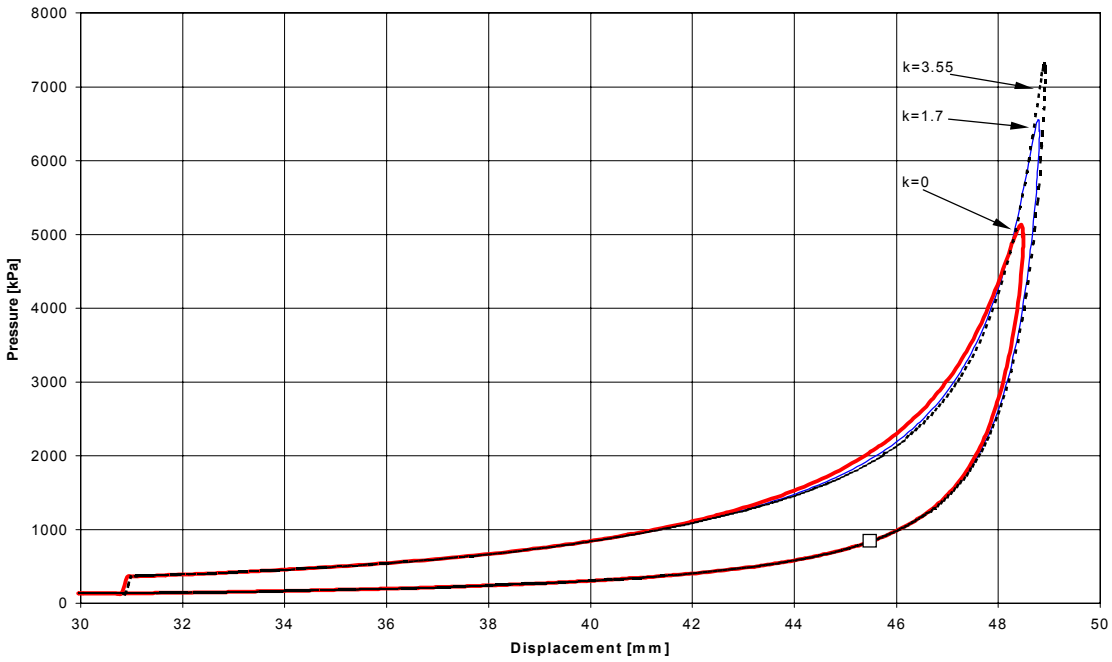

Figure 3.8: In-Cylinder Pressure vs. Piston Displacement for Different Profiles of the Load

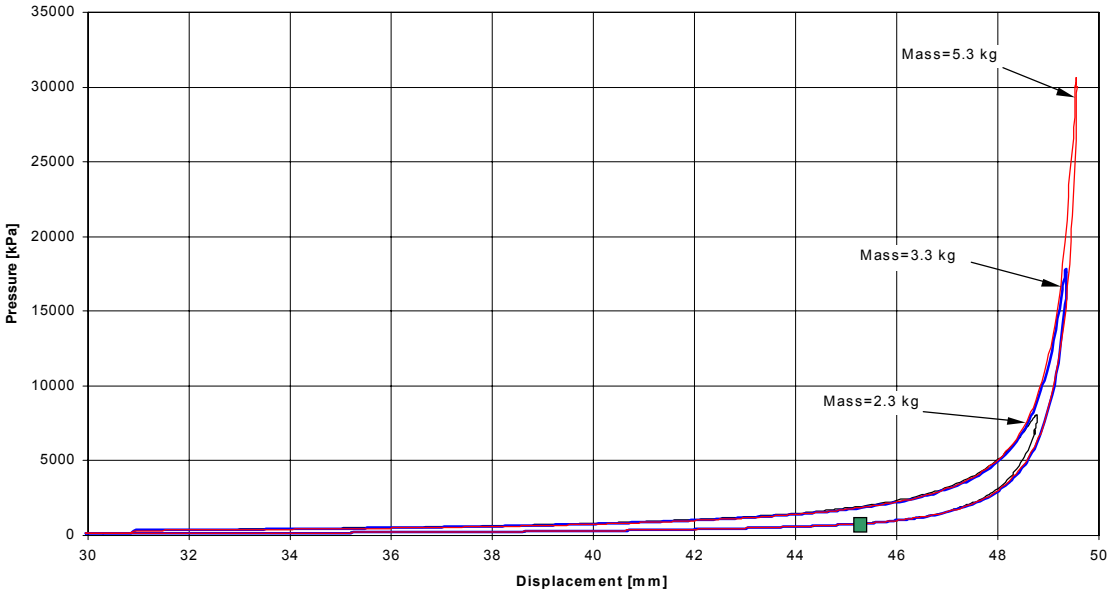

Figure 3.9: In-Cylinder Pressure vs. Displacement for different values of the Reciprocating Mass

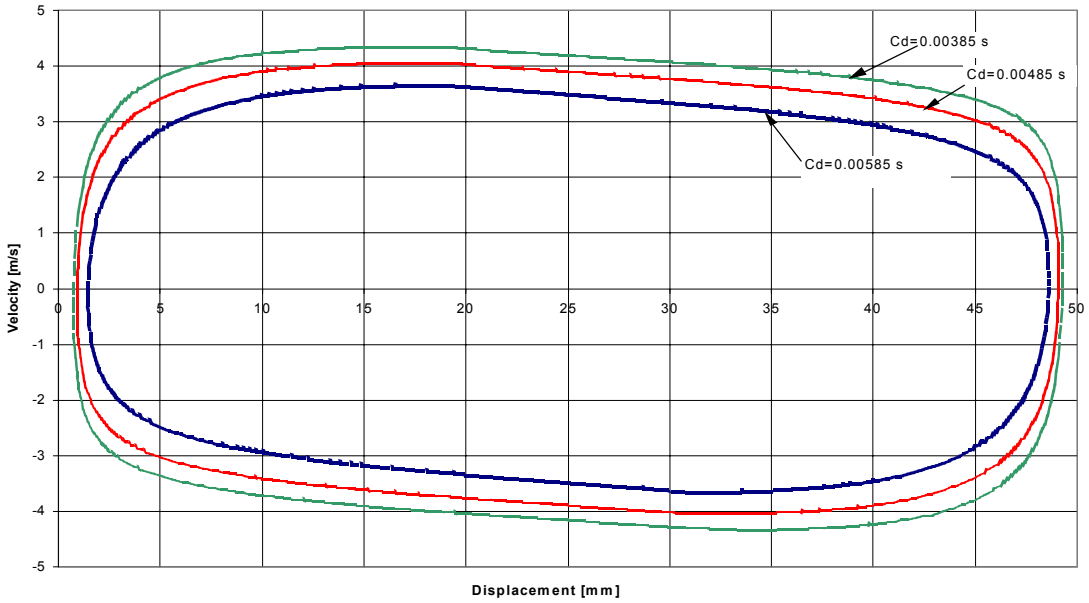

Figure 3.10: Piston Velocity vs. Displacement for different values of the Reciprocating Mass

A compression ignition prototype version of the two stroke linear engine was also built and developed in the past two years at the Engine and Emissions Research Center at West Virginia University. A schematic of this prototype engine is presented in Figure 3.11.

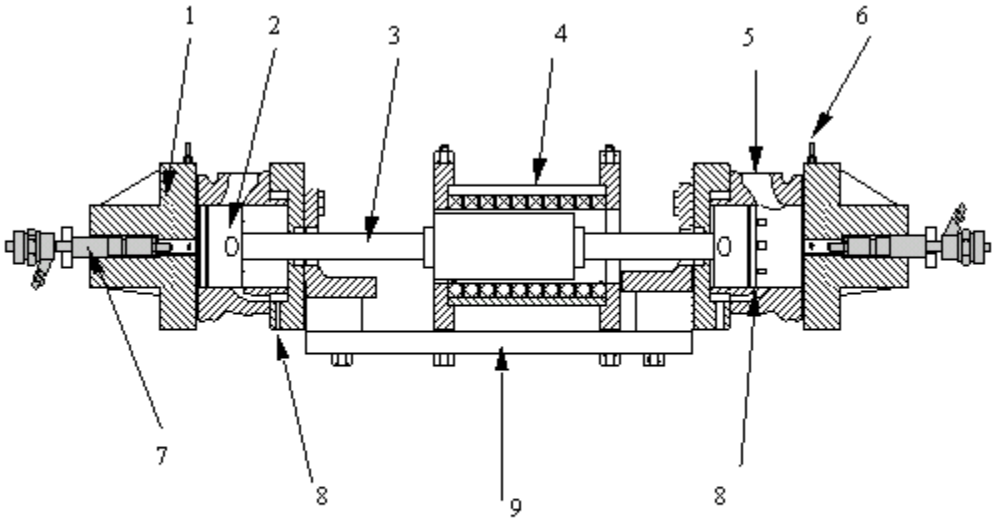

1.Cylinder Head, 2. Piston, 3. Connecting Rod, 4. Linear Alternator, 5. Exhaust Port, 6.Glow Plug; 7. Fuel Injector, 8. Intake Ports, 10. Frame.

Figure 3.11: Prototype Two-Stroke Diesel Cycle Linear Engine-Alternator Combination.

The engine has a similar mechanical arrangement to the spark ignition prototype and the geometric parameters of this engine are presented in Table 3-4. The fuel delivery system for this prototype is performed by a common rail direct injection system. The high-pressure fuel pump supplies the two injectors. The linear alternator interposed with the linear engine operates also as a starting device and, in order to aid the cold start of the engine, each cylinder is equipped with glow plugs. The operation of these auxiliaries namely, injectors, fuel pump and the use of the linear alternator as starting device, are controlled by an

electronic control unit (ECU). Despite the reduced friction losses encountered on these engines there is still need for lubrication on the cylinder-piston ring interface. The solution adopted for the lubrication of the engine (as in the use of in-line air-tools) the lubricant being provided in a spray through the intake air in sufficient amounts to ensure the integrity of the piston rings. The engine is water-cooled, water being forced into the bottom of the cylinder jackets and out through heads of cylinders.

Table 3-4: Geometric Parameters of the Direct Injection Compression Ignition Two-Stroke Linear Engine Prototype

Number Cylinders	2
Bore	75 [mm]
Maximum Possible Stroke	71 [mm]
Exhaust Port Opening	37 [mm] from the end of maximum theoretical stroke
Intake Port Opening	42 [mm] from the end of maximum theoretical stroke
Exhaust Port Height	30.5 [mm]
Intake Port Height	23 [mm]

The compression ignition version of a two-stroke linear engine was tested and it is still under investigation due to some difficulties encountered in the starting process. A two-stroke linear engine design has a number of disadvantages, particularly from an engine efficiency and emissions point of view. For this reason, it was decided to investigate the development of a four-stroke device, as an alternative.

3.3 ADVANTAGES OF THE FOUR-STROKE LINEAR ENGINE

The elimination of the rotating crankshaft mechanism in a linear engine implies a series of advantages over the classical IC engines. First, a linear engine displays a reduction in friction losses that leads to a better overall engine thermal efficiency. Another advantage is the fact that the linear engine can have a more compact construction with lower reciprocating mass per unit power developed, therefore it can offer a higher power density. Since the reciprocating assembly can freely move within the combustion cylinders, the compression ratio is variable; thus permitting the achievement of higher thermal efficiency values than those met by prescribed motion engines. The fact that the engine can operate at variable compression ratio also theoretically permits the use of a large variety of fuels.

From previous studies [16-20] done on the Linear Engine-Alternator Combination, the important features encountered in the operation of this device were observed. These features are summarized as follows. The piston motion is strongly dominated by the reciprocating assembly mass. The reciprocating frequency is a function of reciprocating mass and heat input into cycle and is inversely proportional to the piston diameter [16]. In a numerical analysis performed on a spark ignited gasoline-fueled linear engine [19], it was shown that the combustion duration was longer than expected, resulting in a reduction of the thermodynamic efficiency of the engine cycle. On the other hand, longer combustion duration combined with an unconstrained piston motion permits lower pressure and temperature levels for the same indicated mean effective pressure, with beneficial implications on the engine emissions.

Based on experimental results and analytical considerations, it was also shown that the

scavenging process is a critical for the operation of the Two-Stroke Linear Engine (TSLE). The main problem of two-stroke cylinder processes is that they offer low fuel efficiency due to the imperfect scavenging processes (short-circuiting).

The engine analyzed in this dissertation will operate as a direct injection compression ignition engine for starting and partial loads, and as a HCCI engine under full load regimes. Due to its characteristics (mechanical simplicity, compactness, higher power density) the FSLE has a wide applicability, from the stationary power units to the auxiliary power units for mobile applications.

3.4 THE HOMOGENEOUS CHARGE COMPRESSION IGNITION CONCEPT

The idea of using HCCI for this project derived from the fact that DI does not offer low emission levels at higher loads, especially with regard to oxides of nitrogen emissions. The HCCI concept is a hybrid between the SI and CI engine concepts. The combustion process in common diesel (direct in-cylinder injection) engines has a turbulent-diffusive aspect, the rate of the combustion being dictated by turbulent mixing of fuel with air since the chemical reaction rates are much faster then those of the mixing process [21]. In mixing controlled combustion processes, the flame stabilises at the interface region between the air and the fuel where the combustible volumes are formed, resulting in high local temperatures favorable for NO_x formation. The high local temperatures represent the greatest concern for classic compression ignition engines since they give rise to significant NO_x formation. The combustion process in the Spark Ignition engines is characterised by flame propagation. In these engines, a spark that ignites an already well-mixed homogeneous air-fuel charge initiates the combustion process. The local flame front temperature reaches high values favouring the formation of NO_x. Evidently, for both cases (SI and CI), there are different remedies to avoid the local high temperature formation, such the use of recirculated exhaust gases (EGR), or to reduce the compression ratio, but these tactics represent a compromise resulting in reduced engine performance. HCCI represents an alternative to the in-cylinder injection compression ignition, since for this operation mode, the fuel-air charge is mixed outside the combustion chamber (in the intake system) and it is compression ignited by the temperature of the air-fuel charge in the cylinder after compression. In comparison to SI engine, in HCCI the flame propagation phenomenon does not exist; thus in-cylinder

turbulence does not have a central role in the combustion process. The ignition of the charge occurs spontaneously and simultaneously throughout the mixture, and the combustion process takes place in a homogeneous way thus permitting a homogeneous combustion temperature. Due to the presence of numerous hot ignition spots, the combustion occurs very fast, the overall combustion duration being shorter than that of spark ignition engines. Relevant aspects of the HCCI concept have been presented in several different studies [22-28] over the past twenty years; they all showed significant reductions in exhaust emissions, most notably NO_x. It was shown that in order to achieve well-distributed auto-ignition of the charge, high compression ratios are required. However this combustion concept presents two extremes, one being the detonation in the case of a rich mixture, and the other one is the misfire that occurs in the case of a too lean mixture, and both extremes are to be avoided. The most delicate features of the HCCI operation are the initiation of auto-ignition and the representation of combustion rate.

Important information was disclosed by Ryan et al. [24,25], who have investigated the HCCI on a single cylinder four-stroke engine, using diesel fuel. The investigations were conducted on modified single cylinder engine with variable compression ratio using EGR, intake air temperature, and compression ratio as variable parameters. The air was delivered to the engine using a compressor system that could be used to control the intake air pressure up to 0.3 MPa. It was shown that HCCI is well behaved only for certain regimes corresponding to a relatively high EGR rate, and relatively low compression ratios in the range of 8 to 11. The other regimes corresponding to higher values of compression ratio and to lower EGR rates lead to severe knock. It was also shown that the combustion process especially the

autoignition process has a complex dependency on the EGR rate, compression ratio, equivalence ratio, and also on the charge intake temperature.

The most noticeable work related to this project was done by Van Blarigan et al. [14], who has proposed the use of HCCI implemented on free piston engine coupled with a linear alternator. The HCCI combustion investigations were done on a rapid compression-expansion machine for different types of fuels, other than diesel fuels, for different equivalence ratios and at different compression ratios. The intake charge temperature was also varied. It was shown that HCCI requires higher compression ratios then those seen in conventional diesel engines in order to auto-ignite the cylinder charge, and also the cycle heat addition approaches the Otto cycle for the fuels with a single stage combustion process. NO_x emissions can be controlled by leaning the equivalence ratio and by increasing the intake charge temperature.

In their efforts to analyse the benefits of HCCI, Suzuki et al. [26], have investigated the combustion in a single cylinder that used a hybrid strategy for the charge formation and to control the homogeneous charge combustion. Therefore, the fuel is primarily injected into the intake manifold in a manner similar to HCCI. The lean premixed charge induced into the cylinder is ignited by a small amount of fuel directly injected into the cylinder by a conventional injection system. The premixed fuel used for the experiment was iso-octane, and the direct injected fuel used was light oil, commonly used in Japan for automobile engines. The authors performed a parametric study on HCCI using as variable parameters the ratio of the heating value of premixed fuel to the heating value of the total fuel, the engine load, the EGR rate, and the octane number of the premixed fuel by blending it with normal-

heptane. The results shown that the smoke decreases near-uniformly with the increase of the premixed fuel ratio and the NO_x decreased for higher premixed fuel ratios.

CHAPTER 4 DESCRIPTION OF THE FOUR-STROKE LINEAR ENGINE

The designed engine that makes the subject of this dissertation is an upgraded concept of a linear engine and it is based on a previously designed two-stroke linear engine prototypes. Starting from the same idea of unconstrained motion of the reciprocating device, a new mechanical arrangement proposed is the Four-Stroke Linear Engine (FSLE). This arrangement promises to reduce or to eliminate the disadvantages experienced by the spark-ignition version of the TSLE arrangement. During the operation of the TSLE, noticeable vibrations were observed but they were not of primary concern for the preliminary investigation of the engine operation. Due to its mechanical arrangement, the FSLE has potential to diminish the vibration aspects met in free piston engine operation.

The FSLE has a very similar configuration to the TSLE, and basically it represents a combination of two TSLE's. The FSLE consists of two pairs of opposed-pistons connected by a rigid shaft that oscillates back and forth within the combustion cylinders (chambers). The shaft that links the pistons is coupled with a linear alternator able to absorb the energy generated by the engine. The proposed arrangement introduces a mechanical complication due to the existence of the linkage between the parallel pair of pistons. Nevertheless, this inconvenience can be overcome by means of a proper design for the reciprocating shaft. The FSLE will be able to reduce the vibration offering a better balance than TSLE version. Based on FSLE configuration, a "H" mechanical arrangement can be obtained by coupling two FSLE. Obviously there can be envisioned different mechanical arrangements of FSLE. The unconstrained motion of the reciprocating device, and therefore the variable compression ratio, makes the engine suitable for operation with Homogeneous Charge Compression

Ignition (HCCI), in which a premixed air-fuel charge is ignited by heating due to the compression. A schematic of the engine under investigation is presented in Figure 4.1.

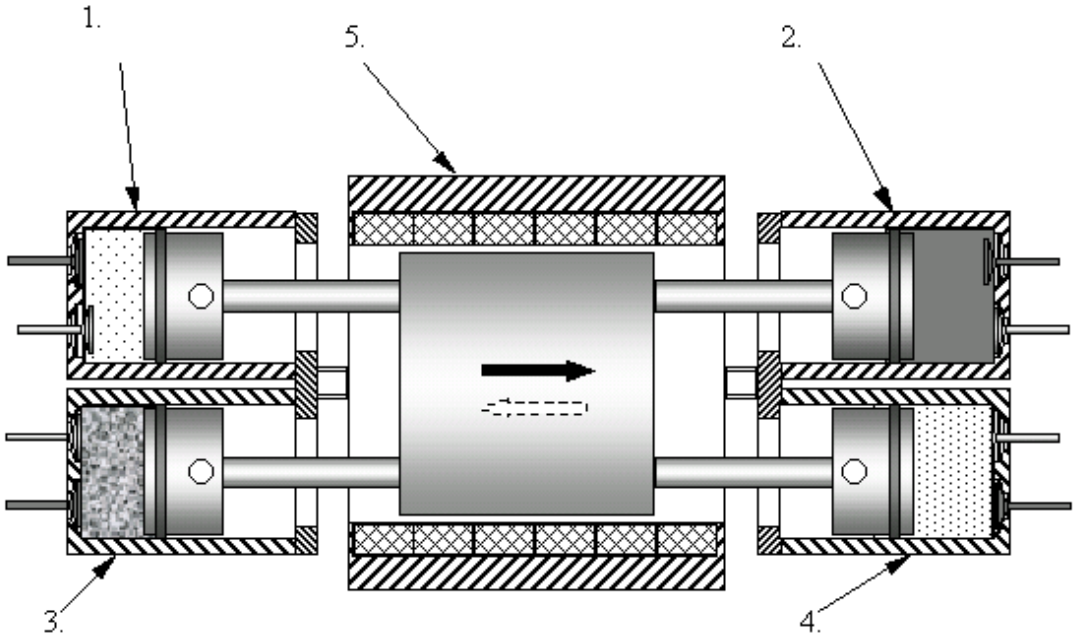

1. Cylinder 1 (Intake); 2. Cylinder 2 (Exhaust); 3. Cylinder 3 (Expansion); 4. Cylinder 4 (Compression); 5. Linear Alternator;

Figure 4.1: Four Stroke Linear Engine Alternator Combination

4.1 ENGINE DESIGN

The engine consists of four cylinders symmetrically arranged, in two pairs of opposite cylinders. The reciprocating device consists of four pistons rigidly connected by an H-shaped connecting rod. The cylinders are equipped with intake and exhaust valves.

The linear alternator attached to the reciprocating assembly is responsible for converting the mechanical energy developed by the engine to electrical energy, which can then be used by

external devices. It should be noted that the mechanical load on the engine (as a function of the displacement of the reciprocating assembly) can be tailored actively or passively to any function of displacement.

For a better understanding of the operation of the four-stroke linear engine, Table 4-1 illustrates the engine cycle phasing.

Table 4-1: Four-Stroke Linear Engine Cycle Description

	CYLINDER 1	CYLINDER 2	CYLINDER 3	CYLINDER 4
Stroke 1 →	Combustion + Expansion	Compression + Combustion	Intake	Exhaust
Stroke 2 ←	Exhaust	Combustion + Expansion	Compression + Combustion	Intake
Stroke 3 →	Intake	Exhaust	Combustion + Expansion	Compression + Combustion
Stroke 4 ←	Compression + Combustion	Intake	Exhaust	Combustion + Expansion

4.1.1 INTAKE AND EXHAUST SYSTEM

The four-stroke arrangement requires intake and exhaust valves for the gas exchange processes. Since there is no rotational motion and therefore no camshaft, the engine design requires a different solution for the valves operation. The solution adopted for this engine is that the cylinders employ intake and exhaust electromagnetic valves to ensure the gas

exchange process, and the valves being operated by the engine control unit (ECU). In Table 4-2 it is presented the valve timing for the FSLE.

Table 4-2: Valve Timing for FSLE

	CYLINDER 1		CYLINDER 2		CYLINDER 3		CYLINDER 4	
	INT.	EXH.	INT.	EXH.	INT.	EXH.	INT.	EXH.
STROKE 1	C	C	C	C	O	C	C	O
STROKE 2	C	O	C	C	C	C	O	C
STROKE 3	O	C	C	O	C	C	C	C
STROKE 4	C	C	O	C	C	O	C	C

O: Open
C: Closed

4.1.2 ENGINE CONTROL UNIT

Due to the fact that the linear engine displays unconstrained piston motion, it is necessary to measure the piston displacement as a function of time throughout the stroke. The instantaneous piston velocity and acceleration can be obtained from successive derivatives of displacement with respect to time. To control the engine power output, the fuel quantity and injection timing need to be controlled by the engine control unit (ECU) which is also designed to control intake and exhaust valve operation (and hence EGR rate), engine starting and electrical load shaping.

In order to control the engine on a cycle by cycle basis, the ECU requires a response time of 10 ms or less, modest by modern microprocessor standards.

4.1.3 INJECTION SYSTEM

In order to satisfy the operational requirements of the proposed engine, the injection system chosen consists of two subsystems that work independently. The first subsystem, which is a high-pressure fuel system, is used only when the engine operates as a compression ignition engine for starting and partial load operation, and the second subsystem only for the HCCI operation mode during full load regime. The lack of any rotational output from the engine obviates the use of a mechanically driven injection system; therefore the high-pressure pump used will be electrically driven.

The high-pressure fuel injection system for this project is of the "common rail" type. This type of fuel system is characterized by the use of a single pressurized rail that supplies fuel to all the injectors. These injectors are electronically operated by the engine control unit.

The high-pressure fuel system consists of:

- high pressure gear pump, able to deliver the fuel at pressures around 20 MPa,
- rail pressure control valve,
- electronically controlled injectors, type Bosch CRI1

For the HCCI operation mode the fuel injection occurs in the intake manifold and it does not require high injection pressures. Therefore the fuel is delivered by the low-pressure fuel system through an electronic port fuel injector installed in the intake of the engine. This system is similar to the injection systems used for a spark-ignition engine and does not complicate the engine design.

The low-pressure fuel system consists of:

- low-pressure fuel pump

- pressure regulator

- electronically controlled injectors (low-pressure)

4.1.4 COOLING SYSTEM

The engine is water-cooled in order to avoid the high temperature gradients developed during the combustion process. This solution was chosen because it represents the most convenient one, water being the most convenient heat sink. The cooling water is required for the cylinder jacket and the cylinder heads to control the temperature. The cooling water can be delivered from a cooling tower, for the case of stationary applications, or from a radiator for mobile applications.

4.1.5 LUBRICATION

The frictional forces are much lower than those in the crankshaft IC engines, and the only frictional aspect that needs to be considered appears between the piston ring(s), the skirts and the cylinder. Therefore the lubrication requirements will be minimal since there are no large-scale hydrodynamic bearings.

4.1.6 STARTING

Previous designs for free-piston engines have proposed using the linear alternator as a starting device. For this operating regime the linear alternator is used to motor the engine. However, at these low values of the speed there is insufficient in-cylinder pressure to generate the spontaneous ignition, and therefore the cylinders will be equipped with glow plugs. The power required to motor the engine, and for all the auxiliaries involved in this operation may be supplied by an external source, such as an auxiliary battery, to be charged

by the linear alternator during normal operation.

CHAPTER 5 ENGINE COMBUSTION MODELING REVIEW

The objective of this chapter is to make a short general introduction to engine modeling and to review a couple of relevant mathematical models for this dissertation. The internal combustion engine modeling field represents a very vast area, therefore it is very complicate to elaborate a comprehensive literature review. Books such as Heywood [21] and Ramos [29], were an important guide for this modeling work, even though they offered just a hint of what is available in the literature. The engine models can be classified can be classified into two main groups as, thermodynamic or zero-dimensional models and dimensional models. The thermodynamic models are often referred as zero-dimensional models because they do not have spatial resolution in describing a particular thermodynamic evolution. The first category, the thermodynamic models can be also classified into two subgroups, based on the way the cylinder charge is approached, as single-zone models or multi-zone models. In single-zone models the temperature the pressure and the composition of the cylinder charge are assumed to be uniform throughout the combustion chamber. These single-zone models represent a very useful tool in engine modeling, they can be used in analysis of the heat release rate from pressure-volume diagrams, where the heat release rate is accepted as being a measure of the rate at which the fuel's energy is added to the cylinder charge. Single-zone models can also be used as predictive tools if the heat release rate is specified. These models yield a system of ordinary differential equations for the pressure, temperature and the mass of the cylinder mixture.

In comparison to the single zone models where the cylinder mixture is considered homogeneous, in the multi-zone models the cylinder mixture is divided into burning and

nonburning zones, each zone being treated as separate thermodynamic system. These models they account for air entrainment and fuel jet penetration. In the multi-zone models the burnt zone corresponds to the injected fuel, and the unburnt zone corresponds to the surrounding air. The fuel jet penetration and the air entrainment process are in most cases based on empirical relations. Two-zone models attribute the burnt zone to the injected fuel assuming that the injected fuel represents a uniform gaseous medium [41,42], processes such as atomisation, evaporation of the fuel droplets are completely neglected, therefore the accuracy of two-zone models is limited. More complex multi-zone models [43-46], which consider more than two zones, account for the fuel jet characteristics by dividing the fuel spray injected into the cylinder into parcels which are analysed separately. Although multi-zone combustion models vary in complexity the main strategy is to model the fuel jet into various elements (zones), which entrain air and ignite as the mixture is prepared for combustion. In this type of models simplified quasi-steady equations are used to describe various processes of fuel injection, atomisation, droplet formation, air entrainment, droplet evaporation, ignition, heat release, and heat transfer. Despite they present a certain degree of empiricism, multi-zone models are powerful tools in predicting with accuracy the exhaust emissions. More complex than the zero-dimensional models, the multidimensional models of diesel engine combustion account for engine geometry and the spatial and temporal variation of the flow field, temperature, composition, pressure, and turbulence within the combustion chamber. The multidimensional models are based on computational fluid dynamics (CFD) computations. In these models the governing equations that describe the flow field are solved numerically with different numerical schemes. The KIVA code, for example, has the ability

to calculate three-dimensional flows in engine cylinders with arbitrary shaped piston geometries, including the effects of turbulence, sprays and wall heat transfer. These particular models based on are very expensive since they require high computational resources.

The last category of models used in the modeling of the combustion process is represented by the models that are based on the chemical equations governing the combustion process. In these models, the combustion process is considered the result of a series of chemical reactions, called reaction mechanism, through which the cylinder charge is transformed into products of combustion. In the chemical process of combustion the fuel is broken down and the constituent atoms combine in different ratios and at certain rates. However, since there are millions of atoms that undergo billions of combinations, it is practically impossible to predict with accuracy what occurs. Chemical kinetics models can be classified based on the type of kinetic mechanism employed as detailed or reduced. The detailed chemical kinetics models include a large number of possible chemical reactions that characterises the combustion process. A chemical equation for the combustion of a hydrocarbon fuel $C_a H_b$ has the following form:

$$C_a H_b + \alpha(O_2 + 3.773N_2) \rightarrow \beta CO_2 + \delta H_2O + \varepsilon N_2 + \gamma CO + \\ + \eta NO + \kappa OH + \mu H + \nu C_x H_y + ... \tag{5.1}$$

The fuel oxidation represents a complex process, it occurs in many steps called base reactions. The simplest base reaction can be written as follows:

$$\alpha A + \beta B \leftrightarrow \delta C + \gamma D \tag{5.2}$$

where A, B ,C, and D represent the chemical species of the reaction, and $\alpha, \beta, \delta,$ and γ are the corresponding stoichiometric coefficients.

According to the law of mass, the rate at which product species are produced and the rate at which reactant species are removed is proportional to the product of the concentrations of reactant species, with the concentration of each species raised to the power of its stoichiometric coefficient.

$$R^{+} = -\frac{d[A]^{+}}{dt} = \frac{d[C]^{+}}{dt} = k^{+}[A]^{\alpha}[B]^{\beta} \tag{5.3.a}$$

$$R^{-} = -\frac{d[C]^{-}}{dt} = \frac{d[A]^{-}}{dt} = k^{-}[C]^{\delta}[D]^{\gamma} \tag{5.3.b}$$

where R^{+} and R^{-} represent the forward and backward rate respectively, and k^{-} and k^{+} represent the proportionality constants for forward and backward rate respectively. More generally, any reaction can be written as

$$\sum_{i=1}^{n} \nu_i M_{R_i} \leftrightarrow \sum_{i=1}^{m} \nu_i M_{P_i} \tag{5.4}$$

where: ν_{R_i} and ν_{P_i} represent the stoichiometric coefficients of the species M_i, and

subscripts R and P denote reactants and products respectively.

The rate of reaction for a chemical reaction when the process undergoes forward can be written as

$$R^{+} = -k^{+}\prod_{i=1}^{n}[M_{R_i}]^{\nu_{R_i}} \tag{5.5.a}$$

Similarly the backward rate for a chemical reaction can be expressed as

$$R^{-} = -k^{-}\prod_{i=1}^{m}[M_{P_i}]^{\nu_{P_i}} \tag{5.5.b}$$

The brackets indicate the appropriate concentration quantity such as molarity or partial

pressure. The proportionality constant also called the specific reaction-rate constant, is independent of the concentration and it depends only on the temperature. The specific reaction-rate constant is given by the Arrhenius law:

$$k = A\exp\left(-\frac{E_A}{\widetilde{R}T}\right)$$

where A is Arrhenius constant,

E_A is the activation energy,

$\widetilde{R}$ is the universal gas constant, and

T is the absolute temperature

The Arrhenius constant also called the collision frequency factor accounts for the effect of collision terms, $A = BT^{\alpha}$. The exponential term is the Boltzmann factor, specifying the fraction of collisions that have an energy greater than the activation energy E_A.

The net rate of removal of reactant species M_{R_i} is

$$-\frac{d[M_{R_i}]}{dt} = \nu_{R_i}\left(R^{+} - R^{-}\right) \tag{5.6.a}$$

and the net rate of production of product species M_{P_i} is

$$\frac{d[M_{P_i}]}{dt} = \nu_{P_i}\left(R^{+} - R^{-}\right) \tag{5.6.b}$$

When chemical equilibrium is reached, the forward and the backward reaction rates are equal, it then follows

$$K_c = \frac{k^{+}}{k^{-}} = \frac{[C]^{\delta}[D]^{\gamma}}{[A]^{\alpha}[B]^{\beta}} \tag{5.7}$$

where K_c is the equilibrium constant.

In order to evaluate the rate of combustion it is necessary to determine the rate of each individual reaction that characterises a particular chemical kinetic mechanism. Complete detailed reaction schemes are only available for the simpler hydrocarbon fuels such as methane, propane or butane. For the blended hydrocarbon fuels the detailed chemical mechanisms are not completely known and therefore the use of reduced chemical kinetics scheme is usually adopted. However, these models are very complex due to the large number of chemical reactions involved, and also expensive, since they require a large amount of computational resources [47]. More often used due to their relative simplicity are the reduced or simplified chemical kinetics models, or global kinetics. In these models the combustion process is considered to be governed by a series of chemical reactions, which consists of a reduced number of chemical reactions. Although they do not represent very accurate the oxidation process of a hydrocarbon, the reduced chemical kinetics schemes of varying degrees of details require much less computational resources and they represent a useful tool for the engineering purposes. A reduced scheme or a quasi-global reaction scheme for lean combustion of propane or of a hydrocarbon C_nH_{2n+2} is presented as follows:

$$C_nH_{2n+2} \rightarrow \left(\frac{n}{2}\right)C_2H_4 + H_2 \tag{5.8.a}$$

$$C_2H_2 + O_2 \rightarrow 2CO + 2H_2 \tag{5.8.b}$$

$$CO + \frac{1}{2}O_2 \rightarrow CO_2 \tag{5.8.c}$$

$$H_2 + \frac{1}{2}O_2 \rightarrow CO_2 \tag{5.8.d}$$

And the corresponding reaction rates expressed in $\frac{gmol}{cm^3 s}$ are:

$$\frac{d[C_nH_{2n+2}]}{dt} = -10^{17.32} \exp\left(-\frac{49{,}600}{\widetilde{R}T}\right)[C_nH_{2n+2}]^{0.5}[O_2]^{1.07}[C_2H_4]^{0.40} \tag{5.9}$$

$$\frac{d[C_2H_4]}{dt} = -10^{14.7} \exp\left(-\frac{50{,}000}{\widetilde{R}T}\right)[C_2H_4]^{0.9}[O_2]^{1.18}[C_nH_{2n+2}]^{-0.37}$$

$$\frac{d[CO]}{dt} = -10^{14.6} \exp\left(-\frac{40{,}000}{\widetilde{R}T}\right)[CO]^{1.0}[O_2]^{0.25}[H_2O]^{0.5} + 5\cdot 10^{8} \exp\left(-\frac{40{,}000}{\widetilde{R}T}\right)[CO_2]$$

$$\frac{d[H_2]}{dt} = -10^{13.52} \exp\left(-\frac{41{,}000}{\widetilde{R}T}\right)[H_2]^{0.85}[O_2]^{1.42}[C_2H_4]^{-0.56}$$

In these equations the concentations are expressed in gmol/cm^3, the temperature in Kelvin, the activation energies in calories, and the universal gas constant in cm^3 atm/(gmol K). Westbrook and Dryer [51] present the global rates equations for each of these reactions above presented. This reduced chemical kinetics scheme may also be complicated to some extent and for practical use it is preferred the use a two-step or a single-step global reaction. In single step global reactions the hydrocarbon oxidation is considered to obey the following reaction:

$$C_nH_m + \alpha O_2 \rightarrow \beta CO_2 + \gamma H_2O \tag{5.10}$$

where α,β, and γ are stoichiometric coefficients and the corresponding global rate equation is:

$$\frac{d[C_nH_{2n+2}]}{dt} = -A\cdot \exp\left(-\frac{E_A}{\widetilde{R}T}\right)[C_nH_{2n+2}]^{a}[O_2]^{b} \tag{5.11}$$

In Figure 5.1 it is represented the calculated history of reaction is represented using a single-step global reaction for $C_{10}H_{22}$ at 1500 K and 1 atm.

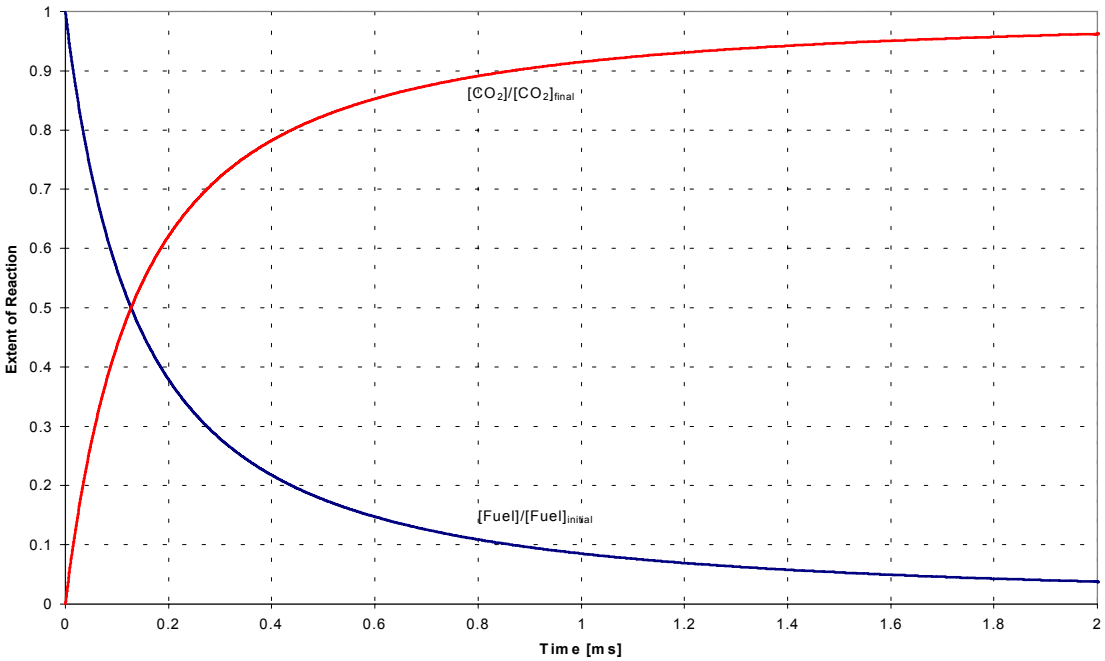

Figure 5.1: Calculated History of Reaction for Stoichiometric $C_{10}H_{22}$-*Air* at 1500K and 1atm., using a Single-Step Global Reaction.

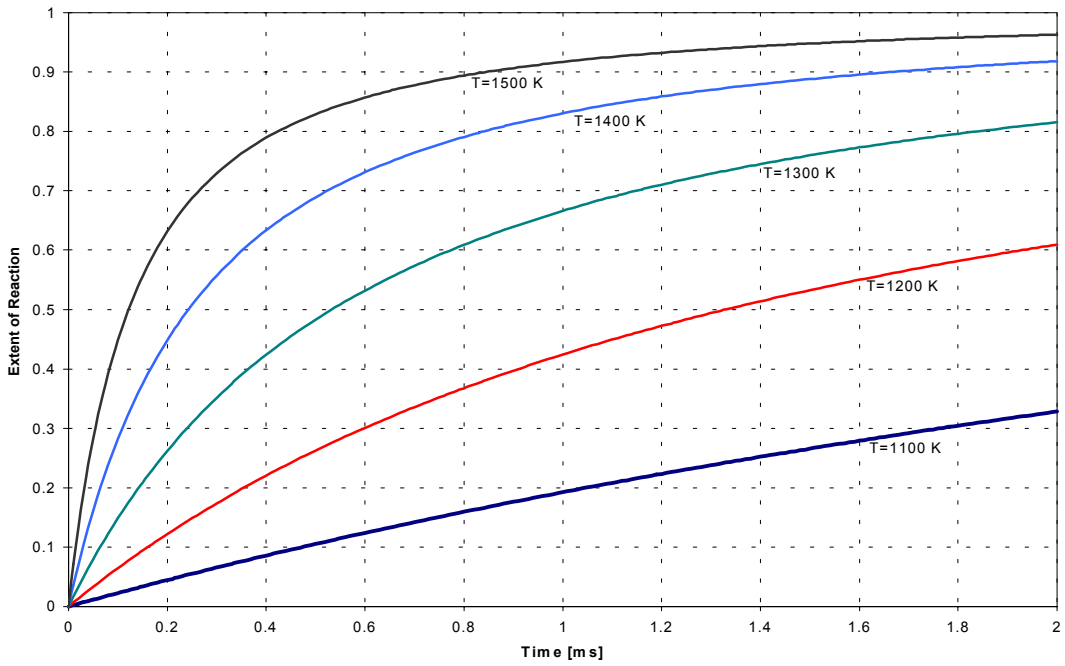

Figure 5.2: Rate of Reaction Variation with Temperature for Stoichiometric $C_{10}H_{22}$-*Air* at 1 atm., using a Single-Step Global Reaction.

The rate of reaction depends on pressure and temperature and the temperature dependence is presented in Figure 5.2 In Section 5.1 and Section 5.2 several relevant mathematical models for compression ignition and HCCI engines respectively, will be reviewed.

5.1 DIRECT INJECTION COMPRESSION IGNITION ENGINE MODELS

Before reviewing some of the mathematical models of combustion in compression ignition engine a very brief review of the fundamental features of the combustion process for this engines will be synthesised as follows. The combustion process in compression ignition engines is characterised by the fact that has distinct stages, a period of ignition delay, a period ignition and rapid pressure rise called premixed combustion, a period of continuous combustion and gradual pressure change called diffusive combustion and a period of post flame reactions.

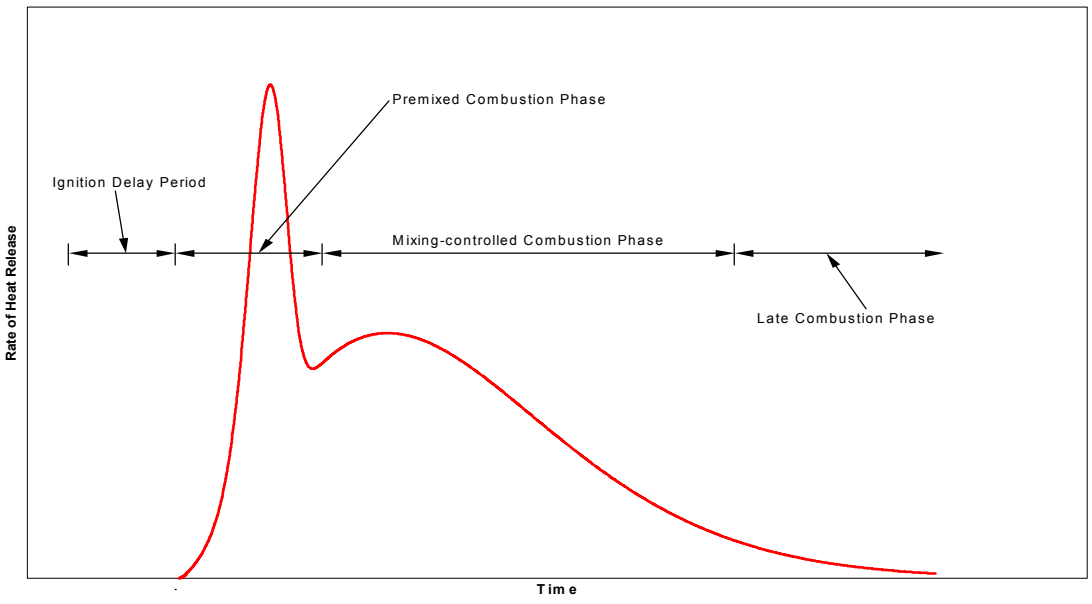

Figure 5.3: Typical Combustion Stages in a Compression Ignition Engine

Unlike the homogeneous charge engines, where the cylinder charge is prepared before its induction into the cylinder, in compression ignition engines the fuel is injected during compression into the high pressure and high temperature cylinder charge which is composed usually of air and a small amount of residual gases from the previous cycle, unless the EGR presence is not mentioned. The time-period from the start of fuel injection to the beginning of combustion is known as the ignition delay. During this particular time-period, the already injected fuel undergoes a series of physical and chemical processes, such as atomisation, vaporization and mixing in the hot, compressed cylinder charge and a chemical kinetics stage during which fuel pyrolysis begins. Therefore the ignition delay can be considered as having a physical component and a chemical component. The physical component accounts for the atomization of the liquid fuel jet, the vaporization of the fuel droplets, and the mixing of fuel vapor with air. The chemical component of the ignition delay accounts for the mechanism of chemical processes involved in the autoignition. The chemical processes depend on the fuel characteristics and composition, the cylinder charge pressure and temperature, as well as on the physical processes enumerated above which govern the distribution of fuel throughout the air charge. Although the ignition delay has been the subject of many studies, it cannot be predicted accurately and this due to its complex dependency on the large numbers of parameters involved. In different models, there are different mathematical correlations used for the ignition delay expression, most of them based on empiric relations. Hardenberg and Hase [35], developed an empirical formula for predicting the duration of the ignition delay in direct injection engines. The expression developed has shown good results for direct injection IC engines and is a function of cylinder pressure, temperature, mean speed, and also

a function of fuel characteristics.

$$\tau_{id} = \frac{0.36 + 0.22\overline{S}_p}{0.006 \cdot N} \exp\left[E_A \cdot \left(\frac{1}{\widetilde{R}T} - \frac{1}{17{,}190} \right) \left(\frac{21.2}{p - 12.4} \right)^{0.63} \right] \tag{5.12}$$

where τ_{id} is the ignition delay in $\text{sec} \times 10^{-3}$

$\overline{S}_p$ is the mean piston speed in m/s,

N is the engine speed in rev/min,

E_A is the apparent activation energy in J/mole,

T is the cylinder charge temperature in Kelvin, and

p is the cylinder pressure in 10^5 Pa .

The apparent activation energy is given by

$$E_A = \frac{618{,}840}{\text{CN} + 25}$$

where CN represents the fuel Cetane Number.

Other empirical correlations often used in the evaluation of the ignition delay, were derived based on the studies of autoingnition process in rapid compression machine, or in constant volume bombs, or in steady-flow reactors and, and they have the form of the Arrhenius equation.

$$\tau_{id} = A \cdot p^{-n} \exp\left(\frac{E_A}{\widetilde{R}T} \right) \tag{5.13}$$

where A and n depend on the fuel.

To account for effect of continuous changing conditions affecting the ignition delay, accounted by the physical parameters from Equation 5.2, the following empirical integral

relation is used:

$$\int_{t_{si}}^{t_{si}+ID} \left(\frac{1}{\tau_{id}} \right) dt = 1 \tag{5.14}$$

where t_{si} represent the time at which the injection starts,

ID is the ignition delay period, and

τ_{id} represents the ignition delay calculated for the corresponding conditions at time t.

Once the ignition delay period is over the combustion process in this stage is characterised by a high rate of heat release. During the ignition delay period, the fuel injection continues and, part of the previous injected fuel has mixed with air and has formed some regions of combustible mixture. The regions that have reached the combustion requirements burn fast, and therefore the cylinder pressure and temperature increase aiding the injected liquid fuel to vaporise. As mentioned before, this stage is associated with high heat release rates and, the duration of this stage of combustion is dictated to a certain extent by the injection strategy adopted.

Diffusive Combustion

The third stage of combustion, also called the diffusive combustion due to its character, represents the phase of the combustion process in which the process itself is controlled by the rate at which the combustible mixture becomes available. The fuel vapor-air mixing process controls this phase of the combustion process. Compared to the premixed combustion, in which the fuel encounters rapid oxidation and thus a rapid pressure rise, the diffusive combustion stage has a steady aspect with regards to the pressure variation and the heat release rate.

Having the combustion process in compression ignition engines features summarized in the previous review, in the following

Single zone models yield a system of ordinary differential equations for the mixture pressure, temperature and mass. These models do not account for the presence of vaporizing liquid droplets, fluid flow, combustion chamber geometry, and spatial variations of the mixture composition and temperature. In single-zone models the cylinder charge is assumed to be a homogeneous mixture of ideal gases. Considering the cylinder an open system, the state of the mixture can be described at every instant by the pressure p, temperature T, and equivalence ratio ϕ. In these models the rate of combustion is prescribed by specifying the mass fraction burnt. The fraction of heat release or the mass fraction burned, is most commonly expressed by using the Wiebe function, Ramos [29] presents a extensive analysis for the Wiebe function. The Wiebe function represents an empirical correlation an has the following form:

$$\chi(t) = \frac{m_b}{m_{inj}} = 1 - \exp\left[- a \left(\frac{t - t_0}{Cd} \right)^{b+1} \right] \tag{5.15}$$

where χ is the mass fraction burned,

m_b is the mass burned,

m_{inj} is the mass injected,

a and b are shape factors,

t_0 is the time at which the combustion process starts, and

Cd is the combustion duration.

The use of two Wiebe functions for the heat release is often met in phenomenological models for CI engines [37-40], one function being assigned to the premixed combustion process, and the other to the diffusive combustion process. The heat release rate equation was expressed as indicated in Equation 5.16:

$$\frac{dQ}{d\theta} = a\frac{Q_p}{\theta_p}\left(M_p + 1\right)\left(\frac{\theta}{\theta_p}\right)^{M_p} \exp\left[-a\left(\frac{\theta}{\theta_p}\right)^{M_p+1}\right] + a\frac{Q_d}{\theta_d}\left(M_d + 1\right)\left(\frac{\theta}{\theta_d}\right)^{M_d} \exp\left[-a\left(\frac{\theta}{\theta_d}\right)^{M_d+1}\right] \tag{5.16}$$

In the multi-zone models the cylinder mixture is divided into burning and nonburning zones, each zone being treated as separate thermodynamic system. These models they account for air entrainment and fuel jet penetration. In the multi-zone models the burnt zone corresponds to the injected fuel, and the unburnt zone corresponds to the surrounding air. The fuel jet penetration and the air entraining process are in most cases based on empirical relations. Two-zone models attribute the burnt zone to the injected fuel assuming that the injected fuel represents a uniform gaseous medium [41,44], processes such as atomisation, evaporation of the fuel droplets are completely neglected, therefore the accuracy of two-zone models is limited. In their work Kamimoto et al. [42] present a two-zone model in which the combustion chamber was divided into two zones. First zone was considered as being formed by two sub-regions, a mixture of unburned fuel and unburned air at temperature T_u and a region of burned gas at temperature T_b. Zone two was considered as being formed by only air at temperature T_2, the pressure was assumed to be uniform throughout the combustion

chamber. Sastry and Chandra [44] developed a three-zone model for direct injection engines. In this model the three zones considered were fuel, unburnt, and burnt gases. In order to simplify the model, the authors considered the fuel enters the combustion chamber in a gaseous form. The unburnt zone is the gas mixture in which the fuel is injected is assumed to consist of fresh air inducted during the intake stroke and residual gases from the previous cycle. Once the combustion begins, the burnt zone comes into existence separating the fuel and unburnt gases are assumed to enter the burnt zone in such a manner that the fuel and oxygen bear a stoichiometric proportion, react spontaneously and completely resulting CO_2 and H_2O. Some complex multizone models account for the droplet vaporisation by dividing the fuel jet into droplets groups, and they use experimental correlations for entrainment and spray penetration.

More complex than the phenomenological models, multidimensional engine models account for the engine geometry and the temporal and spatial variation of the flow field. These models do not account for the liquid fuel break up. However, these models are more accurate but they require more computational resources.

5.2 HCCI ENGINE COMBUSTION MODELS

Different aspects of the HCCI combustion process for different fuels were presented in Section 3.4, and for convenience they will be reiterated in this section especially those encountered in HCCI combustion of diesel fuel. In HCCI engines the fuel is injected outside the cylinder into the intake air. The already prepared fresh mixture is inducted into the cylinder and compressed up to the point when autoignition appears, when the cylinder charge starts burning rapidly. The ignition of the cylinder charge occurs simultaneously throughout the mixture due to the presence of numerous hot ignition spots, resulting in a homogeneous combustion throughout the body of the mixture, thus permitting a homogeneous combustion temperature. Investigations of the HCCI combustion process have revealed the absence of flame propagation, a fact that considerably reduces the conditions for NO_x emissions even though HCCI operates with lean mixtures. It was observed that combustion process during the HCCI operation was well behaved over a relatively reduced range of load regimes. However, two limits were encountered, misfire and detonation, and both are to be avoided. The high rates of energy release encountered during the experiments could be harmful for the engine operation, and therefore the requirement of different techniques for the control of combustion process. In the literature the HCCI combustion process has been controlled by means of a combination of EGR, compression ratio, and variable intake temperature.

The literature is relatively sparse in models for HCCI engines, and that is because the HCCI concept is relatively new. Nevertheless there are some remarkable models in this particular area of interest. Najt and Foster [48] investigated the HCCI combustion process on a four-stroke CFR engine, and used a semi-empirical model to represent the autoignition, and an

empirical energy release equation to evaluate the HCCI combustion process. The authors considered that the HCCI combustion process was purely a chemical kinetic process. However, the HCCI combustion process was divided into two stages, the first stage was that of low temperature chemical kinetics (below 950 K) leading to autoignition, and the second was that of high temperature chemical kinetics (above 1000 K) associated with the energy release. The ignition process was modelled by using a semi-empirical model. The high temperature chemical kinetics are characterised by fuel radical thermal decomposition.

$$C_nH_{2n+2} + \left(\frac{3n+1}{2}\right)O_2 \rightarrow nCO_2 + (n+1)H_2O + heat \tag{5.17}$$

It was considered that the high temperature oxidation of a paraffinic fuel obeys the following chemical kinetics scheme

$$fuel + O_2 \rightarrow alkene + H_2O$$

$$alkene + O_2 \rightarrow CO + H_2O$$

$$CO + O_2 \rightarrow CO_2$$

The CO_2 formation considered to release most of the combustion energy, has the following chemical reaction scheme.

$$CO + OH \leftrightarrow CO_2 + H$$

In the early combustion process, fuel and radicals compete with CO for the OH radicals.

$$F + OH \leftrightarrow F + H_2O$$

Assuming that the energy release is controlled by the CO oxidation, the expression for the energy release was based on an empirical equation formulated by Dryer and Glassman [51, 52] for the rate of reaction of CO_2

$$\frac{d[CO_2]}{dt} = 10^{14.6} \exp\frac{(-40000)}{RT}[CO]^1[O_2]^{0.25}[H_2O]^{0.50} \quad (5.18)$$

Reitz et al. [53] modelled the combustion process in a four-stroke HCCI engine using a modified KIVA-II code. In their complex multidimensional model, the authors included numerous effects such as turbulence, crevice flow, and wall heat transfer. In their detailed study, the authors performed a sensitivity analysis evaluating the effects of the turbulence mixing characteristics, initial temperature, turbulence parameters, and swirl ratio. Their studies presented a different point view about HCCI combustion mechanisms than the one adopted by Najt and Foster [48], who considered the HCCI combustion to be purely a chemical kinetic controlled process. The results indicated that although there are no flame propagation phenomena, the high pressures and temperatures can extend the flammability and sustain flamelets within the turbulent eddies. The combustion mechanism was described as during the early stages of combustion the development of flame kernels is controlled by the laminar ignition chemistry. It was also concluded that the turbulence phenomena has a dominant role in HCCI combustion. In the sensitivity study it was shown that initial charge temperature influences the autoignition process. Also the autoignition is affected by the turbulence diffusivity and by the swirl ratio through affecting the wall heat flux, by increasing these parameters the autoignition is delayed because of the enhanced wall heat flux. The HCCI combustion process was considered as being related to the premixed burned of diesel combustion.

The key for the combustion modeling of the HCCI is represented by the evaluation of the conditions for the autoignition process. This is probably the most delicate problem of the HCCI combustion modeling, since the heat release can be easily approached by means of an

empirical mass burned function. In their efforts to model the HCCI combustion process, Ryan et al. [24,25], used an empirical expression for the "ignition delay", based on experimental studies conducted on combustion bomb testing [54]. The ignition delay was considered to be the time period from the closing of the intake valve to the moment of autoignition of the fuel. The developed expression for the ignition delay is a function of oxygen concentration, fuel concentration, and of air density and temperature at the start of injection.

$$\tau_d = 0.00221[O_2]^{-0.053}[Fuel]^{-0.05}\rho^{0.13}\exp\left(\frac{5914}{T}\right) \tag{5.19}$$

where τ_d is the ignition delay in milliseconds

The autoignition occurs when

$$\frac{X}{X_c} = \int_0^{\tau_c} \frac{1}{\tau_d} dt = 1 \tag{5.20}$$

where $\frac{X}{X_c}$ is the fraction of pre-reactions completed at time t.

The correlation for the ignition delay previously mentioned, was integrated in a computer model able to simulate the HCCI operation. Goldsborough [56] modeled the HCCI combustion applied to a free piston linear engine- alternator combination, by means of a detailed chemical kinetics model using the CHEMKIN [57] libraries package. The modeling task was simplified by the fact that the fuel used was Hydrogen where the chemical reactions that characterize the combustion process are very well known. In their efforts to model the HCCI combustion of natural gas, Fiveland and Assanis [58] developed a single-zone simulation model. The combustion model was incorporated into a cycle simulation code

originally developed for direct injection diesel engines. The simulation couples models for mass, species, and energy in a zero-dimensional framework. The autoignition and combustion processes in their engine cycle simulation, were represented by using CHEMKIN libraries. Recently, there were issued different HCCI models and, most of them, were developed used detailed chemical kinetics libraries offered by CHEMKIN.

Taking into consideration the peculiarities of the HCCI combustion process, a direct way to model the HCCI combustion is to use the chemical kinetics approach. Although Reitz et al. [53] recommended the computations for the HCCI combustion be made by using detailed chemical kinetics mechanism in order to assess the influence of the chemistry, the proposed model for this dissertation will be one based on a highly simplified chemical kinetics scheme.

CHAPTER 6 COMPUTATIONAL MODEL DERIVATION

6.1 DYNAMIC ANALYSIS OF THE FOUR-STROKE LINEAR ENGINE

Consider the case of a FSLE with four reciprocating pistons linked by a solid shaft that oscillates back and forth in a left-to-right motion. The reciprocating mass represented by the pistons, piston rings, connecting rod, and the magnets the subject of the following forces, the pressure force from each cylinder, the mechanical load imposed by the linear alternator, and the frictional force.

The equation that describes the motion of the system derives from Newton's second law.

$$m\frac{d^2x}{dt^2} = \sum_i F_{i_x} \tag{6.1}$$

The right hand side of Equation 6.1 represents the summation of the forces that act in the plane of motion. The only forces are considered to act on the moving assembly are the resultant pressure forces given by the difference between the pressures in the four cylinders, a frictional force, and the load. The load represents the electromagnetic force introduced by the linear alternator coupled to the linear engine.

Thus, the Equation 6.1 can be written as

$$m\frac{d^2x}{dt^2} = F_p - F_f - F_l \tag{6.2}$$

where F_p represents the resultant pressure force,

F_f is the resultant friction force, and

F_l is the electromagnetic force representing the load introduced by the linear alternator.

The integration of this differential equation will permit us to determine the equation of motion for the linear engine. The analytic integration is very difficult due to the complex variation of the three forces in space and time. The piston assembly does not follow a prescribed motion but rather its resultant motion is established as a result of the net balance in the in the applied forces. Thus, the numerical integration is imposed.

6.1.1 FRICTION FORCE EVALUATION

Although the linear engine is crankless, the frictional force cannot be neglected. The friction in this case is attributed to the piston assembly only. There have been done a lot of studies with regards to the friction in the internal combustion engines, and according to these, the piston assembly friction represents the major source of engine mechanical friction. Elements of the piston assembly that contribute to friction are the piston rings and the piston skirt. There is also friction in the wrist pin that should be noted even though is small in comparison to the other friction forces previous mentioned. Rosenberg [30], describes the frictional causes for internal combustion engines and presents a couple of design solutions towards diminishing the effects of the frictional phenomena. The author shows that the friction coefficient varies between 0.2 for boundary lubricated engine components to 0.001 for hydrodynamically lubricated engine components. According the lubrication theory there are three lubrication regimes, and these are known as boundary, hydrodynamic, and mixed lubrication. In the boundary lubrication regime the friction is proportional to the normal load applied and this is referred as the Coulomb friction.

$$F_f = c_f \cdot N$$

where c_f is the coefficient of friction, and

N is the normal load.

Although the lubricant is present between the two surfaces, the coefficient of friction is independent of the bulk lubricant viscosity, the sliding speed and the unit load. The hydrodynamic regime occurs when the two surfaces in relative motion in the presence of a lubricant between the two surfaces, have no physical contact. The resistance to motion results from the shear forces within the film.

The shear stress τ, developed in a liquid film between two surfaces in relative motion is given by

$$\tau = \mu \frac{dU}{dy} \tag{6.3}$$

where μ is the fluid dynamic viscosity, and

$\frac{dU}{dy}$ is the velocity gradient across the film.

The friction in the hydrodynamic regime depends on geometry, speed and lubricant viscosity, and the fiction force has the form

$$F_f = \frac{\mu A U}{\delta} \tag{6.4}$$

where μ is the fluid viscosity,

A is the area,

U is the relative velocity, and

δ is the film thickness.

The mixed lubrication regime occurs when the film thickness becomes so thin that asperities touch. This way the two surfaces in relative motion have a physical contact, therefore to

viscous friction is added to the solid friction effect. As it was mentioned before, the piston assembly represents the only friction source for case of the Linear Engine. Elements of the piston assembly, which contribute to the friction, are the piston rings the piston skirt and the wrist pin. The analyses developed on the piston assembly friction showed that the ring friction has a dominant role in the overall frictional aspects (more than 50%).

Based on the assumption that the piston ring operates in hydrodynamic regime, the frictional effects can be evaluated from the Reynolds equation:

$$\frac{\partial}{\partial x}\left(h^3 \frac{\partial p}{\partial x} \right) = 6U\mu \frac{\partial h}{\partial x} + 12\mu \frac{\partial h}{\partial t} \tag{6.5}$$

where h is the instantaneous film thickness.

Equation 6.5, along with the appropriate force balance on the ring, can be solved for the couple film and ring behavior.

The calculation of the friction force for the experimental model is a very complicated process; thus the use of an existing correlation permits a faster evaluation far the friction forces. Blair [31], suggests an empiric expression for the calculation of the friction mean effective pressure. This correlation used for the evaluation of the friction force for the SI model, is a function of engine length and speed.

$$fmep = a + bL_{st}N \tag{6.6}$$

where a and b are constants,

L_{st} is the stroke length in meters

N is the engine speed in cycles/min

The constants a and b have different values based on the type of the engine, size of the

engine, and also based on the type of the bearing. In the case of a rolling element the value of the constant a is zero. In the previous modeling work [19] the calculation of the friction force was based on the same type of correlation. In this dissertation the evaluation of the frictional force due to the presence of represents a simple but effective approach similar to the one used in the numerical modeling of the two-stroke spark-ignition linear engine, using a similar correlation with the one suggested by Blair [31].

Considering the friction force as being constant along the stroke does not alter the computation, this assumption was justified by the fact that in the operation of the TSLE it was observed that the engine operation was not influenced substantially by the variation in shape of the applied load. Another reason for this assumption is that the frictional force magnitude is small in comparison to the one of the load introduced by the linear alternator.

Considering the friction mean effective pressure as given by:

$$fmep = 200 \cdot L_{st} \cdot N \quad [\text{Pa}] \tag{6.7}$$

where L_{st} is the stroke length in meters,

N is the reciprocating frequency in cycles/min.

It follows that the corresponding average friction force can be written as:

$$F_f = \frac{fmep \cdot V_d}{4 \cdot L_{st}} \tag{6.8}$$

6.1.2 LOAD INTRODUCED BY THE LINEAR ALTERNATOR

Another variable needed to solve the Equation 6.1, is the load introduced by the linear alternator F_l. This variable is very important for the evaluation of the engine performances and it depends mainly of the design of the linear alternator. It is quite complicated to make an assumption for the this particular variable since it is a result of engine operation and alternator design From the previous work [20] it was shown that the resistant force introduced by the linear alternator has a shape similar with a sinusoidal function. This observation permitted the assumption that the engine load has a sinusoidal shape. In the numerical simulation of the FSLE, the load introduced by the linear alternator was considered as being a function of piston position only and that can be expressed as a different power of a sinusoidal. In each case considered for expression of the load

$$F_{l_i}(x) = A_i \cdot \sin^i\left(\frac{\pi x}{L}\right) \tag{6.9}$$

where: A_i represents a proportionality constant and it depends on the power "i",

x represents the piston position, and

L is the total maximum stroke.

In the order to obtain the same equivalent constant load, it considered for each analysed case that

$$\int_0^L A_i \cdot \sin^i\left(\frac{\pi x}{L}\right) dx = \text{Constant}$$

6.2 THERMODYNAMIC ANALYSIS OF THE FOUR-STROKE LINEAR ENGINE

In this dissertation the thermodynamic analysis conducted for the FSLE is based on First Law of Thermodynamics. Considering the modeled engine an open thermodynamic system as shown in Figure 6.1 it follows:

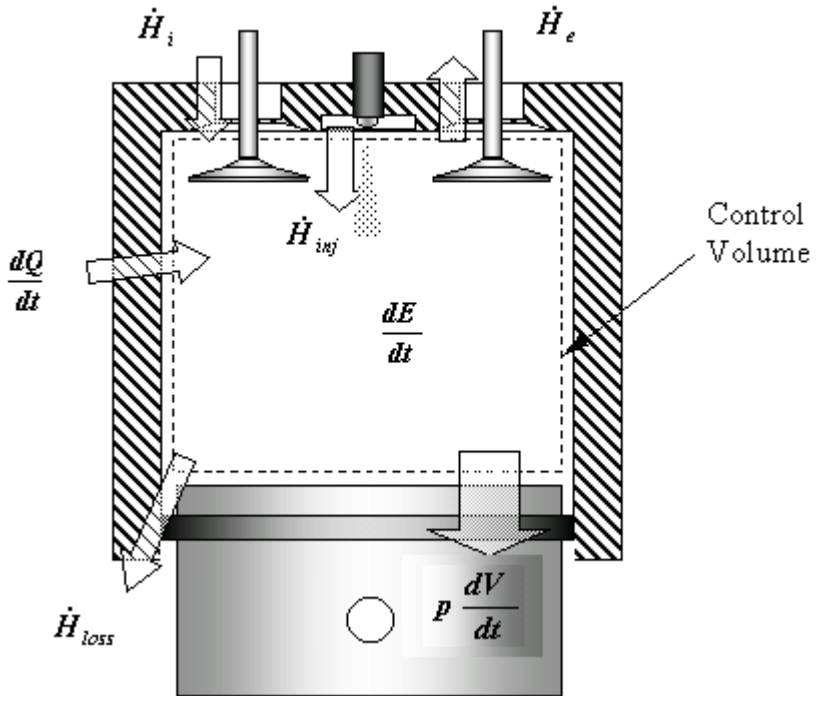

Figure 6.1: First Law of Thermodynamics applied to the cylinder gases.

The analysis assumes that at any instant in time there is a state of thermodynamic equilibrium over the control volume. The cylinder content is treated as being a homogeneous mixture of perfect gases at each instant. In this analysis, phenomena such as mixing, fuel vaporization, are neglected. The equations that describe the thermodynamic state of the cylinder gases are the conservation of mass and the First Law of Thermodynamics as follows:

Conservation of Mass

$$\frac{dm}{dt} = \sum_i \frac{dm_i}{dt} \tag{6.10}$$

where $\sum_i \frac{dm_i}{dt}$ represents the mass flow rates through the intake and exhaust valves, the mass flow rate through the injector and the mass flow rates associated with the crevice flow and leakeage through the piston rings.

Conservation of Energy

$$\frac{dE}{dt} = -p\frac{dV}{dt} + \frac{dQ}{dt} + \sum_i \dot{H}_i \tag{6.11}$$

where $\frac{dE}{dt}$ represents the rate of change of total energy of the control volume,

$p\frac{dV}{dt}$ is the rate of mechanic work done by the system on its boundaries,

$\frac{dQ}{dt}$ is the rate of heat transfer into the control volume through the control volume boundaries

$\sum_i \dot{H}_i$ is the sum of enthalpy fluxes through the intake and exhaust valves and the enthalpy flux associated with the fuel injection.

$$\frac{dE}{dt} = \frac{d(m \cdot u)}{dt} = m\frac{du}{dt} + u\frac{dm}{dt} \tag{6.12}$$

$$H_i = \frac{dm_i}{dt} h_i \tag{6.13}$$

$$m\frac{du}{dt}+u\frac{dm}{dt}=-p\frac{dV}{dt}+\frac{dQ}{dt}+\sum_i\frac{dm_i}{dt}h_i \tag{6.14}$$

For the case of compression, combustion and expansion process neglecting the crevice flow and the leakage, the first law of thermodynamics applied to the cylinder content becomes.

$$m\frac{du}{dt}+u\frac{dm}{dt}=-p\frac{dV}{dt}+\frac{dQ}{dt}+\frac{dm_{fuel}}{dt}h_{fuel} \tag{6.15}$$

where the mass conservation equation is:

$$\frac{dm}{dt}=\frac{dm_{fuel}}{dt}$$

If the enthalpy flux due to the fuel injection is neglected, Equation 6.15 becomes:

$$m\frac{du}{dt}=-p\frac{dV}{dt}+\frac{dQ}{dt} \tag{6.16}$$

Considering that the cylinder content is an ideal gas, then at every instant the ideal gas law is satisfied

$$pV=mRT \tag{6.16}$$

it allows $u=c_vT$, so

$$m\frac{d(c_vT)}{dt}=-p\frac{dV}{dt}+\frac{dQ}{dt} \tag{6.17}$$

Taking the derivative of the ideal gas law and assuming that R is constant it follows that:

$$V\frac{dp}{dt}+p\frac{dV}{dt}=mR\frac{dT}{dt} \tag{6.18}$$

considering $R=c_p-c_v$ and $\gamma=\frac{c_p}{c_v}$ and substituting the Equation 6.18 into Equation 6.17

and it yields:

$$\frac{dQ}{dt} = \frac{V}{\gamma - 1}\frac{dp}{dt} + p\frac{\gamma}{\gamma - 1}\frac{dV}{dt} \tag{6.19}$$

The net heat flux term, $\frac{dQ}{dt}$ is a result of the heat transfer out of the system and the chemical input energy from the fuel combustion process and it can be explicitly written as:

$$\frac{dQ}{dt} = \frac{dQ_{chemical}}{dt} - \frac{dQ_{ht}}{dt} \tag{6.20}$$

Substituting Equation 6.20 into Equation 6.19, then the cylinder pressure variation is given by:

$$\frac{dp}{dt} = -\gamma\frac{p}{V}\frac{dV}{dt} + (\gamma - 1)\frac{1}{V}\left(\frac{dQ_{chemical}}{dt} - \frac{dQ_{ht}}{dt}\right) \tag{6.21}$$

6.3 INDIVIDUAL THERMODYNAMIC PROCESS MODELING

6.3.1 GAS EXCHANGE PROCESS MODELING

The purpose of the exhaust and inlet processes is to remove the burned gases at the end of power stroke and induct the fresh charge for the next cycle. Needless to say that the gas exchange process affects both the performances and the emissions of an internal combustion engine, and therefore it requires a careful approach. The effectiveness of this process is evaluated by the volumetric efficiency, which depends on the flow field in the intake and exhaust manifolds, and especially on valves. The volumetric efficiency is defined as the ratio of the volume flow rate of air into the intake system, to the rate at which volume is displaced by the system. It was mentioned previously that the gas exchange process (scavenging) for the case of TSLE, was critical for the performances of the linear engine, although in the numerical simulation [19] the scavenging process was considered ideal for simplicity reasons. The operation of the proposed FSLE is more complex than that of the TSLE since the FSLE has two operation modes, one as a direct injection CI where the cylinder charge is form in the cylinder, and the other as a HCCI engine where the cylinder charge is formed externally. Basically the gas exchange process modeling comprehends two aspects, one is the modeling of flow in the intake and exhaust manifolds, and the other one is the modeling of the flow around valves. Manifold flow models can be classified in two groups: one-dimensional and multidimensional models. One-dimensional models often used in engine modeling, use the mass, momentum, and energy conservation equations for the unsteady flow, together with the equation of state for the gas. The set nonlinear differential equations can be solved numerically by using different numerical techniques presented in the literature

[21-23]. Benson [34], used the method of characteristics to solve the one-dimensional, unsteady, compressible flow problem in ducts.

Multi-dimensional models permit a better evaluation of the gas exchange process and of the calculation of the flow field around the intake and exhaust valve, but they are more complex, and they require expensive computational devices.

The valves represent the most important flow restriction, in the intake and exhaust system. The instantaneous flow area depends on the valve lift and the geometry of the valve, head, seat, and stem. Similarly to the flow in manifold models, the flow through valve models can be classified as one-dimensional and multi-dimensional models.

The model used in these engine cycle simulations for the calculation of the flow around valves, is a quasi-steady, one-dimensional model. The equations used in these models are derived from the one-dimensional isentropic flow analysis, and real flow effects are accounted for by means of experimentally determined discharge coefficient.

$$\frac{dm}{dt} = C_D A_v p_0 \left(RT_0\right)^{-\frac{1}{2}} \left(\frac{p_R}{p_0}\right)^{\frac{1}{\gamma}} \left\{\frac{2\gamma}{\gamma-1}\left[1-\left(\frac{p_R}{p_0}\right)^{\frac{\gamma-1}{\gamma}}\right]\right\}^{\frac{1}{2}} \tag{6.22}$$

where C_D is the discharge coefficient

For the case when the flow is choked, which represents the case when pressure ratio becomes less than the critical value defined by $\frac{p_R}{p_0} \le \left(\frac{2}{\gamma+1}\right)^{\frac{\gamma}{\gamma-1}}$, the flow rate is given by

$$\frac{dm}{dt} = C_D A_v p_0 \gamma^{\frac{1}{2}} \left(RT_0\right)^{-\frac{1}{2}} \left(\frac{2}{\gamma+1}\right)^{\frac{\gamma+1}{2(\gamma-1)}} \tag{6.23}$$

In order to avoid eventual calculation complications, for this dissertation, the gas exchange process will be calculated by means of one-dimensional model for the flow in intake and exhaust manifold, and by means of a one dimensional quasi-steady model for flow through valves, although considering ideal intake and exhaust processes does not affect very much the engine performances. The proposed gas exchange calculation is considered to be accurate enough for this modeling work.

6.3.2 COMPRESSION AND EXPANSION PROCESS MODELING

The compression process for this model is considered to start when the intake valve closes, and it continues until the start of the fuel injection (for the case when the engine operates as a CI), and until the cylinder pressure rise rate differs from the that of the motoring pressure (for the HCCI case). During this process the cylinder charge receives external mechanical work, increasing its internal energy. The compression process can be mathematically modeled by using the first law of thermodynamics. If we neglect the crevice flow, and after some mathematical manipulations the equation becomes:

$$\frac{dQ}{dt} = \frac{\gamma}{\gamma - 1} p \frac{dV}{dt} + \frac{1}{\gamma - 1} V \frac{dp}{dt} \tag{6.24}$$

The pressure variation during the compression process is given by:

$$\frac{dp}{dt} = -\gamma \frac{1}{V} \frac{dV}{dt} + (\gamma - 1) \frac{1}{V} \frac{dQ_{ht}}{dt} \tag{6.25}$$

If the heat transfer process is neglected the Equation 6.25 reduces to:

$$\gamma p \frac{dV}{dt} + V \frac{dp}{dt} = 0 \tag{6.26}$$

The solution for this differential equation represents the law for an isentropic process.

$$pV^{\gamma} = Const.$$

The expansion process or the power stroke is considered to start at the end of the combustion process, and ends when the exhaust valve opens. The expansion process can be modelled in a similar manner considering the evolution as an isentropic process. In the numerical simulation of a two-stroke linear engine [19], the two evolutions were considered as being polytropic processes, and thus they were mathematically expressed as:

$$pV^{m_{c,d}} = Const.$$

$$TV^{m_{c,d}-1} = Const$$

where m denotes the polytropic coefficient, and

the subscripts c and d denote the compression and expansion process respectively.

6.3.3 COMBUSTION PROCESS MODELING

6.3.3.1 COMBUSTION MODELING FOR DIRECT INJECTION COMPRESSION IGNITION OPERATION

For the direct injection case, there were elaborated two combustion models and both models used were zero-dimensional, single zone models. In these combustion models the energy release was simulated using Wiebe functions. The first approach for the combustion model for FSLE operating in the direct injection, compression ignition mode, used a single Wiebe function for the representation of the heat release. This preliminary model was used to represent the general behavior of the engine. A more accurate approach of the combustion process representation for the FSLE operating in direct injection mode was done using a double Wiebe function. By using a double Wiebe function or two Wiebe functions for the

heat release rate, has permitted to put in evidence the two characteristic stages encountered at the combustion process in compression ignition engines, the premixed combustion and the diffusive combustion, respectively. Figure 6.2 illustrates the heat release rate represented by using two Wiebe functions.

$$\chi_p = 1 - \exp\left[-a\left(\frac{t - t_s}{C_{D_p}}\right)^{M_p}\right] \tag{6.27}$$

$$\chi_d = 1 - \exp\left[-a\left(\frac{t - t_s}{C_{D_d}}\right)^{M_d}\right] \tag{6.28}$$

where χ_p and χ_d represent the fraction of heat release for the premixed combustion and diffusive combustion, respectively,

C_{D_p} and C_{D_d} represent the combustion durations for the premixed and diffusive combustion, respectively.

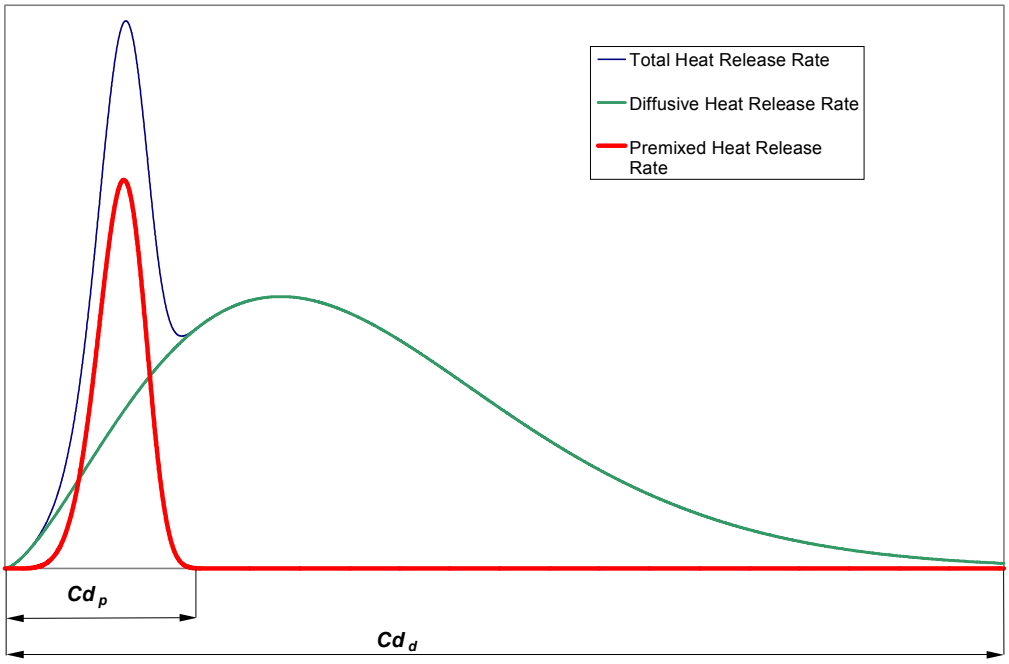

Figure 6.2: Heat release rate represented by using two Wiebe functions.

Considering that during the premixed combustion period the amount of heat released is Q_p and the amount of heat released is Q_d, then the corresponding rates of heat release these two combustion stages are given by:

$$\frac{dQ_p}{dt} = Q_p \frac{d\chi_p}{dt} \tag{6.29}$$

$$\frac{dQ_d}{dt} = Q_d \frac{d\chi_d}{dt} \tag{6.30}$$

or

$$\frac{dQ_p}{dt} = a\frac{Q_p}{C_{d_p}}\left(M_p + 1\right)\cdot\left(\frac{t - t_s}{C_{d_p}}\right)\cdot \exp\left[-a\left(\frac{t - t_s}{C_{d_p}}\right)^{M_p+1}\right] \tag{6.31}$$

$$\frac{dQ_d}{dt} = a\frac{Q_d}{C_{d_d}}\left(M_d + 1\right)\cdot\left(\frac{t - t_s}{C_{d_d}}\right)\cdot \exp\left[-a\left(\frac{t - t_s}{C_{d_d}}\right)^{M_d+1}\right] \tag{6.32}$$

Thus, the heat release write can be written as:

$$\frac{dQ}{dt} = \frac{dQ_p}{dt} + \frac{dQ_d}{dt} \tag{6.33}$$

The equations that describe the thermodynamic parameters are given by:

The ignition delay expression has the form of Arrhenius equation.

$$\tau_{id} = A \cdot p^{-n} \exp\left(\frac{E_A}{R \cdot T}\right) \tag{6.34}$$

where A and n are constants dependent on the fuel,

E_A is an apparent activation energy, and

R is the universal gas constant.

The coefficients A and n used in the ignition delay expression were those determined by Spadaccini and TeVelde [36].

$$n = 1$$

$$A = 0.0405$$

$$\frac{E_A}{R \cdot T} = 20080$$

The ignition delay was evaluated in both models, by accounting for the continuous change of the conditions during this period.

$$\int_{t_{si}}^{t_{si}+\tau_{id}} \frac{1}{\tau} dt = 1 \tag{6.35}$$

6.3.3.2 COMBUSTION MODELING FOR HCCI OPERATION

A general description of the homogeneous charge compression ignition engines was presented in section 3.4, and for convenience it will be summarised in the following. In HCCI engines the cylinder charge is prepared before the induction process. The cylinder charge is compressed to a point when autoignition occurs. The ignition of the charge occurs spontaneously and simultaneously throughout the mixture, and the combustion process takes place in a homogeneous way thus permitting a homogeneous combustion temperature. Due to the presence of numerous hot ignition spots, the combustion occurs very fast, the overall combustion duration being shorter than that of spark ignition engines. However this combustion concept presents two extremes, one being the detonation in the case of a rich mixture, and the other one is the misfire that occurs in the case of a too lean mixture, and both extremes are to be avoided. The most delicate features of the HCCI operation are the

initiation of auto-ignition and the representation of combustion rate.

In order to model the combustion process for this case, it is necessary to evaluate the two features of this complex process, the autoignition of the mixture and the combustion rate. Definitely it is a great challenge to evaluate these two aspects of the HCCI combustion process, however the combustion model presented in this dissertation employed a simple and effective approach. The ignition delay represents the time period from the close of the intake valve to the start of the combustion. This parameter has been calculated using an empirical expression developed by Ryan and Callahan [24].

$$\tau_{id} = 0.0221 \cdot [O_2]^{-0.53} \cdot [Fuel]^{0.05} \cdot \rho^{0.13} \cdot \exp\left(\frac{5914}{T}\right) \tag{6.36}$$

where: τ_{id} represents the ignition delay in ms,

$[O_2]$ is the oxygen concentration in moles/m^3,

$[Fuel]$ is the fuel concentration in moles/m^3,

ρ is the air density, and

T is the air temperature.

Since the fuel is mixed with air during the intake process, it means that the fuel is present in the cylinder charge during the compression event and, therefore there is a continuous variation of the parameters taken into account for the ignition delay calculation expression. The continuous change of the ignition delay during the compression, is accounted by using theory of conservation of delay in which it is considered that the ignition delay period is consumed when:

$$\int_{IVC}^{IVC+ID}\left(\frac{1}{\tau_{id}}\right)\cdot dt = 1 \tag{6.37}$$

Once the autoignition delay period is consumed, the combustion process begins. The combustion process in HCCI engines is characterized by a high rate of energy release, in section 3.4, were presented the features of the HCCI combustion process. It was established previously that the HCCI combustion process is governed in essence by the chemical kinetics, therefore for the combustion process was decided to be modeled by using a single-step global reaction. This simplistic approach represents a non-expensive tool and it permits a rapid and general evaluation of the HCCI combustion process. Global reactions as discussed in Chapter 5, have their limitations since do not capture the details of hydrocarbon oxidation but they permit a relatively good approximation for the overall oxidation process.

$$\frac{d[Fuel]}{dt} = -A\cdot T^{n}\cdot p^{m}\cdot \exp\left(-\frac{E_A}{\widetilde{R}T}\right)\cdot [Fuel]^{a}[O_2]^{b} \tag{6.38}$$

where $[Fuel]$ represents the instantaneous fuel concentration in gmol/cm^3,

$[O_2]$ represents the instantaneous oxygen concentration in gmol/cm^3,

T and p are the temperature and the pressure of the reactor, respectively,

A, m, n, a, and b, are coefficients characteristics for the considered fuel.

A major assumption in this model was that the rate of energy release was considered to be the same with the rate of reaction and, this permits:

$$\frac{dQ}{dt} = LHV\cdot\frac{dm_{Fuel}}{dt} \tag{6.39}$$

$$\frac{dm_{Fuel}}{dt} = \frac{V}{M_{Fuel}}\frac{d[Fuel]}{dt} \tag{6.40}$$

where $\frac{dm_{Fuel}}{dt}$

LHV represents the fuel lower heating value, in J/kg,

V is the instantaneous combustion chamber (the reactor) volume, in cm^3,

M_{Fuel} represents the molar mass of the fuel, in gmol/kg.

In the numerical simulation of the HCCI combustion of diesel fuel was considered that the decane

($C_{10}H_{22}$) combustion can closely represent the diesel fuel. Hence, combining Equation 6.13 and Equation 6.14 the fuel energy release rate can be written as:

$$\frac{dQ}{dt} = -LHV \frac{V}{M_{Fuel}} \cdot A \cdot T^n p^m \exp\left(-\frac{E_A}{\tilde{R}T}\right)[Fuel]^a [O_2]^b \tag{6.41}$$

In Equation 6.26 the temperature and pressure exponents, n and m respectively are considered to be equal to zero, therefore the fuel energy release rate has the following expression:

$$\frac{dQ}{dt} = -LHV \frac{V}{M_{Fuel}} \cdot A \cdot \exp\left(-\frac{E_A}{\tilde{R}T}\right)[Fuel]^a [O_2]^b \tag{6.42}$$

The reactor model used in this combustion model is the constant volume, constant mass type; for this type of reactor the first law of thermodynamics reduces to:

$$m\frac{du}{dt} = \frac{dQ}{dt} \tag{6.43}$$

The relationship between the instantaneous fuel molar concentration and oxygen molar concentrations is determined by considering the complete combustion of the fuel, in this case $C_{10}H_{22}$.

6.3.4 HEAT TRANSFER MODELING

The heat transfer process in an internal combustion engine and particularly for a CI engine represents a very complex process and this due to the fact that all three forms of heat transfer known are present in the overall heat transfer process, namely conduction, convection, and radiation. In diesel engines radiation heat transfer has much greater importance than in homogeneous charge engines where the radiation energy of water and carbon dioxide represent a less than 10% of the convective heat loss and, usually neglected. The radiation heat transfer in diesel engines is important component in the overall heat transfer process during the combustion phase due to the presence of the soot particles.

The conductive component of the overall heat transfer process is also of a great importance especially when it comes to the engine cylinder design, however for the thermodynamic analysis of the engine this component is not going to be taken into account since the subject of this analysis represent the heat transfer process on the gas side.

Generally, the equations used for heat transfer modeling in internal combustion engine modeling are of the standard convection form

$$\frac{dQ_{ht}}{dt} = h \cdot A \cdot \left(T_{cyl} - T_w\right) \tag{6.46}$$

where $\frac{dQ_{ht}}{dt}$ is the instantaneous heat transfer rate,

h is the overall heat transfer coefficient,

A is the instantaneous area over which heat transfer occurs,

T_{cyl} is the instantaneous cylinder fluid temperature, and

T_w is the cylinder wall temperature.

The most delicate problem resides in the evaluation of the overall heat transfer coefficient, *h*. Considering the heat transfer process from the cylinder gas to the cylinder wall as being a steady process it can be written that:

$$\frac{dQ_{ht}}{dt} = \frac{dQ_c}{dt} + \frac{dQ_r}{dt} \tag{6.47}$$

In an internal combustion engine the heat transfer process engine is dominated by a convective mechanism, therefore this particular form of heat transfer has been a subject to numerous investigations and so far, there are known two types of models, spatially uniform models and, boundary layers models.

Spatially uniform models consider the cylinder gases as a uniform medium. More realistic are the boundary layers models, which account for the variation of the physical properties of the in-cylinder gas in a thin layer formed near the cylinder wall. In boundary layer models two regions are considered, one in which the physical properties of the gas are subject to high gradients, and the other region outside the boundary layer in which the physical properties can be assumed to be uniform. These models are more accurate for the evaluation of the heat transfer process but they require information about the in-cylinder flow-field, fact that can create computational complications.

A very accurate evaluation of the heat transfer coefficient represents a very complicate task due to the complexity of the heat transfer process itself, and it does not represent the main priority for this work. Therefore the use of spatially uniform model that uses a heat transfer correlation, a common practice in engine modeling, will be used to simplify the modeling task. There are numerous heat transfer correlations in the IC engines literature [59], and most of them give satisfactory results despite their empiricism. These correlations relate the

Nusselt, Reynolds, and Prandtl numbers in the following general form.

$$\mathrm{Nu} = a\,\mathrm{Re}^{d}\,\mathrm{Pr}^{e} \tag{6.48}$$

where the dimensionless parameters are $\mathrm{Re} = \frac{\rho \hat{U} L}{\mu}$; $\mathrm{Pr} = \frac{\mu c_p}{k}$; $\mathrm{Nu} = \frac{hL}{k}$;

Another correlation used, probably the most popular, for the evaluation of the instantaneous convective heat transfer in IC engines is the one developed by Woschni [61].

$$\mathrm{Nu} = \frac{hL}{k} = 0.035\,\mathrm{Re}^{m} = 0.035\left(\frac{\rho \hat{U} L}{\mu}\right)^{m} \tag{6.49}$$

where Nu is the Nusselt Number,

h is the instantaneous space-averaged heat transfer coefficient

L is the Characteristic Dimension,

k is the fluid Thermal Conductivity,

Re is the Reynolds Number,

m is the Reynolds Number Exponent.

ρ is the Fluid Density,

$\hat{U}$ is the Characteristic Velocity, and

μ is the Fluid Viscosity.

Woschni postulated that the average gas velocity should be proportional to the piston speed. In his correlation, Woschni assumed that the ideal gas law was applicable, that the characteristic dimension was the cylinder diameter D, that m=0.8, that $\mu \propto T^{0.62}$ and that $k \propto T^{0.75}$.

Substituting these in the Woschni correlation it follows that

$$h_c = 0.00326 \frac{p^{0.8} \hat{U}^{0.8}}{D^{0.2} T^{0.53}} \tag{6.50}$$

where h_c is the film heat transfer coefficient,

p is the cylinder pressure,

$\hat{U}$ is the characteristic velocity

D is the cylinder diameter, and

T is the cylinder gas temperature

The characteristic velocity was evaluated throughout different evolutions of the engine cycle as follows.

$$\hat{U} = C_1 S_p + C_2 \frac{V_d T_{sc}}{p_{sc} V_{sc}} (p - p_{motored}) \tag{6.51}$$

where C_1 and C_2 are coefficients that denote the combustion and motored conditions respectively,

S_p is the mean piston speed

V_d is the displacement volume

T_{sc}, p_{sc}, and V_{sc} represent the temperature, the pressure, and the volume at the end of ignition delay period

p is the cylinder pressure, and

$p_{motored}$ is the pressure that corresponds to the motored conditions.

The coefficients C_1 and C_2 have different values based on the process the engine performs, these values being shown in Table 6-1. The Woschni correlation represents a very fast and convenient tool in the evaluation of the heat transfer, and therefore it was used for the heat

transfer process calculations for the FSLE model.

Table 6-1: Values for the coefficients used in Woschni correlation.

Evolution	C_1	C_2
Compression	2.28	0
Combustion and Expansion	2.28	0.00324
Gas Exchange	6.18	0

Although the convective mechanism dominates the entire heat transfer process, in the DI case due to the diffusive flame presence, the radiation heat transfer component has to be considered.

The heat flux due to the radiation has the following form:

$$\frac{dQ_r}{dt} = \varepsilon \cdot \sigma \cdot A \cdot \left(T^4 - T_w^4\right) \tag{6.52}$$

where ε represents the gas emissivity, and

$\sigma = 5.66 \cdot 10^{-8} \frac{W}{m^2 K^4}$, is the Stefan-Boltzmann constant.

Considering that the total heat transfer flux can be written as having two components, one being the convective component and the other one the radiation component, it follows from Equation 6.47 that:

$$\frac{dQ_{ht}}{dt} = A \cdot \left(h_c + h_r\right) \cdot \left(T - T_w\right) \tag{6.53}$$

where h_r is the radiation heat transfer coefficient.

From the Equation 6.47 and 6.52 it follows that radiation heat transfer coefficient can be written as:

$$h_r = \varepsilon \cdot \sigma \cdot (T - T_w) \cdot (T^2 - T_w^2) \tag{6.54}$$

The emissivity term value was taken from the Annand [60] correlation, in which it was considered that the emissivity term for compression ignition engines as being $\varepsilon = 0.58$.

For the HCCI operation case, the radiation component is practically absent due to the HCCI combustion nature, in other words, due to the absence of flame propagation phenomena or absence of the diffusive flame, radiation heat transfer component can be neglected. Therefore for the HCCI case the only term considered for the heat transfer model was the convective one. Similarly to the direct injection case, for the evaluation of the convective heat transfer for the HCCI model was used the fast approach offered by Woschni's correlation.

CHAPTER 7 DESIGN CONSIDERATIONS SUGGESTED BY MODELING

The purpose of this dissertation was to design a four-stroke linear engine able to produce a power output of 15 kW, and to operate in two different modes, as a direct injection compression ignition and, as a homogeneous charge compression ignition engine. In the following sections of this chapter is presented the analysis conducted for the FSLE operating in direct injection mode and the analysis of the FSLE operating in HCCI mode. The geometrical parameters for this linear engine were taken as being identical with the ones from the direct injection version of the two-stroke linear engine prototype shown in Table 3-4.

7.1 ENGINE ANALYSIS OPERATING IN DIRECT INJECTION COMPRESSION IGNITION MODE

Before presenting the results obtained from the numerical simulation of the cycle it is necessary to underline the fact that the design of the engine has two major restrictions imposed to the engine operation. First restriction is represented by the limitation of the in-cylinder pressure, for the designed engine the in-cylinder pressure in limited at a value of 15000 kPa, and the second one is represented by the limitation of the average reciprocating assembly speed, limiting this way the friction losses. The considered limit value for the average piston speed was of 12 m/s. In Table 7-1 besides the geometric parameters of the engine, bore, and maximum possible stroke, are presented the valve timing specifications. In this numerical simulation the scavenging process is not taken in consideration due to the fact that there is no valve overlapping. The exhaust valve opens at the end of the expansion process, which is considered to end in the moment the piston reverses its motion. Similarly,

the intake valve opens in the moment the piston in the exhaust stroke reverses its motion, which coincides with the closing of the exhaust valve.

Table 7-1: Geometric Specifications of a Direct Injection Compression Ignition Four-Stroke Linear Engine

Number Cylinders	4
Bore	75 [mm]
Maximum Possible Stroke	71 [mm]
Reciprocating Assembly Mass	3-6 [kg]
Exhaust Valve Opening	At the end of the expansion stroke considered when the reciprocating assembly reverses its motion
Intake Valve Opening	At the end of the exhaust stroke considered when the reciprocating assembly reverses its motion
Exhaust Valve Closing	At the end of the exhaust stroke considered when the reciprocating assembly reverses its motion
Intake Valve Closing	Variable

Another important parameter for the engine simulation was the friction force. As mentioned before in section 6.1.1, the friction force in this simulation was considered constant along the stroke. This assumption will not alter the operation of the linear engine due to the fact that its order of magnitude is much smaller in comparison to the load introduced by the linear alternator and therefore, this do not affect the engine behavior. The friction force in this simulation is a function of displaced volume and reciprocating frequency, therefore for a stroke length of 71 mm and a reciprocating frequency of 3000 cycles/min, the friction mean effective pressure was found to be:

$$fmep = 0.034\,MPa$$

$$fmep = \frac{W_f}{V_d} \tag{7.1}$$

where W_f is the work required to overcome the friction force, and

V_d is the displaced volume

$$W_f = 4 \cdot L_{st} \cdot F_f \tag{7.2}$$

From equation, the average friction force was found to be:

$$F_f = \frac{fmep \cdot V_d}{4 \cdot L_{st}} = 37.6N \tag{7.3}$$

In Table 7-1 besides the geometric parameters of the engine, bore, and maximum possible stroke, are presented the valve timing specifications. In these simulations the scavenging process is not taken in consideration since there is no valve overlapping. The exhaust valve opens at the end of the expansion process, which is considered to end in the moment the piston reverses it motion. Similarly, the intake valve opens in the moment the piston in the exhaust stroke reverses its motion, which coincides with the closing of the exhaust valve. The investigations done on the spark ignition version of the two-stroke linear-engine prototype, in essence a parametric study performed to determine the interdependence among different engine parameters, did not establish any range of operation for this type of engine. Therefore, in this dissertation, one of the primary goals was to determine the operation domain for this type of engines. The numerical simulation programs for the analyzed case of operation, were run and tested for a wide range of the engine input parameters such as, manifold intake pressure and temperature, air to fuel ratio, injection timing and duration, combustion duration, and valve timing. After several runs of the engine simulation, it was observed that

one way to control the engine operation was to delay the closing of the intake valve. Initially the engine was designed to have the intake valve closing in the moment the piston ends it intake evolution, more precise, in the moment it reverses its motion.

During the first set of runs of the engine simulation, the engine's input parameters (intake air temperature and pressure, air to fuel ratio, combustion duration, injection timing, injection duration, combustion duration, and valve timing) were varied for a wide range of values in order to determine the general behavior of the engine. It was observed that it was not possible to obtain a steady operation for the engine unless the intake valve closing was delayed. This delay was found to be greater than or at least equal to the height corresponding to operating the clearance volume.

The engine operation is result of the balance between the in-cylinder pressure forces, friction force and load and, as expected the engine reaches its operation regime very fast. In the simulation program there is a period of about 1.5 s of simulated engine operation until the engine operation becomes stable. The results obtained from running the numerical simulation are presented in the following figures and they correspond to a typical FSLE cycle. Figure 7.1 presents the in-cylinder pressure variation and the corresponding motoring pressure variation versus time. It was mentioned before that the motoring pressure for the case of free-piston engines, different than the crankshaft engines case, represents an artificial parameter and it corresponds to a cycle without combustion for which it is obtained the same displacement to a cycle with combustion. Figure 7.2 illustrates the in-cylinder pressure variation vs. displacement assumed a "P-V" diagram and, Figure 7.3 presents the same in-cylinder pressure variation but in logarithmic coordinates

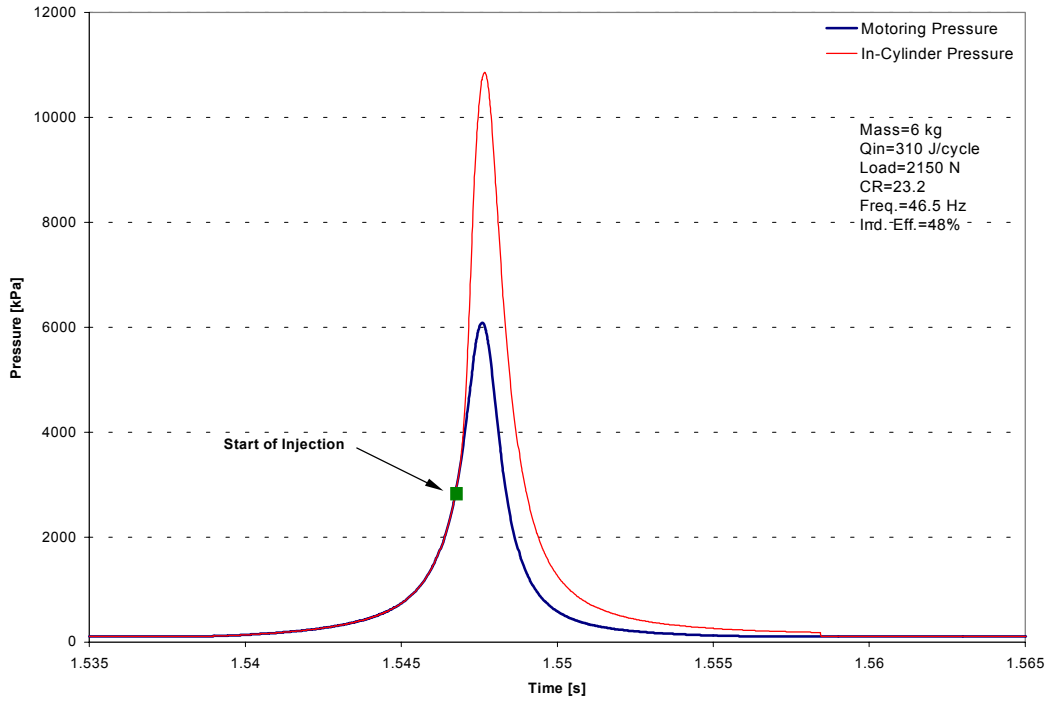

Figure 7.1: In-Cylinder Pressure Variation vs. Time

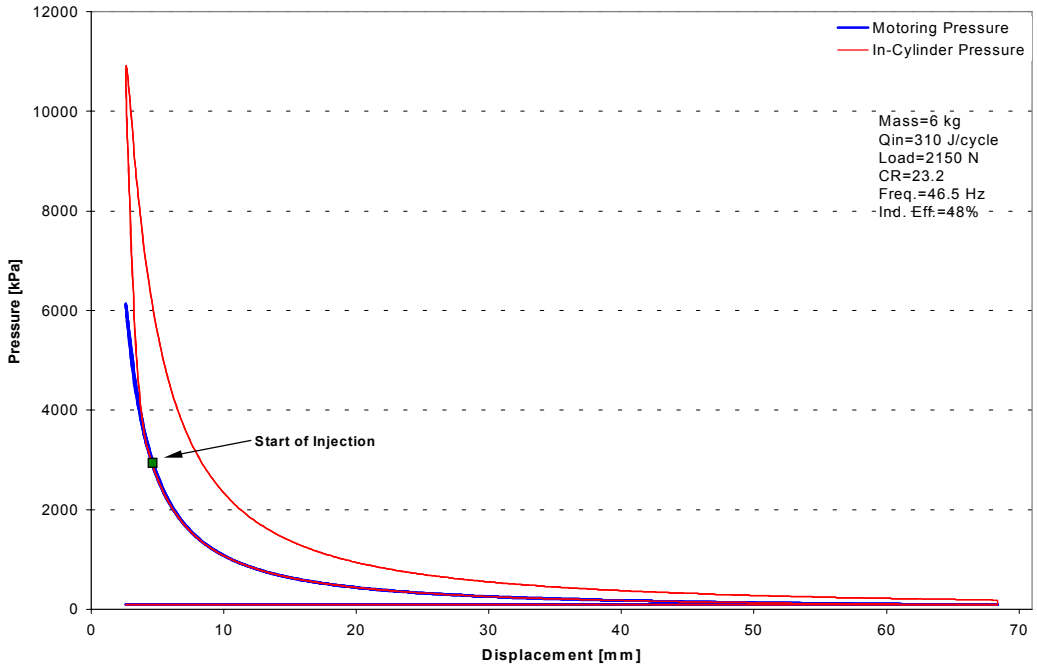

Figure 7.2: A Pressure vs. Displacement Diagram

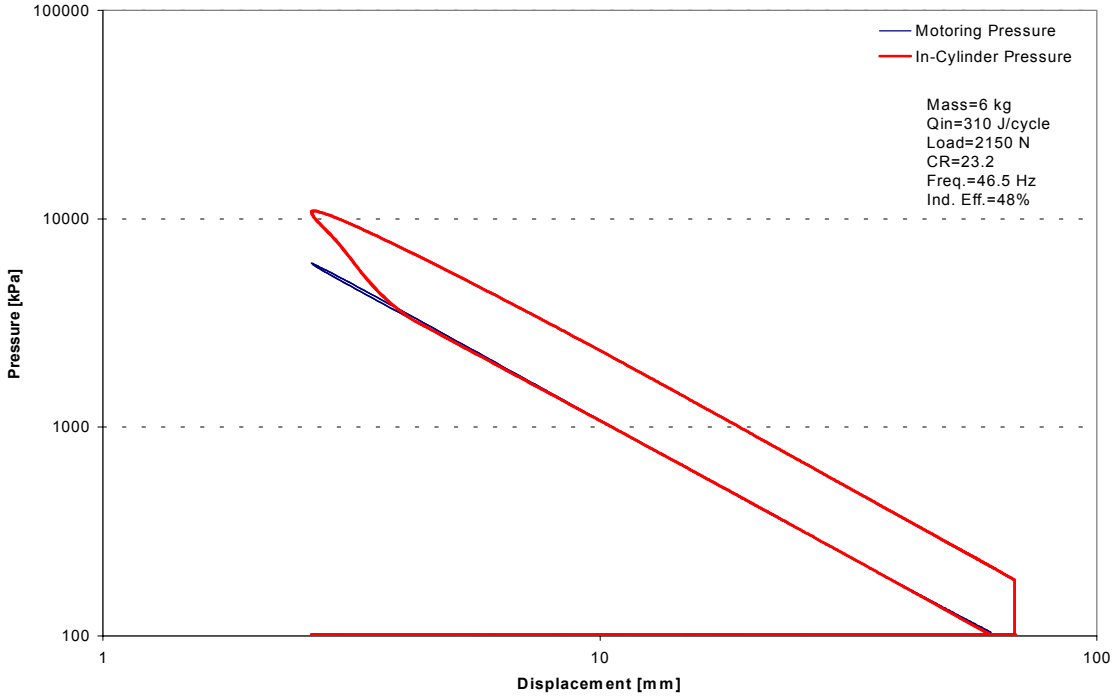

Figure 7.3: Log (Pressure) – Log (Displacement) Representation of a typical cycle of FSLE

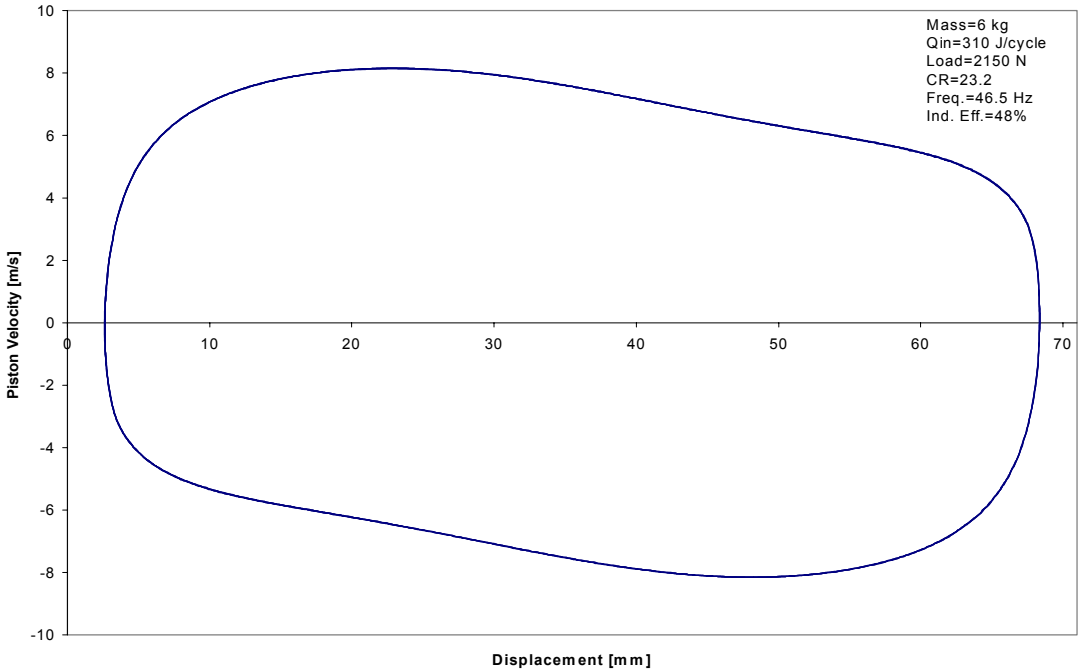

Figure 7.4: Piston Velocity vs. Displacement for a typical cycle of FSLE

The corresponding velocity profile associated to the operation regime shown in Figures 7.1-7.3 is illustrated in Figure 7.4. Once the steady operation for the engine was obtained, the analysis of the engine operation was performed considering the baseline input parameters as indicated in Table 7-2.

Table 7-2: Baseline Parameters used in the Analysis of the FSLE Direct Injection Compression Ignition

Intake Manifold Temperature	370 [K]
Intake Manifold Pressure	0.1013 [MPa]
Injection Timing	5 [mm] from the very end of the maximum possible stroke.
Injection Duration	Variable
Combustion Duration	0.0035 [s]
lambda	1.1 – 3

For convenience in this analysis, the reference to the cylinder mixture quality is done using the relative air to fuel ratio, lambda. By definition, λ represents the ratio between the actual fuel to air ratio to the stoichiometric air to fuel ratio.

$$\lambda = \frac{(A/F)_{actual}}{(A/F)_{stoichiometric}} \tag{7.4}$$

In order to determine the operation domain for this engine, the relative air to fuel ratio was varied within a reasonable large range typical for a compression ignition engine maintaining the others parameters fixed. The variation of the relative air to fuel ratio was associated with a variation of load introduced by the linear alternator. Thus, for each considered value of λ it

was determined the maximum supported load establishing this way the upper limit of the engine operation domain. The upper operation limit for the considered parameters is presented in Figure 7.5.

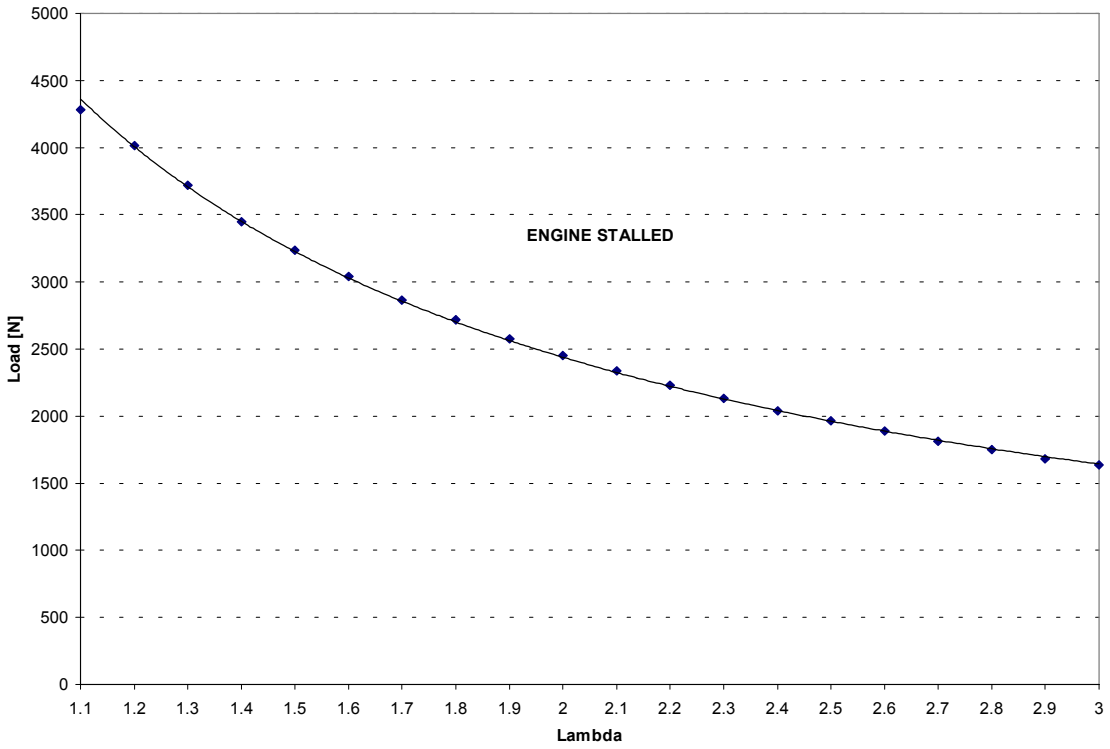

Figure 7.5: An Upper Limit of FSLE Operation

It is evident that the boundary obtained is characteristic to the operation of this type of engines and it corresponds to a certain combination of input parameters. Figure 7.5 shows that as the cylinder mixture becomes richer, the maximum load that can be overcome evidently increases it. During these particular runs it was observed that the engine compression ratio was relatively constant for this par ticular range of operation having a value of around 20. The reciprocating frequency registered an increase in value for lower values of λ. It was also observed that the reciprocating frequency has an increase in value as

the mixture becomes leaner. Figure 7.6 illustrates the power output variation with λ, corresponding to the limit of the operation domain. It can be observed that towards richer regimes associated with a higher power output, the indicated efficiency decreases, this aspect can be associated with the slight decrease in compression ratio towards low values of λ.

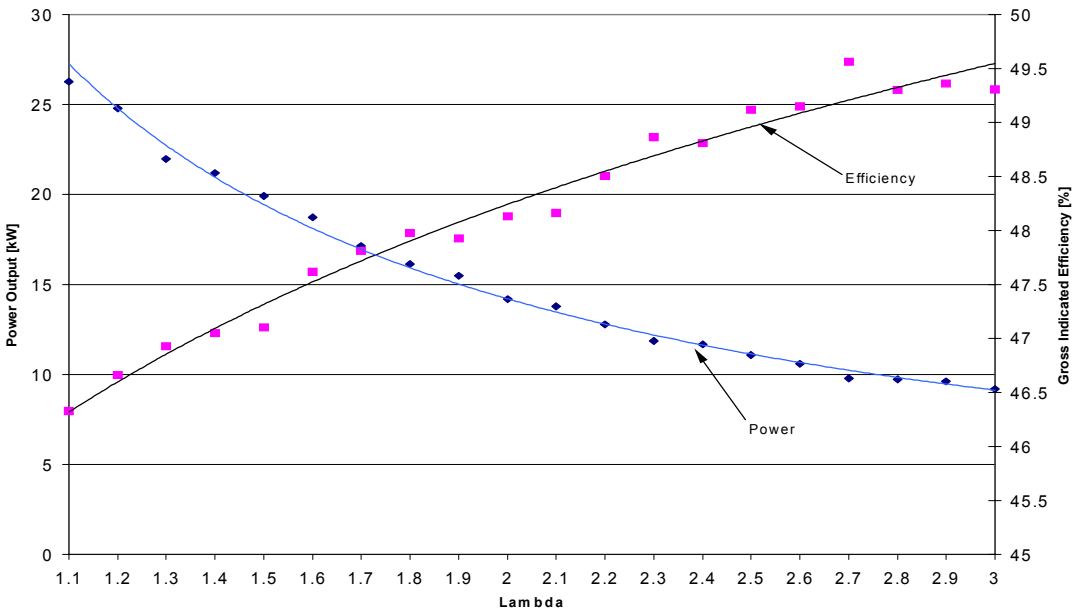

Figure 7.6: Power Output Variation Corresponding to the Upper Limit of Operation

The numerical simulation of the FSLE has shown that for a certain value of heat input and for a value of the load lower that the limit load, the engine will increase its reciprocating frequency implying an increase in compression ratio, due to inertial effects, resulting in high values of the in-cylinder pressure. Due to mechanical and emissions constrains, the in-cylinder pressure for this engine was limited to a limit value of 15000 kPa. This design constrain will practically set the lower limit of the engine operation domain. Figure 7.7 presents the domain of operation for the FSLE for the input parameters from Table 7-2. It can be observed that the operation domain extends as the value of λ increases. At low values of

relative air to fuel ratio, around stoichiometric combustion limit, this domain gets very narrow limiting the option for operation in rich regimes.

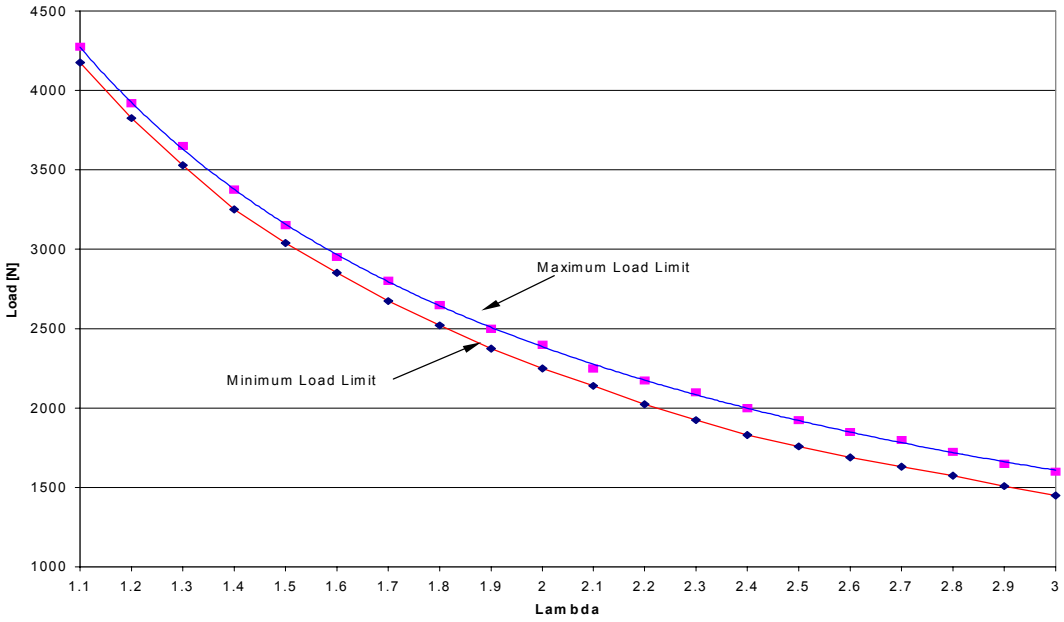

Figure 7.7: Typical Operation Domain for the FSLE

The power output variation associated to these two limit-regimes that define the operation domain is presented in Figure 7.8. The upper power output curve corresponds to the lower limit of the operating regime presented in Figure 7.7, and this can be explained by the fact that at lower loads, for the same input parameters, there is an increase in the reciprocating frequency which evidently implies a higher power output. The corresponding gross indicated efficiency registered a slight decrease in comparison to the maximum-load operation regime despite the fact that the minimum-load operation regime is characterised by a higher compression ratio operation, the values varying from 24 to 34 with higher values for the leaner mixtures, Figure 7.9.

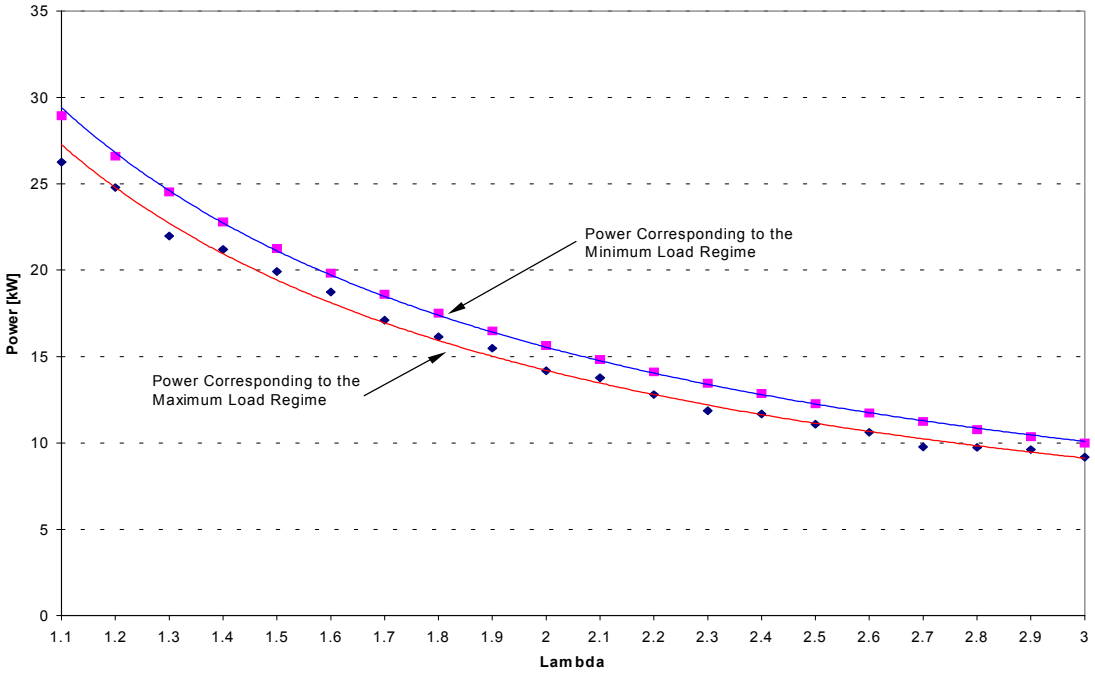

Figure 7.8: Power Output Associated with the FSLE Operation Domain

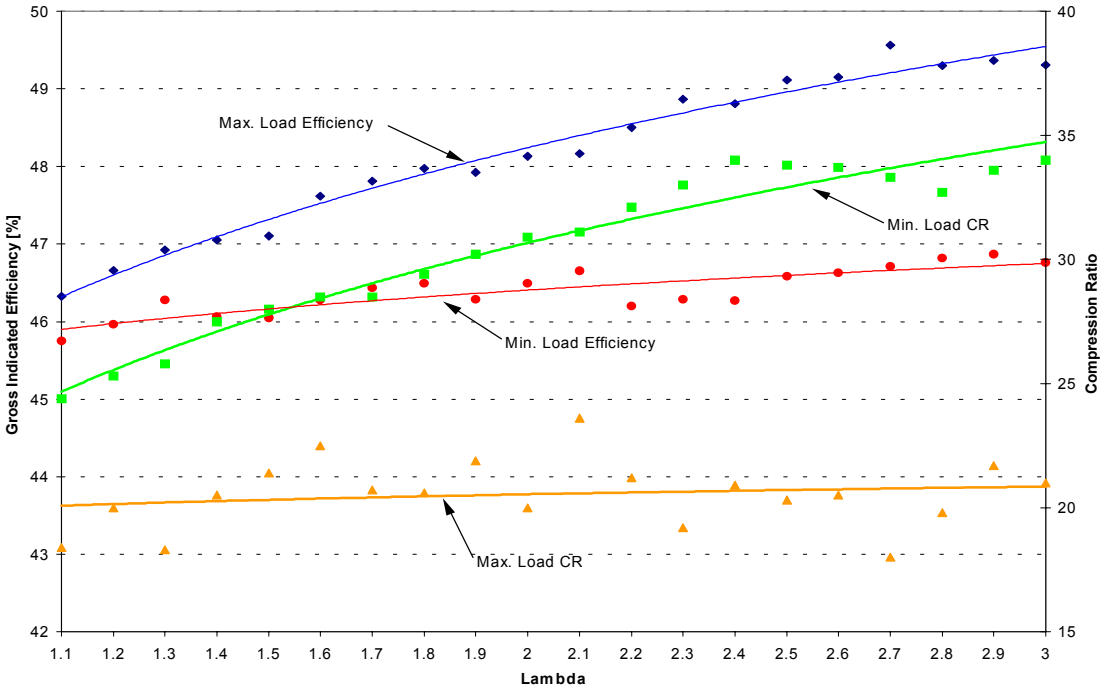

Figure 7.9: Indicated Efficiency and Compression Ratio Variation

The fact that engine operation in the domain that corresponds to the lower values of the relative fuel to air ratio implies higher power output is very attractive, the only problem that arises is that the range for the load variation becomes narrower. The lower lambda operation regimes for this engine on the other hand is not quite indicated due to the high tendency of soot formation.

The higher air to fuel ratio domains, despite their higher range for the load and their high values of indicated efficiency, they offer a poor power output, and also they are more predisposed to nitrogen oxides emissions. Therefore as a compromise, it was decided to choose the engine operation in the region that corresponds to a value of relative air to fuel ratio around 2.

7.1.1 INFLUENCE OF RECIPROCATING MASS

The free piston engine operation is dominated by inertia introduced by the mass of the reciprocating assembly, thus the reciprocating mass requires special attention. In the previous analysis [19] of the two-stroke engine prototype it was shown the reciprocating mass dictates the reciprocating frequency at which the engine operates. It was also shown that the higher the mass the lower the operation frequency, and also the fact that for the same engine parameters and for high values of mass the peak pressure increases due to the increase of the compression ratio in the engine operation, Figure 3.9 and Figure 3.10. In the analysis for the FSLE case, the engine numerical simulation model was run for different values of the reciprocating mass trying to determine the way it affects the operation domain for the engine. It was observed that the engine operation domain shifts up with for lower values of the reciprocating mass. The analysis was done for three values of the reciprocating mass as

indicated in Figure 7.10 in which is illustrated the variation of the "maximum load" boundary vs. lambda for different values of the reciprocating mass. This behavior is explained by the fact that the lower the values of the reciprocating mass the higher the reciprocating frequency and therefore the higher the power output necessary to overcome the resistant load.

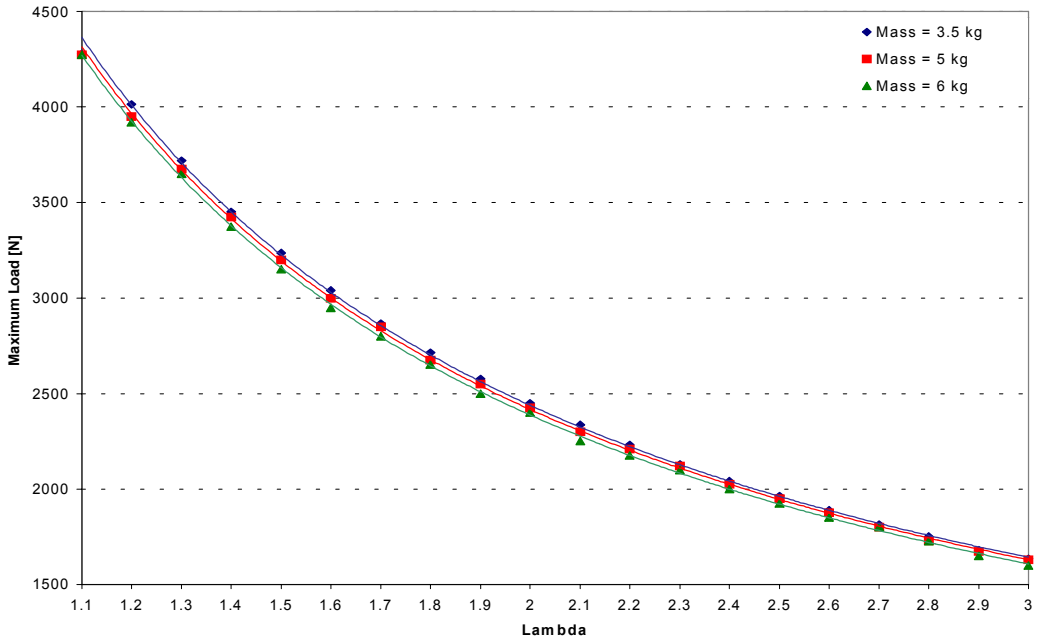

Figure 7.10: "Maximum Load" operation boundary variation for different values of the Reciprocating Mass

As expected the "minimum load" boundary of the engine operation shifts up with a decrease in value of the reciprocating mass, implying an increase of the reciprocating frequency therefore higher compression ratios operation regimes The "minimum load" boundary variation for different values of the reciprocating mass in shown in Figure 7.11. In Figure 7.12 it is presented the power output domain for two values of the reciprocating mass. It can be observed that for the lower value of the reciprocating mass the power output range for a given value of lambda, becomes wider.

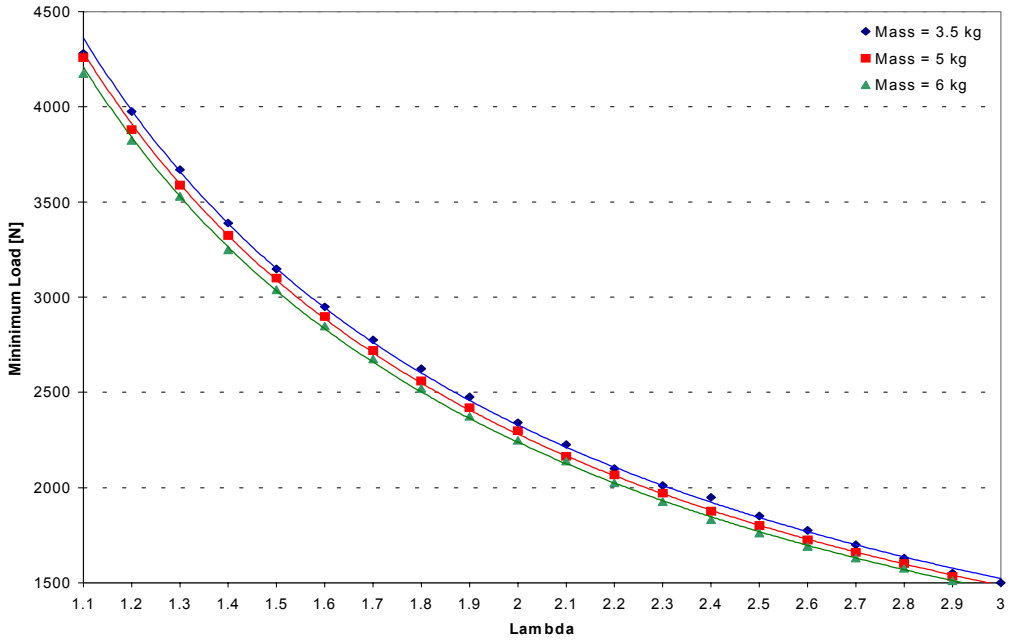

Figure 7.11: "Minimum Load" Operation Boundary Variation for different values of the Reciprocating Mass

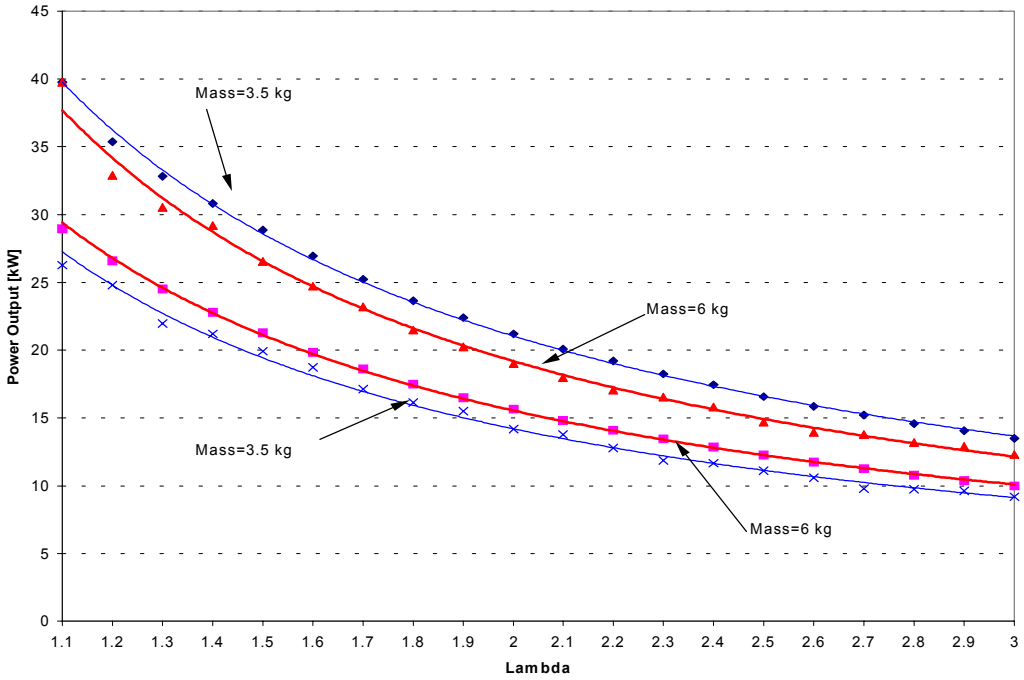

Figure 7.12: Power Domain for different values of the Reciprocating Mass

In the same Figure 7.12, it is obvious that the lower limit of the power output domain corresponds to the "Maximum Load" operation regime.

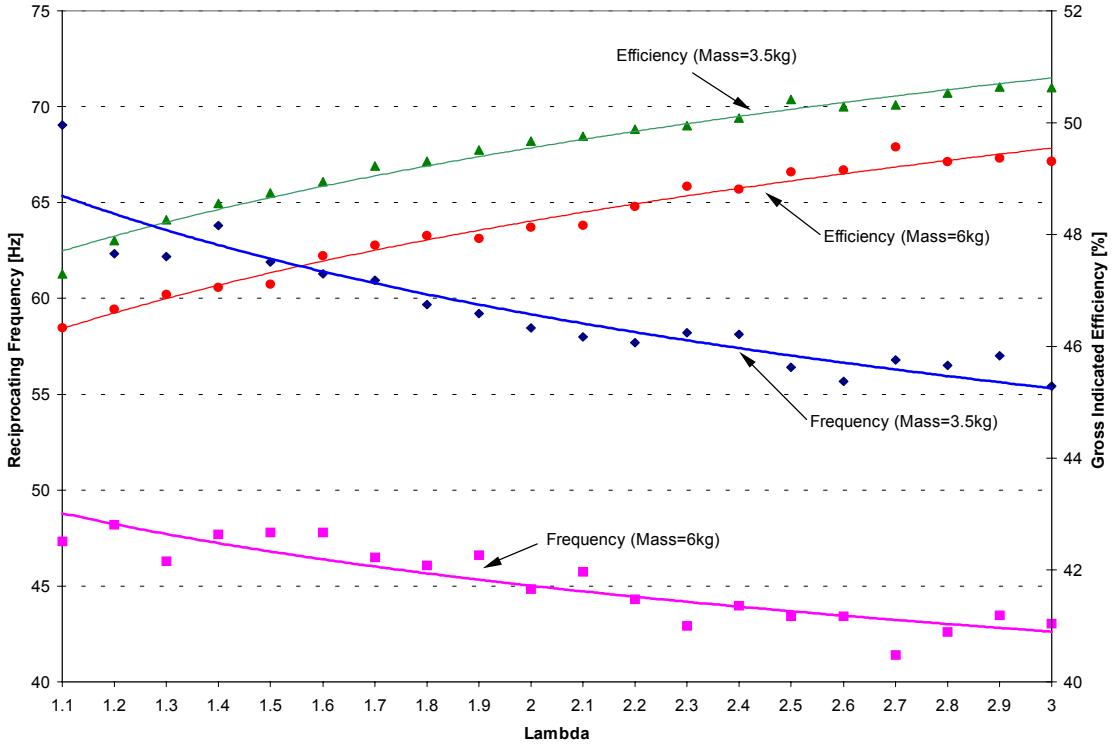

Figure 7.13: Gross Indicated Efficiency and Reciprocating Frequency Variation for Different values of the Reciprocating Mass

For lower values of the reciprocating mass the indicated efficiency increases due to the fact that the engine operates at a slightly higher compression ratios, this is shown in Figure 7.13 where the indicated efficiency variation vs. lambda is plotted for two values of the reciprocating mass, the values considered were 3.5 kg and 6 kg.

From the analysis conducted so far on the engine, it can be concluded that it is advantageous to use a low reciprocating mass due to the fact the engine operation becomes more efficient implying a higher power output. The value of the air to fuel ratio at which the engine

operation will be considered, therefore further investigations on different parameters that influence the engine operation will be performed using this value (λ=2).

7.1.2 INFLUENCE OF INJECTION TIMING

Another important parameter that influences the engine operation is the injection timing. The way the combustion process takes place relatively to the engine cycle depends on the injection process. The heat release rate depends to a certain extent on the injection timing accounted as the moment when injection starts and, on the injection strategy. Through the injection strategy is understood the shape of the rate at which injection process occurs, or more explicit the rate at which the fuel is injected into the combustion chamber with respect to the injection process. In the numerical model, the injection process was taken in account by assuming the amount of fuel burned during the premixed combustion period. Myamoto et al. [37] in their phenomenological combustion model considered that the amount of burned in the premixed combustion stage represents 50% of the fuel injected during the ignition delay period. It is quite complicated to estimate the amount of fuel burned in the premixed combustion, unless is the injection rate is known, since it is mainly a function of injection strategy adopted by the engine designer. In the presented numerical model this particular aspect has been caring out by specifying the amount of burned in during the premixed and diffusive combustion periods. This approach represents an effective tool for the present analysis which up to this stage considered that the injection starts at 5 mm from the very end of the maximum stroke, and the amount of heat released associated to the premixed combustion represented 20% of the total heat released during the combustion period. In this section it will evaluated the effect of the fuel injection towards the engine operation. The

analysis will be performed considering the engine has the geometrical parameters from Table 7-1, for a relative air to fuel ratio λ=2 and for a value of the reciprocating mass, mass=3.5 kg. In the analysis performed on FSLE the start of injection was considered fixed every operation condition taken in account. The start of injection value considered was 5 mm from the very end of the maximum possible stroke. The following analysis will be focusing on the effects of this important parameter on engine operation. Thus there were considered two cases, a first case in which the start of injection is advanced (considered at 6 mm from the very end of maximum possible stroke) and, a second case when the start of injection delayed (considered at 4 mm from the very end of maximum possible stroke), both cases are considered relative to the start of injection used so far (5 mm from the very end of maximum possible stroke).

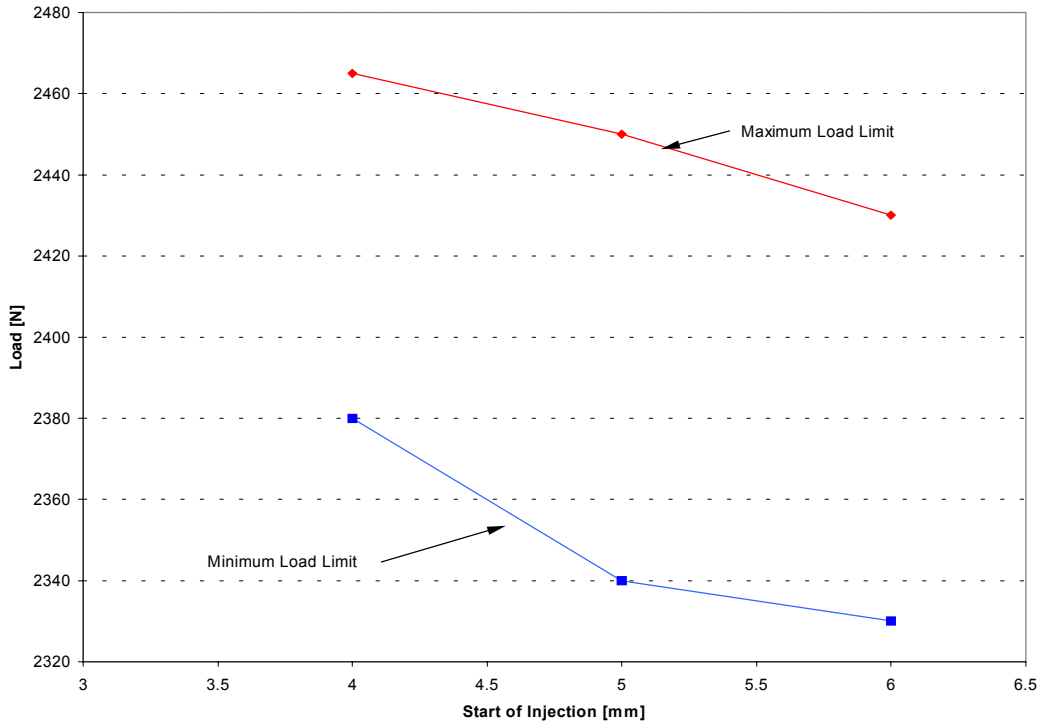

Figure 7.14: Start of Injection Effect on the Engine Operation

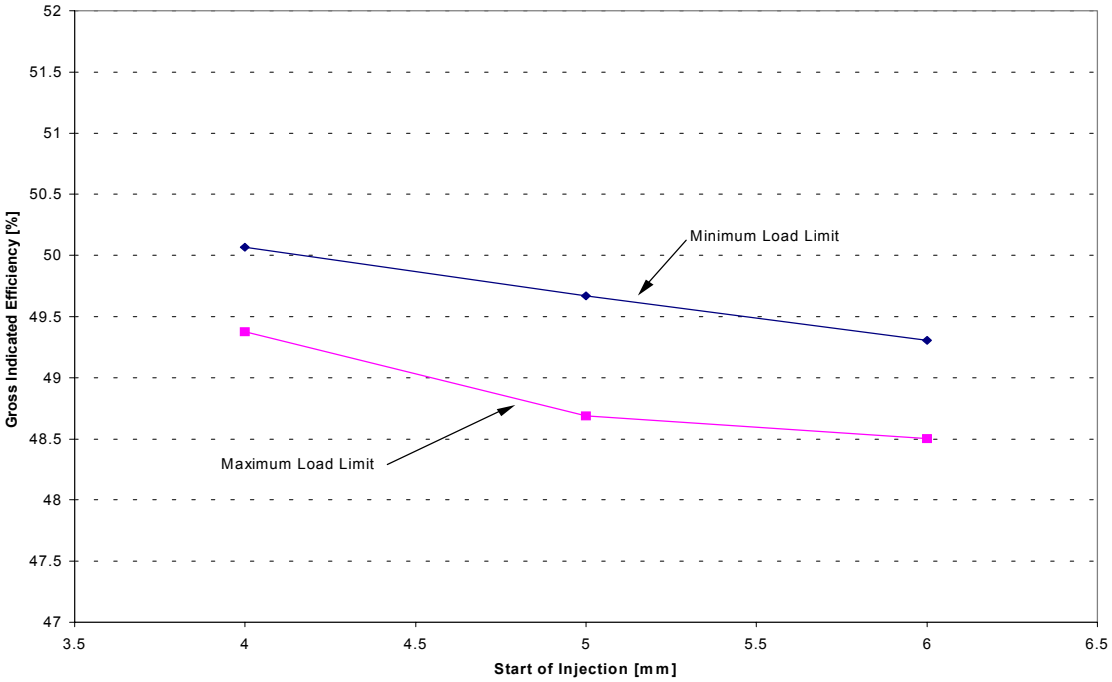

Figure 7.15: Indicated Efficiency variation for different cases of Injection Timing

It was observed that for an advanced injection timing there is a downshift of the operation domain the load values corresponding the maximum load regime and maximum pressure regime decreasing and, for the case of late injection timing the boundaries of the operation domain shift up as shown in Figure 7.14. Figure 7.15 shows the variation of the indicated efficiency for the three cases considered. The indicated efficiency, as expected, increases for the case of the considered delayed start of injection and this due to a better positioning of the combustion process with respect to engine the cycle. The results obtained suggest that the engine operation domain can be expanded to a certain extent, by adopting the optimum injection strategy. For example when it is seek the maximum power operation, by adopting an advanced injection timing it will permit an expansion of the operation domain, evidently with a certain cost in efficiency.

7.1.3 INFLUENCE OF COMBUSTION DURATION

In the FSLE analysis the combustion duration was considered as being constant, its value was considered based on the fact that a typical combustion duration in a diesel engine between 40-70 crank-angle degrees. Considering that the engine speed is 3000 rpm, this corresponds to a combustion duration with values between 2.2-3.8 ms. In the numerical simulation of the FSLE operating in direct injection mode the value adopted for combustion duration was 3.5 ms for a reciprocating frequency of 50 Hz. The fact that the combustion process was evaluated by using a double Wiebe function offered a great flexibility for the parametric study pursued, basically the rate of heat release can be shaped in various ways which permits a complex analysis. Investigations with regards to the importance of this parameter were conducted in the analysis of the TSLE [19], it was shown that a shorter combustion duration affects the in-cylinder pressure peak and the reciprocating frequency. In fact, the same effects are also expected for the case of the FSLE but the main goal is to determine in what way the operation domain is affected by the variation of this parameter. In previous section it was mentioned that the amount of fuel burned during the premixed stage of combustion was considered to be 20% from the total amount of fuel injected into the cylinder also the combustion duration associated to this stage was considered to be 1/6 of the total combustion duration. In order to see influence of combustion duration there were considered two cases: first case corresponds to a combustion duration of 2.5 ms and, the second case corresponds to longer combustion duration of 5 ms. In Figure 7.16 it is shown the in-cylinder pressure variation for the two limit cases of combustion duration. Figure 7.17 shows the operation domain variation for different values of combustion duration.

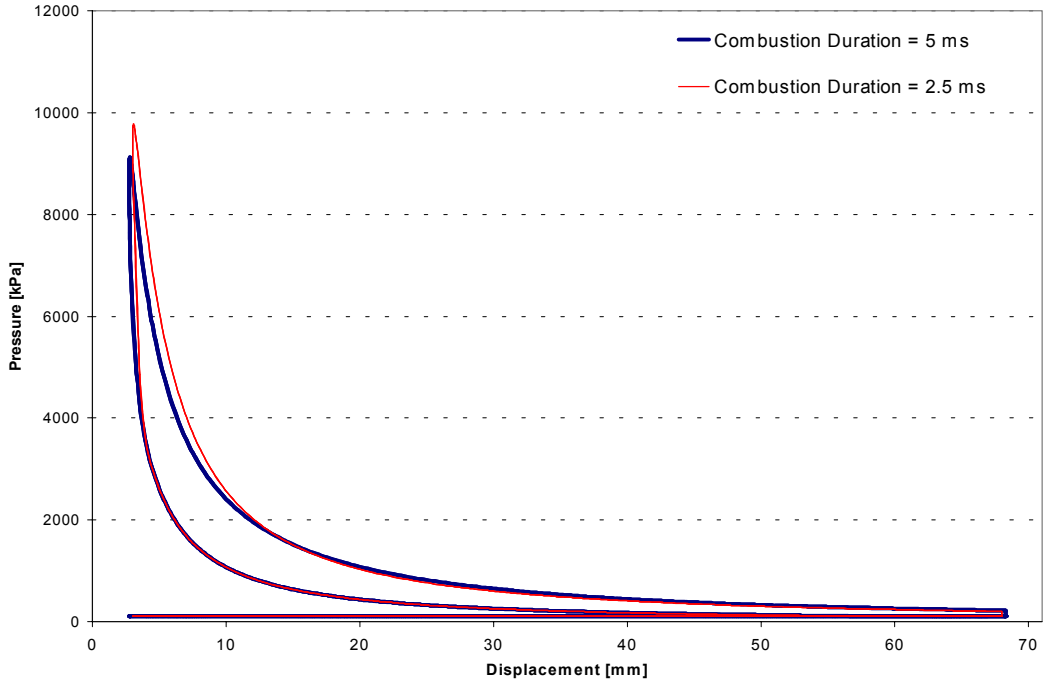

Figure 7.16: In-Cylinder Pressure Variation for Different Values of Combustion Duration

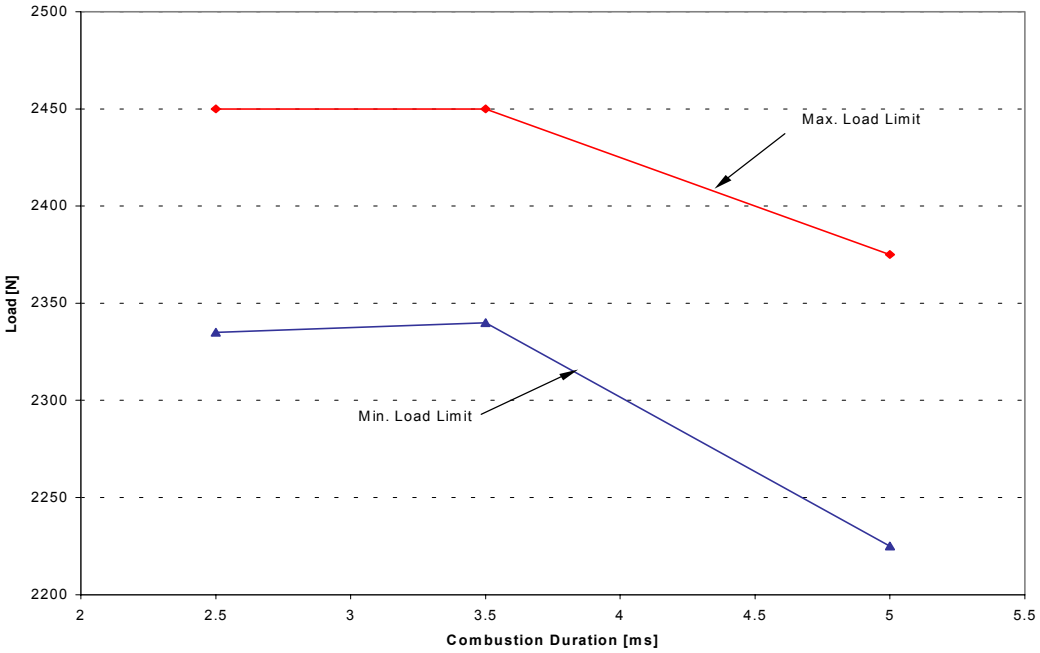

Figure 7.17: FSLE Operation Domain Variation for Different Values of Combustion Duration

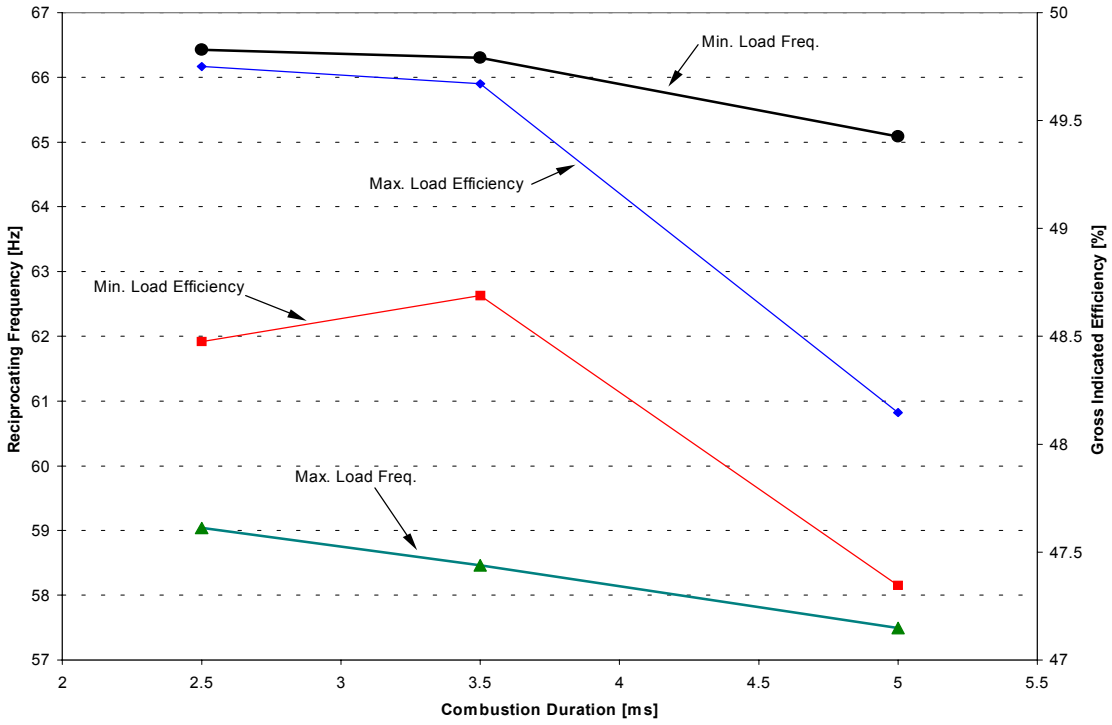

Figure 7.18: Indicated Efficiency and Reciprocating Frequency variation with Combustion Duration

Figure 7.18 illustrates the variation of indicated efficiency and reciprocating frequency with the variation of the combustion duration for the operation boundaries. It can be observed that the higher reciprocating frequency increases for a shorter combustion duration and, the efficiency reaches a within the limit values considered for the combustion duration. In this case the variation of the indicated efficiency is the combined result of the variation compression ration, reciprocating frequency, and heat release rate and in this analysis it is necessary to distinguish which of the three mentioned parameters is dominant. The variation of compression ratio with combustion duration is illustrated in Figure 7.19. It can be observed that for a longer combustion duration the engine operates at higher compression

ratios, although the reciprocating frequency decreases. It is evident that for the case of a longer combustion duration the indicated efficiency has a lower value due to the heat transfer, although it operates at slightly higher compression ratios then for the case of a shorter combustion duration.

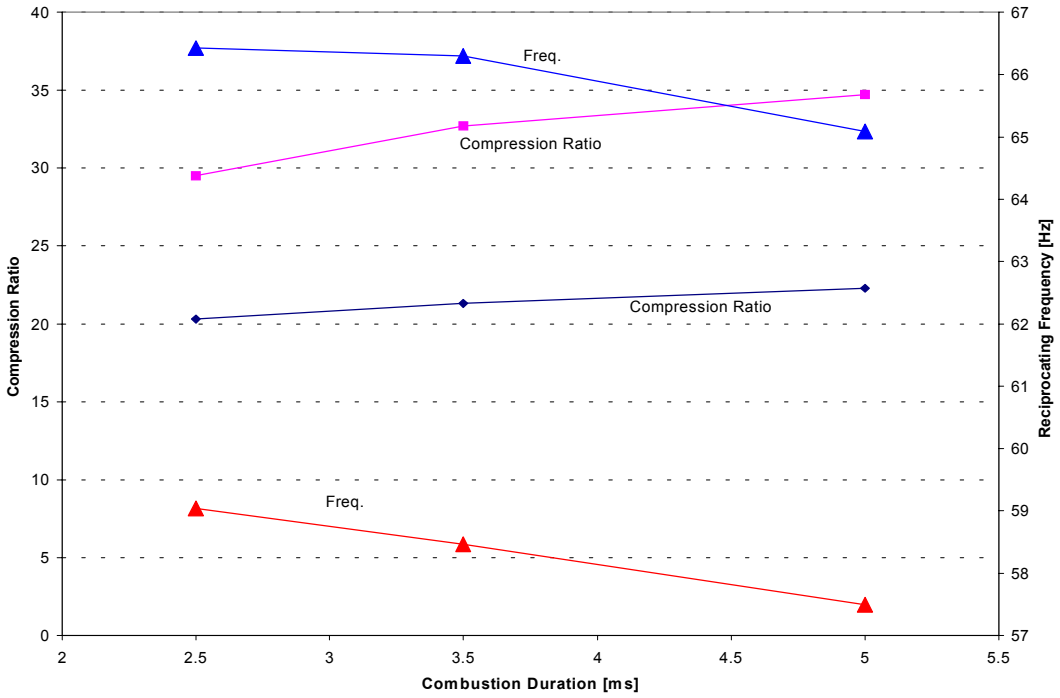

Figure 7.19: Compression Ratio and Reciprocating Frequency variation with Combustion Duration

It also can be observed that for a shortest combustion period considered there is a decrease of the indicated efficiency in comparison to the value the baseline combustion duration, 3.5 ms. This is due mainly to the decrease of compression ratio which is result of positioning the combustion process with respect to the engine cycle, although the reciprocating frequency increased. It was mentioned that the reciprocating frequency has a direct effect on the

compression ratio. In this case, due to the fact that the combustion duration is short there is a higher rate of heat release rate than in the case with a longer combustion duration and therefore a higher pressure rise able to overcomes the inertial effects establishing the clearance volume which in fact defines the compression ratio.

7.1.4 INFLUENCE OF LOAD VARIATION

In the work done for the two-stroke linear engine prototype [19], it was shown that the variation in the shape of the load affects the operation of this type of engines based on the positioning of the load with respect to the engine stroke (Figures 3.6-3.8). However, in this dissertation the load introduced by the linear alternator was considered to have a sinusoidal shape, more precise the load was consider to be shaped as a third order sinusoidal. In this section, it will be presented different aspects observed on engine operation for load variation in shape and magnitude. So far, the analysis was performed mostly on the boundaries of the operation domain, it is interesting to observe the engine's behavior inside the operation domain. The range of load variation corresponding limit of the operation, for a reciprocating mass of 3.5 kg and relative air to fuel ratio λ=2, was 110 N. It was decided to investigate the variation of engine performances, therefore they were considered another there values of the load within the operation domain besides those delimiting the operation domain. The result obtained shown that in general the variation of operation parameters, compression ratio, reciprocating frequency, indicated efficiency, and power output across the operation domain presented a monotonic variation. In order to perform the analysis across the operation domain it was defined a variable DeltaLoad as being the percentage of the applied load, as shown by the following equation:

$$\text{Delta Load} = \frac{MaxLoad - ActLoad}{MaxLoad - MinLoad} \cdot 100[\%]$$

where $MaxLoad$ represents the maximum applied load that the engine can overcome,

$ActLoad$ represents the actual value of the load considered within the operation domain for a given value of relative air to fuel ratio, and

$MinLoad$ represents the minimum applied load corresponding to the maximum in-cylinder pressure, for the considered value of relative air to fuel ratio.

Figure 7.20 illustrates the variation of the compression ratio and reciprocating frequency for different percents of the maximum load. Similarly, the variation of power output and the reciprocating frequency for different load percents is presented in Figure 7.21. An interesting aspect observed was that the piston velocity profile presents symmetric profile as the load varies within the operation domain, this aspect is illustrated in Figure 7.22.

Another stage of this analysis with regards to the influence of the load on the engine operation is represented by the evaluation of the influences of the load shape on engine performances and operation

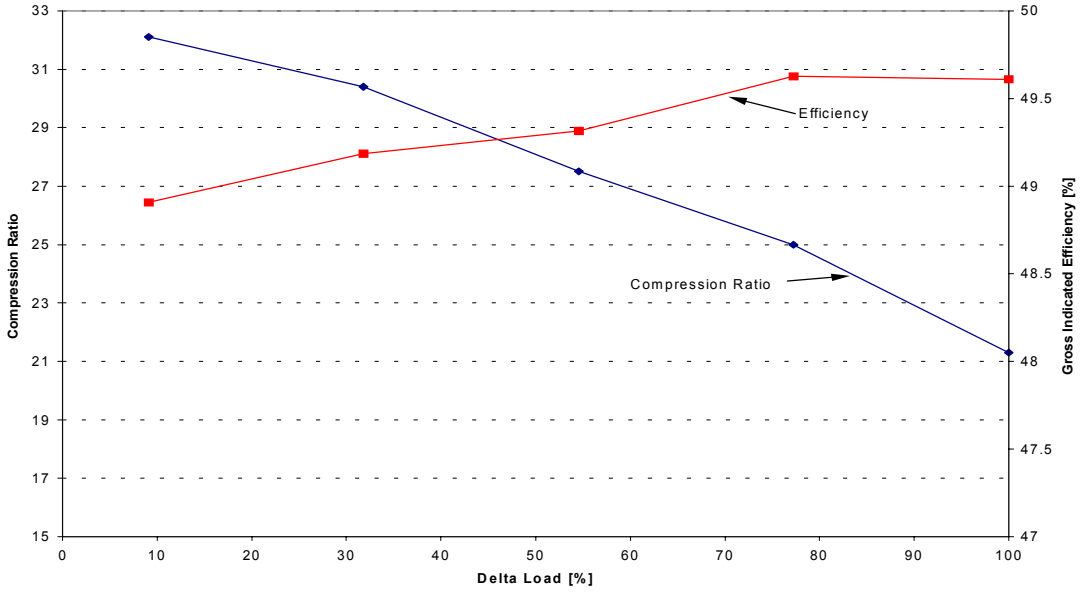

Figure 7.20: Compression Ratio and Indicated Efficiency Variation across the Operation Domain

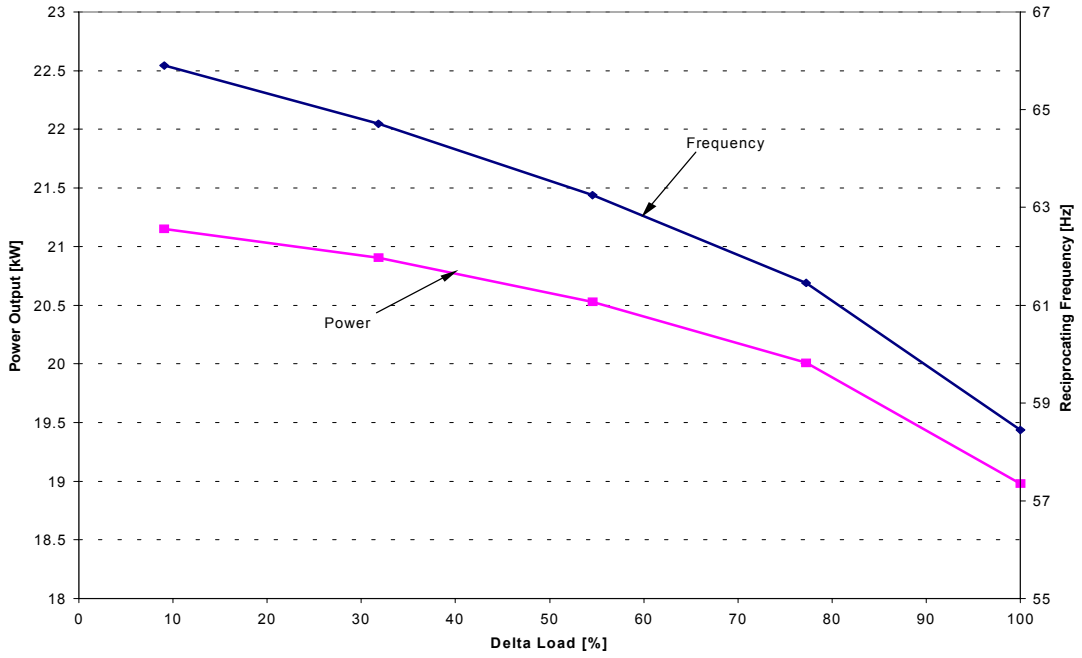

Figure 7.21: Power Output and Reciprocating Frequency Variation across the Operation Domain

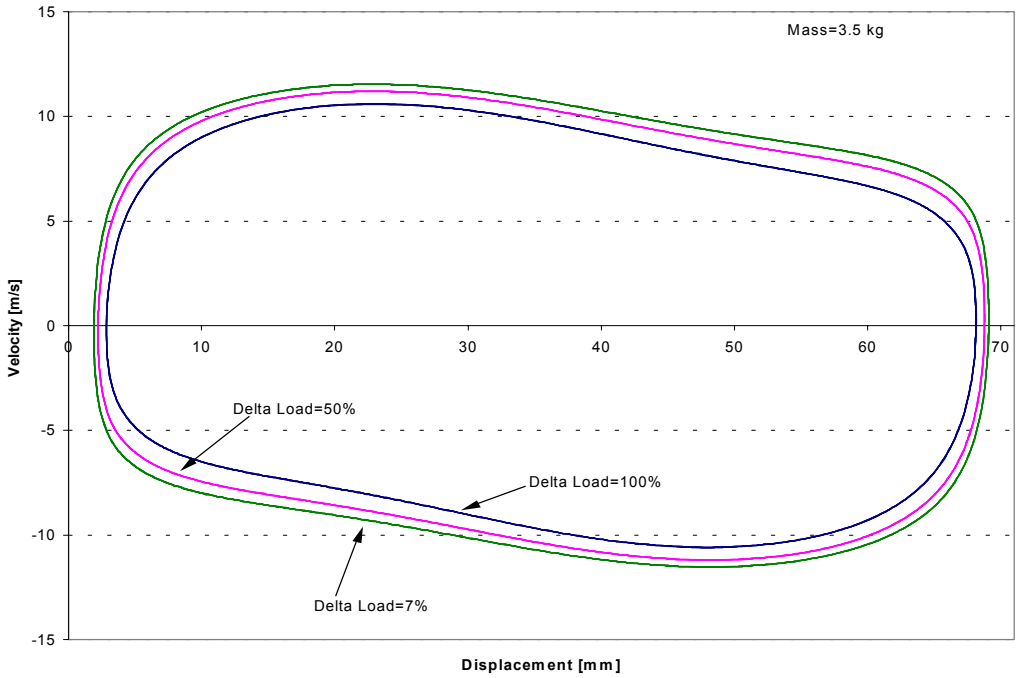

Figure 7.22: Velocity Profile Vs. Displacement for different values of the Load

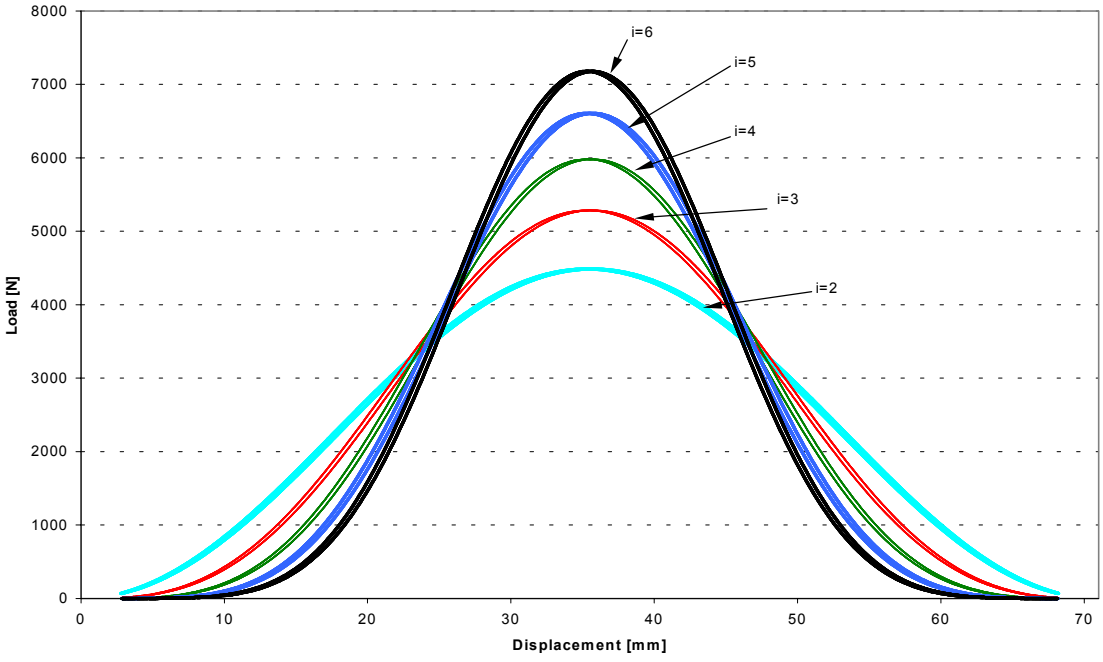

Figure 7.23: Load Shapes considered in the Analysis

There were considered five cases for the load shape, each case representing a power (starting from second power to the sixth power) of a sinusoidal curve, with the remark that in each case the work was equal. As a reminder, the load introduced by the linear alternator was considered as being a function of displacement only and it has the form indicated in Equation 7.5.

$$Load = A_i \cdot \sin^i\left(\frac{\pi x}{L}\right) \tag{7.5}$$

$$\int_0^L A_i \cdot \sin^i\left(\frac{\pi x}{L}\right) \cdot dx = \text{Constant}$$

The results obtained show that the shape variation for load did not affect substantially the engine operation, the reciprocating frequency, the compression ratio, the power output, and the efficiency have a very small variations. Figure 7.24 and Figure 7.25 present these results.

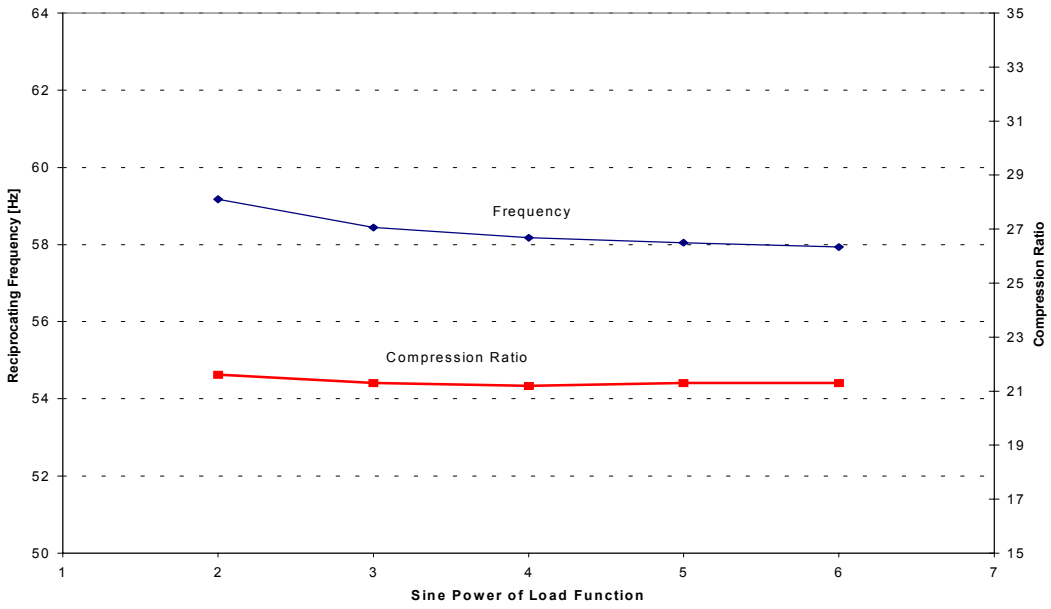

Figure 7.24: Reciprocating Frequency and Compression Ratio variation for different shapes of the Load

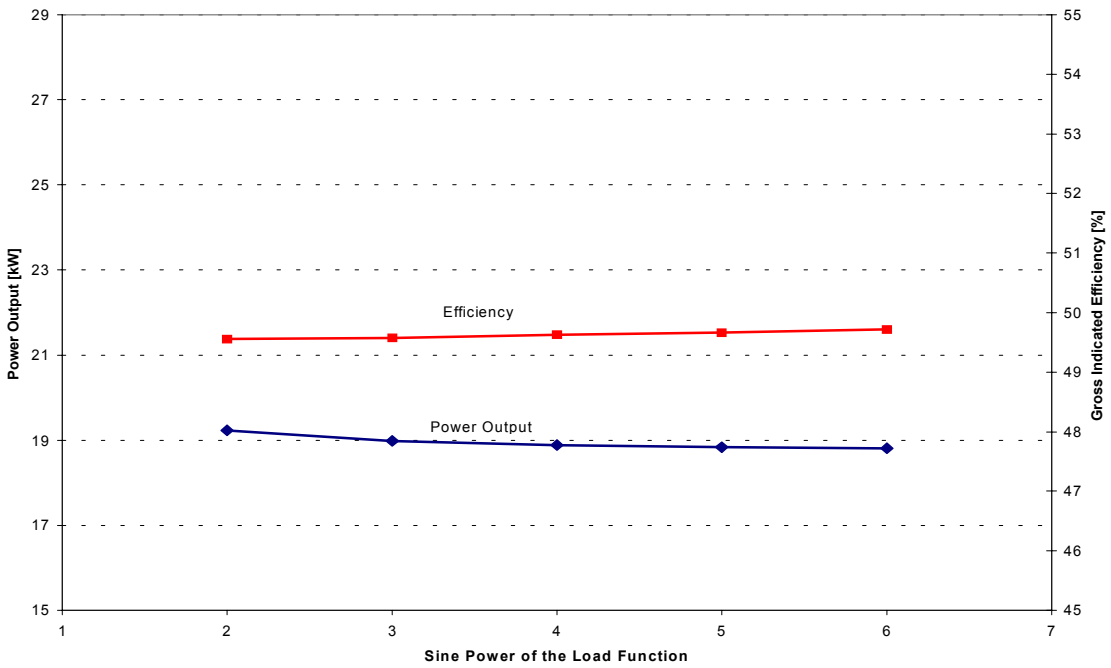

Figure 7.25: Power Output and Indicated Efficiency for different shapes of the Load

From the results obtained it can be concluded that the engine operation is not influenced substantially by a change in shape of the applied load for the case of a sinusoidal shape. Although from the previous analysis of the two-stroke prototype it was shown a relative influence of the shape of the load on engine operation, in this dissertation the considered cases for the load variation along the engine stroke are different. However, these particular load shapes analysed in this work have to be further considered due to the fact that they match much better the shape of the load introduced by the linear alternator.

7.1.5 INFLUENCE OF VOLUMETRIC EFFICIENCY

Volumetric efficiency represents an important parameter in engine operation, this particular parameter is used to measure the effectiveness of the engine's induction process. For a naturally aspired diesel engine this parameter varies between in the range of 80-95%, [20] In the numerical simulation the volumetric efficiency was assumed to be 95% which represent a high value, however this assumption is justified by the fact that there is a late intake valve closing which to a certain extent helps the cylinder filling process. In order to evaluate the effects of this important parameter on engine performances, the volumetric efficiency was varied for a range between 80% to 95%.

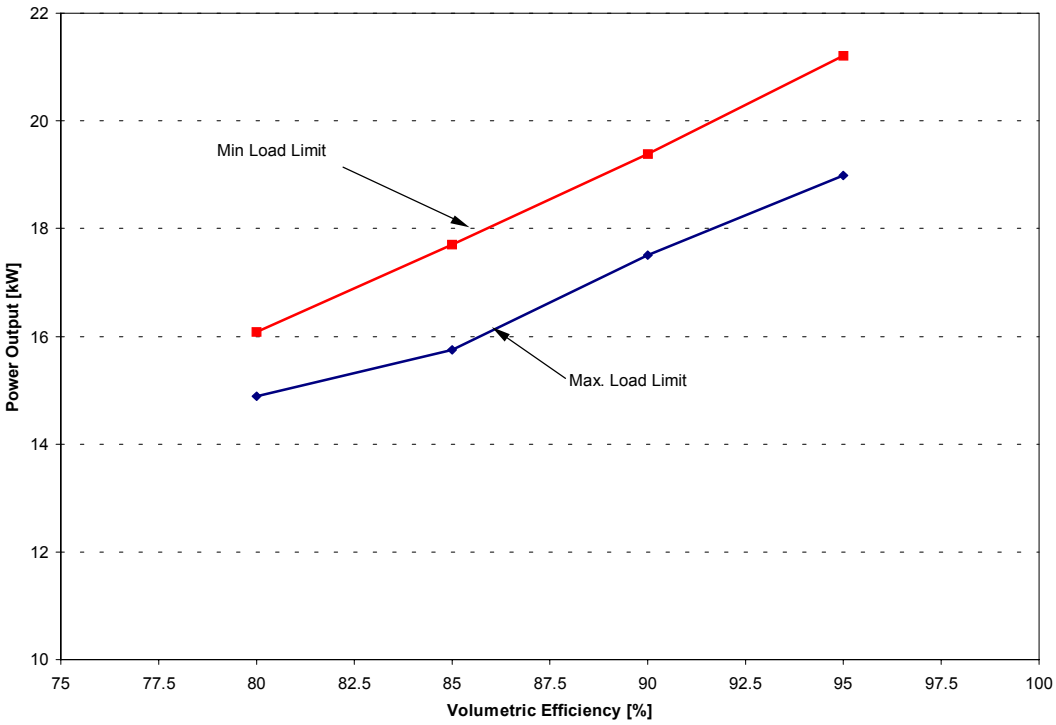

Figure 7.26: Power Output Vs. Volumetric Efficiency

It was observed that the boundary of the operation domain are strongly influenced by the variation of the volumetric efficiency. As expected, the results obtained shown that the power output increases with the volumetric efficiency as a result of a increase of the heat input for the engine cycle and, this variation accounted for the two limits of the engine operation is presented in Figure 7.26.

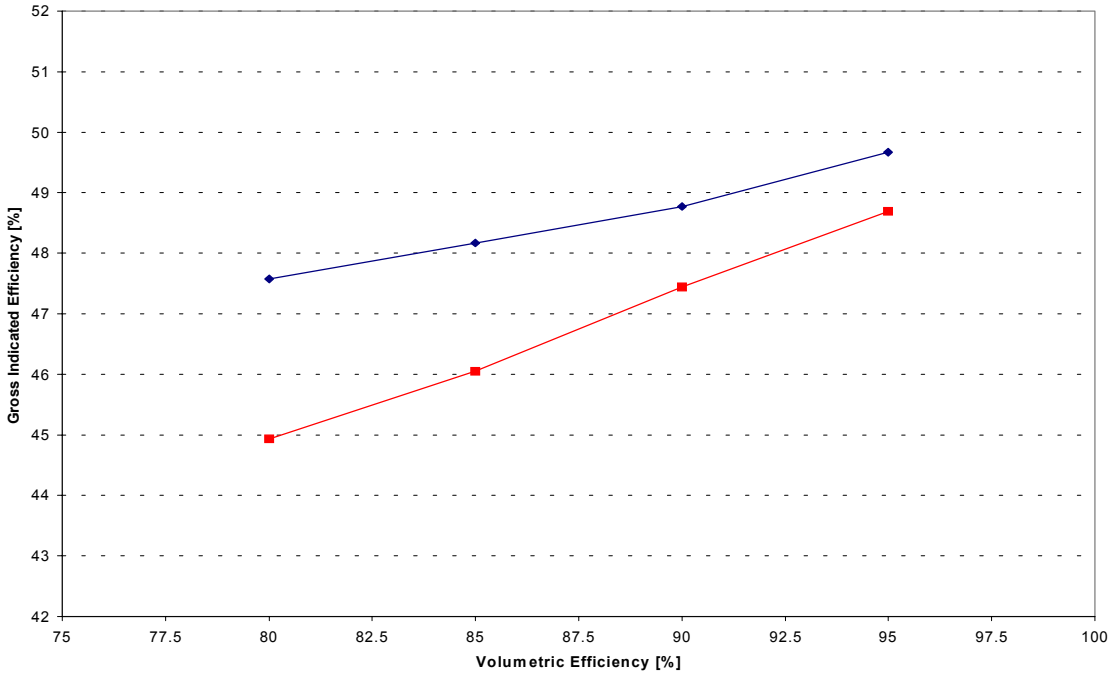

Figure 7.27: Indicated Efficiency Vs. Volumetric Efficiency

In Figure 7.27 it is illustrated the variation of indicated efficiency for values considered for the volumetric efficiency. It can be observed that the indicated efficiency increases with the increase of volumetric efficiency and, this due the higher heat input for the engine cycle.
It was observed that the reciprocating frequency had a relatively small variation with the variation of the volumetric efficiency, this aspect is presented in Figure 7.28.

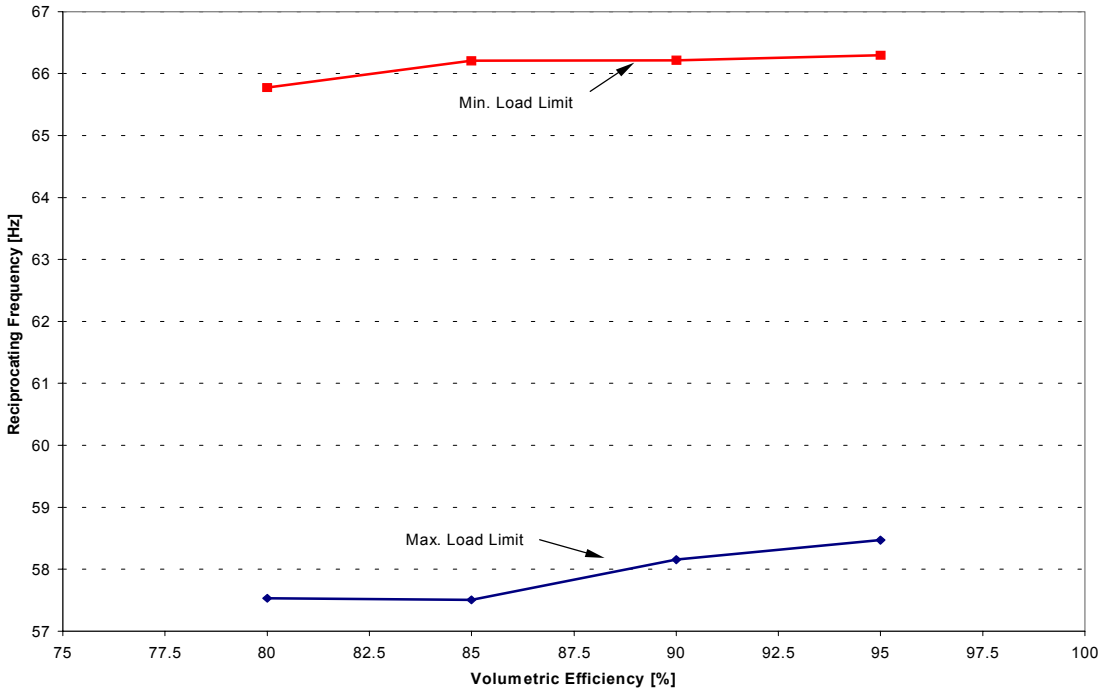

Figure 7.28: Reciprocating Frequency variation with Volumetric Efficiency

From the results obtained for the variation of the volumetric efficiency it can be concluded that this parameter, similarly with the reciprocating mass, has a major importance in establishing the engine operation domain. It is also necessary to mention that this parameter has a complex dependence on intake parameters, intake manifold and exhaust manifold design, intake valve and exhaust valve design, compression ratio and, engine speed, but this particular aspect was not considered in this dissertation.

7.2 ENGINE ANALYSIS OPERATING IN HCCI MODE

The numerical simulation for the HCCI operation mode considered the same geometrical parameters with the case of direct injection compression ignition version of FSLE, these parameters being shown in Table 3-4. Before starting the analysis for this particular case considered, it is necessary to mention that HCCI operation has different features than the previously analyzed case. The expression for autoignition was tested into being incorporated and tested into a numerical model which had a combustion process representation typical for a diesel engine. The autoignition temperature was achieved for values around 1080-1130 K. A first set of runs of the numerical simulation for the HCCI operation mode was performed in order to establish the stability of engine operation. It was observed that the engine behavior was much different that that for the direct injection compression ignition case, and this due to its combustion characteristics. It was also observed that the reciprocating frequency for this engine has a value between 80 and 120 Hz.

The engine operation was found to be very dependent on the value of the reciprocating mass and very sensitive to its variation and also to the variation of the input parameters such as, air to fuel ratio, and mixture intake temperature. The results obtained shown that once the autoignition conditions are reached the combustion occurs very fast and the in-cylinder pressure rise was not able to overcome the inertial effects, leading to a post compression of the cylinder content. These features of are presented in where it can be observed the post compression period immediately after combustion process. Evidently that this feature is undesired due to the fact that it contributes to the in cylinder pressure rise effects.

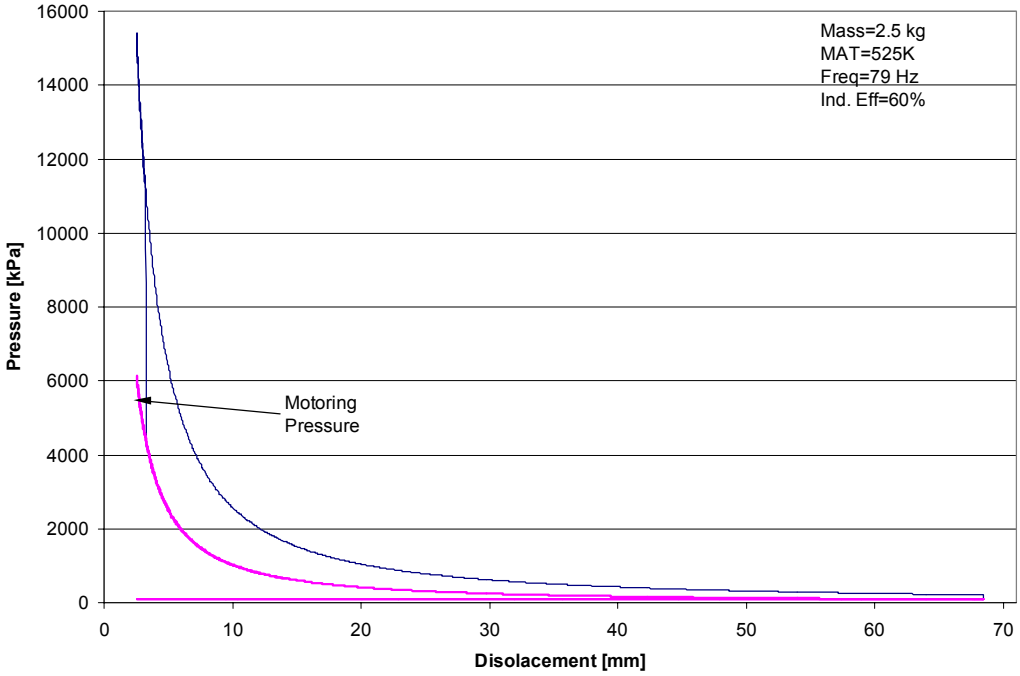

Figure 7.29: Typical Pressure variation profile obtained at FSLE operating as HCCI

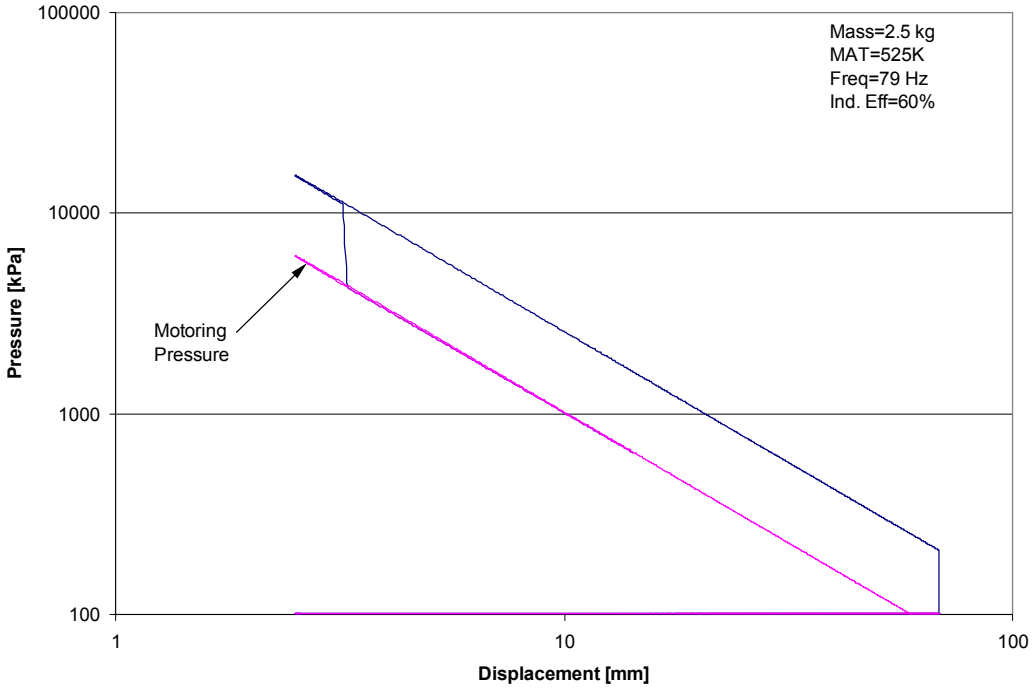

Figure 7.30: LogP-Log Displacement diagram for a typical operation as HCCI of FSLE

A better illustration of this aspect of the in-cylinder pressure variation is shown in The in-cylinder pressure history is presented in Figure 7.31, it can be observed that once the combustion started the in-cylinder pressure occurs almost instantaneously.

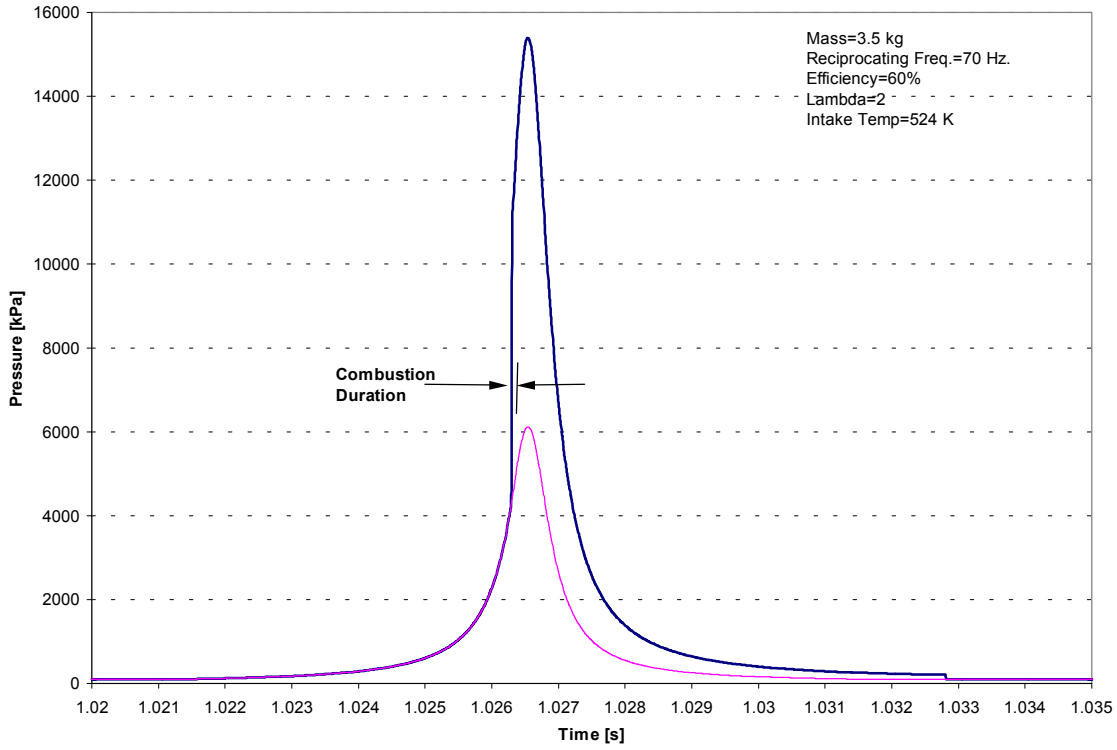

Figure 7.31: In-Cylinder Pressure history for FSLE operating as HCCI

Analyzing the figures, it can be observed that the combustion process ends before the piston reaches the clearance volume, and since the in-cylinder pressure rise is not able to overcame the, the piston continues its motion toward the reverse point causing an additional in-cylinder pressure rise. This undesired phenomenon can be avoided only if the autoignition occurs near the reversing point or the ideal case when the autoignition point coincides with the point of motion reverse. This suggests that ideal case for the engine operation, or the optimum operation regime is the case when it is used the cylinder gas bouncing effect before the

autoignition starts. It was observed that the combustion duration was much shorter than in the case of direct injection compression ignition operation, with typical values between 0.15 and 0.25 ms for a reciprocating frequency of 80 Hz. These values are comparable with the values obtained for the ignition delay in direct injection compression ignition. In this numerical model, the combustion duration is in fact equal to the extent of reaction of the considered fuel, in this case $C_{10}H_{22}$. The frequency of operation for this engine much higher in comparison to that observed at the diesel operation case implying high piston speeds. The typical velocity profile for this type of operation has is illustrated in Figure 7.32.

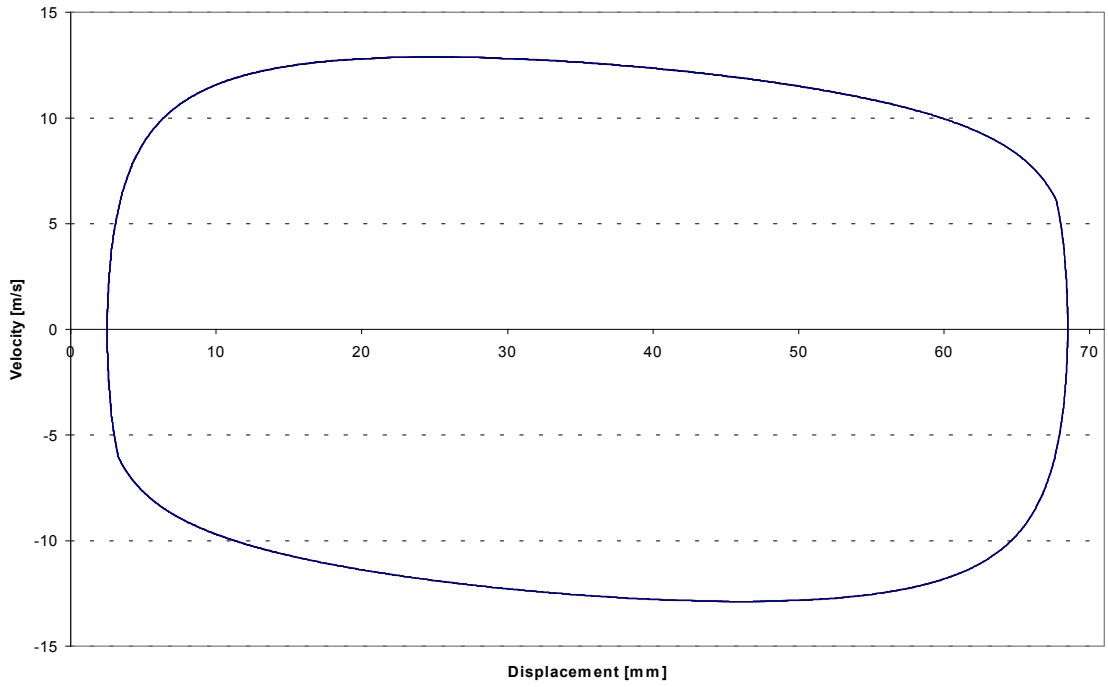

Figure 7.32: Typical Velocity profile for HCCI operation of FSLE

In Figure 7.32 the velocity profile for the HCCI operation was obtained considering the load introduced by the linear alternator as being constant along the engine stroke. It can be observed that for the HCCI the piston is subjected to a much higher acceleration values at the

end of the stroke than in the direct injection case.

Based on the results obtained from the engine simulation it can be concluded that the main challenge of this engine is to determine the optimum operation regime. An important feature of this numerical simulation is represented by the autoignition process. This particular feature of the HCCI process represents a very powerful tool for the combustion process control and thus the engine operation.

CHAPTER 8 SUMMARY AND CONCLUSIONS

The objective of this dissertation was to analyze a new engine with a mechanical configuration derived from free-piston engine, a four-stroke linear engine. The engine design was based on a general analysis of engine operation in two distinct modes, first as a direct injection compression ignition engine and, second as homogeneous charge compression ignition engine. Two time-based phenomenological models were developed and used for the numerical simulation of the four stroke linear engine, first used for the representation of the direct injection compression ignition operation and, the second for the representation of the HCCI operation. The engine analysis was performed based on the results obtained from running the numerical simulation models for each of the two operating mode previously mentioned. In the case of direct injection compression ignition it was shown the engine operation domain although limited, the engine operation was stable over a large value range of the relative air to fuel ratio offering high values for the indicated efficiency (over 45%) and a variable compression ratio which gives the engine a multi-fuel capability. It was also shown that the compression ratio for each operation regime is a result of the engine operation parameters. The engine analysis considered the effect of reciprocating mass, injection timing, combustion duration, volumetric efficiency and shape of the externally applied load. It was shown that the reciprocating mass has a dominant role in the engine operation in establishing of the operation domain.

The engine operation in the HCCI mode was more difficult to control than the case of direct injection, due to the character of its combustion process. The main challenge of this operation case was the determination of the optimum operation point considered to be the same with

the point of piston reverse. The mixture intake temperature was observed to be critical for the control of the engine operation. It was also shown that HCCI operation although more sensitive to the input parameters than the direct injection compression ignition, has certain advantages over the direct injection operation, such as higher efficiency and higher power output for the same heat input.

From both considered operation cases it can be concluded that it is very advantageous to minimize the reciprocating mass due to an increase of engine performances and a better operation control.

8.1 RECOMMENDATIONS FOR FUTURE WORK

The development of this new generation of internal combustion engines will be facilitated by the analysis presented in this work. The numerical model for the HCCI of diesel fuel presented for the designed engine was considered to be satisfactory for the purpose of this dissertation but, a more accurate analysis requires the use of a detailed chemical kinetics model in order to be able to put in evidence particular aspects of this complex combustion process, such as the autoignition process or emissions prediction. Also for the future research should consider the results from the experimental work, recently restarted for the two-stroke direct injection compression ignition prototype, at Engine and Emissions Research Center of WVU. This engine could also be arranged to operate as a HCCI engine. The results obtained from the numerical simulation developed in this dissertation will be taken into consideration for the engine control unit, undergoing development for the two-stroke direct injection prototype. It was shown that the linear alternator operation range should be matched to the engine operation in order to be able to meet the engine operation requirements, therefore the design of the linear alternator should consider a larger range of operation than that of the linear engine.

REFERENCES

1. Cleveland Diesel, “History and description of the free piston engine-gas turbine power”, year unknown.

2. A.F. Underwood, “GMR 4-4 Hyprex Free Piston Turbine Engine”, SAE Journal, June 1956, pp. 60-66.

3. D.N. Frey, P. Klotsch and A. Egli, “The Automotive Free-Piston-Turbine Engine”, SAE Transactions, Vol. 65, 1957, pp. 629-634.

4. E. L. Keating, *Applied Combustion*, Marcel Decker, Inc., 1993.

5. R. P. Heintz, “ Free-Piston Engine Pump ”, U.S. Patent 4,369,021, May 5,1980.

6. R. Bock, “Gas Cushion Free-Piston Type Engine”, U.S. Patent 4,128,083, December 5,1978.

7. P. A. Rittmaster and J. L. Booth, “Hydraulic Engine”, U.S. Patent 4,326,380, April 27,1982.

8. M. D. Iliev, S. S. Kervanbashiev, S. D. Karamanski, F. M. Makedonski, “Method and Apparatus for Producing Electrical Energy from a Cyclic Combustion Process utilizing Coupled Pistons which Reciprocate in Unison” U.S. Patent 4,532,431, July 30,1985.

9. K. A. Galitello, Jr., “Two Stroke Cycle Engine”, U.S. Patent 4,876,991, October 31, 1989.

10. Y. Q. Deng and K. Dong, “Free-Piston Engine without Compressor”, U.S. Patent 4,924,956, May 15, 1990.

11. J. F. Kos, “Computer Optimized Hybrid Engine”, U.S. Patent 5,002,020, March 26, 1991.

12. N. H. Beachley and F. J. Fronczak “Design of a Free-Piston Engine-Pump”, SAE 921740, 1992.

13. S. K. Widener and K. Ingram, “Free-Piston Engine Linear Generator Technology Development”, Final Report, Under Contract to U.S. Army TARDEC, Mobility Technology Center-Belvoir, Fort Belvoir, Virginia, January 1995.

14. P. Van Blarigan, N. Paradiso, and S. Goldsborough, “Homogeneous Charge Compression Ignition with a Free Piston: A New Approach to Ideal Otto Cycle Performance”, SAE 982484, 1998.

15. S. S. Goldsborough and P. Van Blarigan, “A Numerical Study of a Free Piston IC Engine operating on Homogeneous Charge Compression Ignition Combustion”, SAE 1999-01-0619, 1999.

16. N.N. Clark, T.I. McDaniel, R.J. Atkinson, S. Nandkumar, C.M. Atkinson, S. Petreanu, C.J. Tennant, and P. Famouri, “Modeling and Development of a Linear Engine”, 1998 Spring Technical Conference, ASME ICE Division, Fort Lauderdale, FL, ICE-Vol. 30-2.

17. N.N. Clark, S. Nandkumar, C.M. Atkinson, R. J. Atkinson, T. I. McDaniel, and S. Petreanu, P. Famouri, and W.R. Cawthorne, “Operation of a Small Bore Linear Two-Stroke Engine” ASME Fall Internal Combustion Engine Conference, Clymer NY, September 1998, Paper No. 98-ICE-120, ICE Vol. 31-1.

18. S. Nandkumar, “Modeling of a Linear Engine”, MSME Thesis, West Virginia University, 1998.

19. C. M. Atkinson, S Petreanu, N. N. Clark, R. J. Atkinson, T. I. McDaniel, S. Nandkumar and P. Famouri “Numerical Simulation of a Two-Stroke Linear Engine-Alternator Combination”, SAE 990921, 1999.

20. W. R. Cawthorne, P. Famouri, J. Chen, N. N. Clark, T. I. McDaniel, R. J. Atkinson, S. Nandkumar, C. M. Atkinson, and S. Petreanu, “Development of a Linear-Alternator-Engine for Hybrid Electric Vehicle Applications”, IEEE Transactions on Vehicular Technology, Vol. 48, No. 6, November, 1999.

21. J. B. Heywood, Internal Combustion Engines Fundamentals, McGraw-Hill, 1988.

22. S. Onishi, S. H. Jo, K. Shoda, P. D. Jo, and S. Kato, “Active Thermo-Atmospheric Combustion (ATAC) – A New Combustion Process for Internal Combustion Engines”, SAE 790501, 1979.

23. R. H. Thring, “Homogenous Charge Compression Ignition (HCCI) Engines”, SAE 892068, 1989.

24. T. W. Ryan, and T. J. Callahan, “Homogeneous Charge Compression Ignition of Diesel Fuel”, SAE 961160, 1996.

25. A. W. Gray, and T.W. Ryan, “Homogeneous Charge Compression Ignition (HCCI) of Diesel Fuel” SAE 971676, 1997.

26. H. Suzuki, N. Koike, H. Ishii, and M. Odaka, “Exhaust Purification of Diesel Engines by Homogeneous Charge with Compression Ignition Part 1: Experimental Investigation of Combustion and Exhaust Emission Behavior Under Pre-mixed Homogeneous Charge Compression Ignition Method”, SAE 9710313, 1997.

27. M. Christensen, B. Johansson, P. Amneus, and F. Mauss,"Supercharged Homogeneous Charge Compression Ignition",SAE 980787, 1998.

28. R. H. Stanglmaier, and C. E. Roberts, "Homogeneous Charge Compression Ignition (HCCI): Benefits, Compromises, and Future Engine Applications", SAE 1999-01-3632, 1999.

29. J. I. Ramos, *Internal Combustion Engine Modeling*, Hemisphere Publishing Company, 1989.

30. R. C. Rosenberg, "General Friction Considerations for Engine Design", SAE 821576, 1982.

31. P. G. Blair, *Design and Simulation of Two-Stroke Engines*, Society of Automotive Engineers, Inc., 1990.

32. D. A. Anderson, J. C. Tannehill, and R. H. Pletcher, *Computational Fluid Mechanics and Heat Transfer*, Hemisphere Publishing Company, 1984.

33. S. C. Chapra, and R. P. Canale, *Numerical Methods for Engineers 2nd Edition*, McGraw-Hill Publishing Company, 1988.

34. R. S. Benson, The Thermodynamics and Gas Dynamics of Internal Combustion Engines, Vol. 1, Oxford University Press, New York, 1982.

35. H. O. Hardenberg, and F. W. Hase, "An Empirical Formula for Computing the Pressure Rise Delay of a Fuel from its Cetane number and from the relevant Parameters of Direct-Injection Diesel Engines", SAE 790493, 1979.

36. L. J. Spadaccini and J. A. TeVelde, "Autoignition Characteristic of Aircraft-Type Fuels", Combustion and Flame, vol. 46, pp. 283-300, 1982.

37. N. Miamoto, T. Chikahisa, T. Murayama, and R. Sawyer, "Description and Analysis of Diesel Engine Rate of Combustion and Performance Using Wiebe's Functions" SAE 850107, 1985.

38. J. A. Velassquez, and L. F. Milanez, "Analysis of the Irreversibilities in Diesel Engines", SAE 940673, 1994.

39. M. F. J. Brunt, and K. C. Platts, "Calculation of Heat Release in Direct Injection Diesel Engines", SAE 990187, 1999.

40. J. I. Gojel, "A Study of Combustion Chamber Arrangements and Heat Release in D.I. Diesel Engines", SAE 821034, 1982.

41. K. Kumar, M. K. G. Babu, R. R. Gaur, and R. D. Garg, "A Thermodynamic Simulation

Model for a Four Stroke Medium Speed Diesel Engine", SAE 840516, 1984.

42. T. Kamimoto, T. Minagawa, and S. Kobori, "A Two-Zone Model Analysis of Heat Release Rate in Diesel Engines", SAE 972959, 1997.

43. H. Hiroyasu, T. Kadota, and M. Arai, "Development and Use of a Spray Combustion Modeling to Predict Diesel Engine Efficiency and Pollutant Emissions: Part 1. Combustion Modeling, Bulletin of the JSME, vol. 26, no. 214, pp. 569-575, 1983.

44. G. V. J. Sastry, and H. Chandra, "A Three-Zone Heat Release Model for DI Diesel Engines", SAE 940671, 1994.

45. S. Kono, A. Nagao, and H. Motooka, "Prediction of In-Cylinder Flow and Spray Formation Effects on Combustion in Direct Injection Diesel Engines", SAE 850108, 1985.

46. Z. Bazari, "A DI Diesel Combustion and Emission Predictive Capability for Use in Cycle Simulation", SAE 920462, 1992.

47. E. Khalil, P. Samuel, and G. A. Karim, "An Analytic Examination of the Chemical Kinetics of the Combustion of N-Heptane-Methane Air Mixtures" SAE 961932, 1996.

48. P. M. Najt, and D. E. Foster, "Compression-Ignited Homogeneous Charge Combustion", SAE 830264, 1983.

49. S. R. Turns, An Introduction to Combustion Concepts and Applications , McGraw-Hill, 1996.

50. G. L. Borman and K. W. Ragland, *Combustion Engineering*, McGraw-Hill, 1998.

51. F. L. Dryer, and I. Glassman, "Fundamental and Semi-Global Kinetic Mechanisms of Hydrocarbon Combustion" Annual Report, October 1977- September 1978, DOE Contract No. C00-4272-3, 1978.

52. F. L. Dryer, and I. Glassman, "The High Temperature of CO and CH_4" Fourteenth Symposium (International) on Combustion, The Combustion Institute, Pittsburgh, PA., pp 987, 1973.

53. S. C. Kong, N. Ayoub, and R. D. Reitz, "Modeling Combustion in Compression Ignition Homogeneous Charge Engines", SAE 920512, 1992.

54. T. W. Ryan, and T. J. Callahan, "Engine and Constant Volume Bomb Studies of Diesel Ignition and Combustion", SAE 881626, 1988.

55. L. G. Dodge, D. M. Leone, D. W. Naegeli, D. W. Dickey, and K. R. Swenson, "A PC-Based Model for Predicting NO_x Reductions in Diesel Engines", SAE 962060, 1996.

56. S. S. Goldsborough, “A Numerical Investigation of a Two-Stroke Cycle, Hydrogen Fueled, Free Piston Internal Combustion Engine”, Masters Thesis, Colorado State University, 1998.

57. Reaction Design, http://www.ReactionDesign.com/

58. S. B. Fiveland, and D. N. Assanis, “A Four-Stroke Homogeneous Charge Compression Ignition Engine Simulation for Combustion and Performance Studies”, SAE 2000-01-0332, 2000.

59. G. L. Borman, and K. Nishiwaki, “Internal Combustion Engine Heat Transfer”, Progress in Energy Combustion Science, Vol. 13, pp. 1-46, 1987.

60. W. J. D. Annand, “Heat Transfer in the Cylinders of Reciprocating Internal Combustion Engines”, Proceedings of the Institution of Mechanical Engineers, 177, pp. 973-990, 1963.

61. G. Woschni, “A Universally Applicable Equation for the Instantaneous Heat Transfer Coefficient in the Internal Combustion Engine”, SAE 670931, 1967.